

AD-A167 148

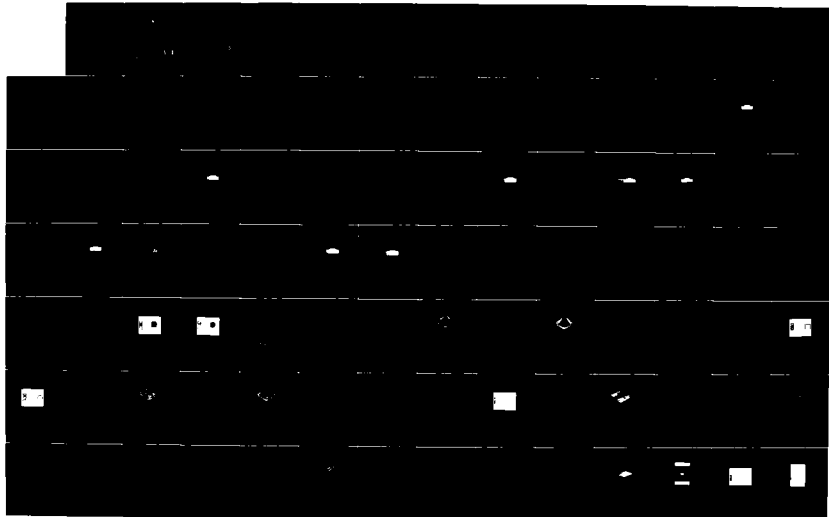
OBJECT RECOGNITION USING RANGE IMAGES(U) AIR FORCE  
INST OF TECH WRIGHT-PATTERSON AFB OH SCHOOL OF  
ENGINEERING J W GRANTHAM DEC 85 AFIT/CEP/ENG/85D-4

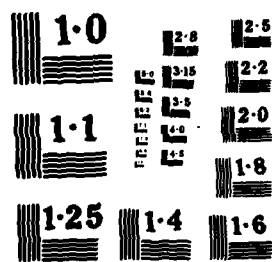
1/2

UNCLASSIFIED

F/C 17/8

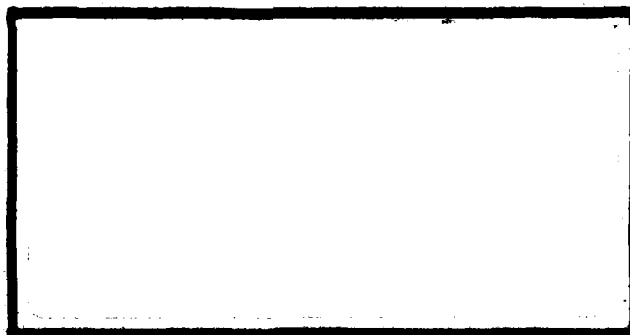
ML





1

AD-A167 148



DTIC FILE COPY

**DISTRIBUTION STATEMENT A**  
Approved for public release;  
Distribution Unlimited

**DTIC**  
**ELECTE**  
**S MAY 12 1986 D**

DEPARTMENT OF THE AIR FORCE  
AIR UNIVERSITY

**AIR FORCE INSTITUTE OF TECHNOLOGY**

Wright-Patterson Air Force Base, Ohio

86 5 12 082

AFIT/GEP/ENP/85D-4

OBJECT RECOGNITION USING  
RANGE IMAGES

THESIS

Jeffrey W. Grantham  
Second Lieutenant, USAF

AFIT/GEP/ENP/85D-4

DTIC  
ELECTE  
MAY 12 1986  
S D  
B

Approved for public release; distribution unlimited

AFIT/GEP/ENP/85D-4

OBJECT RECOGNITION USING  
RANGE IMAGES

THESIS

Presented to the Faculty of the School of Engineering  
of the Air Force Institute of Technology

Air University

in Partial Fulfillment of the  
Requirements for the Degree of  
Master of Science (Engineering Physics)

Jeffrey W. Grantham, B.S.

Second Lieutenant, USAF

December 1985

Approved for public release; distribution unlimited

### Acknowledgements

I would like to first thank the Lord Jesus Christ for giving me the ability and stamina to complete this thesis. I pray that I will be somehow of more service to him because of this experience and education. I thank the CSC system manager, Frank Bakos, for all the time he spent helping me with the computer. I thank the Electrical Engineering Department, especially Captain David King, for allowing me access to the equipment in the Signal Processing Laboratory. I especially want to thank Steve Butler of the Electro-Optical Terminal Guidance Branch, Eglin AFB FL for his time and patience in answering the myriad of questions that I asked him. Thanks also to you, Major John Wharton, for your guidance in this thesis and for listening to my thesis problems at the gym.

Last but certainly not least, I would like to thank my wife, Carrie, for putting up with my moods and listening to my troubles. It will not be too much longer before you will have a husband again.

Jeffrey W. Grantham

|               |   |
|---------------|---|
| Accession For |   |
| THIS COPY     | ✓ |
| THIS TAB      |   |
| REPRODUCTION  |   |
| ORIGINATOR    |   |
| DATE          |   |
| BY            |   |
| QUALITY       |   |
| DATE          |   |
| A-1           |   |



## Contents

|   | <u>Page</u> |
|---|-------------|
| Acknowledgements . . . . .  | 11          |
| List of Figures . . . . .   | v           |
| List of Tables . . . . .  | viii        |
| Abstract . . . . .  | ix          |
| I. Introduction . . . . .   | 1           |
| Background . . . . .  | 1           |
| The Problem . . . . .   | 2           |
| Purpose . . . . .   | 2           |
| Scope . . . . .   | 3           |
| Approach . . . . .  | 3           |
| II. Modeling the Laser Scanner . . . . .  | 5           |
| Determining the Scenario . . . . .  | 6           |
| Formulation of the Mathematics of<br>the Scan . . . . .   | 8           |
| The Images That Can Be Formed by<br>the Computer Program . . . . .  | 13          |
| Investigating the Physical Parameters<br>of a Range Scan . . . . .  | 15          |
| Improving the Modeling of the Laser Scanner . . . . .   | 17          |
| Increasing the Spot Size on the Target . . . . .  | 25          |
| Modeling the Dropouts in Range Images . . . . .   | 28          |
| Repairing the Pixel Dropouts . . . . .  | 33          |
| III. Recognizing Objects from Range Scenes . . . . .  | 38          |
| Using Range Geometry for Scene Analysis . . . . .   | 38          |
| Using Correlation for Object Recognition . . . . .  | 40          |
| IV. Recognizing a Tank from a Range Scene . . . . .   | 65          |
| Establishing Correlation Coefficients<br>for a Tank . . . . .   | 65          |
| Modifying the Model Tank and the Range Scene<br>The Effect of Rotation on the Correlation<br>of a T-72 Tank . . . . . | 72          |
| Enhancing Horizontal Edges Only . . . . .   | 80          |
| Vertical Edge Enhancement . . . . .   | 96          |
|   | 101         |

## Contents

|   | <u>Page</u> |
|---|-------------|
| V. Other Factors Affecting the Correlation Coefficients . . . . .                 | 106         |
| The Effect of the Laser Beam Spot on Correlation . . . . .                        | 106         |
| The Results of Applying the Median Repair Method to Range Images . . . . .        | 114         |
| VI. Scanning and Target Recognition for an Actual Air-to-Ground Missile . . . . . | 121         |
| The Raster Scanning of the Air-to-Ground Missile . . . . .                        | 121         |
| Laser Power and Detector Sensitivity . . . . .                                    | 124         |
| Implementing the Correlation Routine . . . . .                                    | 127         |
| VII. Conclusion and Recommendations . . . . .                                     | 132         |
| Conclusion . . . . .  | 132         |
| Recommendations . . . . .   | 134         |
| Bibliography . . . . .  | 136         |
| Vita . . . . .  | 139         |



# List of Figures

| <u>Figure</u> |   | <u>Page</u> |
|---------------|---|-------------|
| 1             | An Air-to-Ground Missile Raster Scanning<br>with a Laser . . . . .                            | 7           |
| 2             | The Geometric Relationship Between the<br>Sensor's Position and the Scan Point . . . . .      | 11          |
| 3             | Range Image of a Model Russian T-72 Tank . . . . .  | 14          |
| 4             | Range Image of a Model T-72 Tank with<br>"Ghost" Edges . . . . .                              | 19          |
| 5             | Range Image of a Model T-72 Tank without<br>"Ghost" Edges . . . . .                           | 24          |
| 6             | Range Image of a Model T-72 Tank Formed<br>with a Beam Diameter of 29.1 cm. . . . .           | 26          |
| 7             | Range Image of a Model T-72 Tank Formed<br>with a Beam Diameter of 7.3 cm . . . . .           | 27          |
| 8             | Range Image of a Model T-72 Tank That<br>Has Been Degraded by 10% . . . . .                   | 31          |
| 9             | Range Image of a Model T-72 Tank That<br>Has Been Degraded by 40% . . . . .                   | 32          |
| 10            | Range Image of a Model T-72 Tank That Has<br>Been Degraded by 10% and Then Repaired . . . . . | 35          |
| 11            | Range Image of a Model T-72 Tank That Has<br>Been Degraded by 40% and Then Repaired . . . . . | 36          |
| 12            | Range Image of a 2-D Rectangle Function . . . . .   | 46          |
| 13            | Range Image of a 2-D Cylinder Function . . . . .  | 47          |
| 14            | FFT Log-Magnitude of the Rectangle Function . . . . .   | 48          |
| 15            | FFT Log-Magnitude of a Cylinder Function . . . . .  | 48          |
| 16            | FFT Log-Magnitude of a Ellipse Function . . . . .   | 49          |
| 17            | Autocorrelation of the Rectangle Function . . . . .   | 51          |
| 18            | OTF for a Square Exit Pupil . . . . .   | 51          |
| 19            | Correlation of the Cylinder Function with<br>the Rectangle Function . . . . .                 | 53          |

| <u>Figure</u> |  | <u>Page</u> |
|---------------|--|-------------|
| 20            | Enhanced Range Image of the Rectangle Function . . . . .   | 57          |
| 21            | Enhanced Range Image of the Cylinder Function  | 58          |
| 22            | Log-Magnitude of the Enhanced FFT of a Rectangle Function . . . . .                                    | 59          |
| 23            | Autocorrelation of the Enhanced Rectangle Function . . . . .   | 60          |
| 24            | Correlation of the Edge-Enhanced Cylinder Function with the Edge-Enhanced Rectangle Function . . . . . | 62          |
| 25            | Pixel Level vs. Pixel Height for Bidirectional Edge Enhancement . . . . .                              | 63          |
| 26            | Enhanced Range Image of the Model T-72 Tank .  | 66          |
| 27            | Autocorrelation of the Edge Enhanced Model T-72 Tank . . . . .   | 68          |
| 28            | Correlation of a Rectangular Box with the Model T-72 Tank . . . . .                                    | 71          |
| 29            | Correlation of a Range Scene Containing a T-72 Tank and a Tree with the Reference T-72 Tank            | 77          |
| 30            | Range Image of a Model T-72 Tank That Has Been Rotated 45 Degrees . . . . .                            | 82          |
| 31            | Range Image of a Model T-72 Tank That Has Been Rotated 90 Degrees . . . . .                            | 83          |
| 32            | Enhanced Range Image of the Model T-72 Tank That Has Been Rotated 45 Degrees . . . . .                 | 84          |
| 33            | Enhanced Range Image of a Model T-72 Tank That Has Been Rotated 90 Degrees . . . . .                   | 85          |
| 34            | Correlation Maximum vs. Degree of Tank Rotation . . . . .  | 86          |
| 35            | Correlation of a Rotated (45 Degrees) Model T-72 Tank with a Non-Rotated Model T-72 Tank               | 87          |
| 36            | Correlation of a Rotated (90 Degrees) Model T-72 Tank with a Non-Rotated Model T-72 Tank               | 88          |

| <u>Figure</u> |   | <u>Page</u> |
|---------------|---|-------------|
| 37            | The Mellin-Fourier Correlation Process . . .  | 90          |
| 38            | Horizontally Edge Enhanced Range<br>Image of a Model T-72 Tank . . . . .  | 98          |
| 39            | Pixel Level vs. Height for<br>Horizontally Enhanced Edges . . . . .   | 100         |
| 40            | Vertically Edge Enhanced Range Image<br>of a Model T-72 Tank . . . . .  | 102         |
| 41            | Pixel Level vs. Height for<br>Vertically Enhanced Edges . . . . .   | 104         |
| 42            | Correlation Maximum vs. Diameter of the<br>Scanning Laser Beam for a Scanned Tank . . .                             | 109         |
| 43            | Range Image of a Model T-72 Tank<br>Rotated by 90 Degrees and Formed<br>with a Beam Diameter of 7.3 cm . . . . .    | 111         |
| 44            | Range Image of a Model T-72 Tank<br>Rotated by 90 Degrees and Formed<br>with a Beam Diameter of 29.1 cm . . . . .   | 112         |
| 45            | Correlation Maximum vs. Diameter<br>of the Scanning Laser Beam for a<br>Scanned Tank (Rotated 90°) . . . . .        | 113         |
| 46            | Correlation Maximum vs. Percentage of<br>Tank Degraded (for Both Repaired and<br>Non-Repaired Tanks) . . . . .      | 115         |
| 47            | Enhanced Range Image of the 10%<br>Degraded Model T-72 Tank . . . . .   | 117         |
| 48            | Enhanced Range Image of a 40%<br>Degraded Model T-72 Tank . . . . .   | 118         |
| 49            | Correlation of the 40% Degraded Model<br>T-72 Tank with the Non-Degraded Model<br>T-72 Tank . . . . .               | 119         |
| 50            | Correlation of the 40% Degraded (and<br>Then Repaired) Model T-72 Tank with<br>the Non-Degraded T-72 Tank . . . . . | 120         |

List of Tables

| <u>Table</u> |   | <u>Page</u> |
|--------------|---|-------------|
| I            | Correlation Coefficients Resulting from the Correlation of Different Objects with a Model of a T-72 Tank . . . . .  | 69          |
| II           | Correlation Coefficients for Modified T-72 Tanks and for Range Scenes Containing More Than the T-72 Tank . . . . .  | 73          |
| III          | Correlation Coefficients Resulting from the Correlation of the "Horizontally Edge Enhanced" T-72 Tank with Other "Horizontally Edge Enhanced" Objects . . . . . | 99          |
| IV           | Correlation Coefficients Resulting from the Correlation of the "Vertically Edge Enhanced" T-72 Tank with Other "Vertically Edge Enhanced" Objects . . . . .     | 103         |

Abstract

This study involved forming synthetic range images and investigating correlation as a target recognition technique. The synthetic range images were formed with a computer program, which models the laser scanning of an air-to-ground missile. With this range imaging program, a model of a Russian T-72 tank was formed, which was subsequently used in investigating image correlation.

In the investigation into image correlation, the effects of background clutter and target rotation on a range image's correlation coefficient were examined, as well as possible methods of correcting for these effects. Other factors affecting the correlation coefficient that were considered were pixel dropouts and the beam spot size of the laser. Pixel dropouts were shown to be detrimental to a range image's correlation coefficient, but could be corrected by using a "median replacement" technique. Also shown was that for a certain range of "on target" beam diameters, as the diameter of the scanning laser beam increased, so did the correlation's discerning ability. The last part of this study revealed that actually implementing range imaging and correlation into an air-to-ground missile was possible, but would require both digital and optical operations.

## OBJECT RECOGNITION USING RANGE IMAGES

### I. Introduction

#### Background

The Air Force is interested in air-to-ground missiles with stand-off capabilities. To acquire this stand-off capability, a missile must have its own scanning system and a target recognition ability. The Electro-Optical Terminal Guidance Branch at Eglin AFB has recently built and tested a laser scanning system for application in air-to-ground missiles. Laser scanners like the one being developed at Eglin AFB, will provide missiles with a means of target recognition by forming two-dimensional images from time-of-flight range information. These two-dimensional images are called range images because the intensity at each point in the range image, corresponds to the range to an object point in the scanned scene.

Range images preserve the three-dimensional geometry of objects and as a result, they depend only on the shape of the objects. Since range images depend only on the geometry contained in the scanned scene, they are independent of the time of day and most weather conditions. The range images are affected by the weather only in the sense that the pulse

from the scanning laser must be able to return to the missile and be detected. The diurnal and semi-weather independence of range imaging gives it a big advantage over other imaging methods, e.g. infrared imaging.

#### The Problem

The Electro-Optical Terminal Guidance Branch at Eglin AFB FL has shown that it's possible to form range images of targets located long distances, e.g. 1.2 km, away from the laser scanner. The task to be accomplished is to develop a target recognition technique which can be used in air-to-ground missiles. The recognition technique must be extremely fast and must also utilize the range images produced by the missile's laser scanner.

#### Purpose

There was a three-fold objective to this research. The first objective was to form synthetic range images with a computer program. These range images were to be formed in a manner which models the laser scanning of an air-to-ground missile. The second objective was to apply image correlation to the task of recognizing targets from the synthetic range images. In this part of the thesis, factors affecting and problems with image correlation were to be examined. The last objective of this research was to explore some of the problems involved in applying such range imaging and correlation techniques to air-to-ground missiles.

### Scope

Synthetic range images were the only types of images formed in this research, actual range imaging was not performed. The range images that were formed, were only modeled in the context of application to air-to-ground missiles, i.e. where the laser scanner is constantly moving in the forward direction, and the targets are a long distance away. The primary target which was range imaged, was that of a Russian T-72 tank. The investigation into correlation was also primarily performed with this model T-72 tank.

The search into correlation began with the basics, with such topics as edge enhancement being explored. In developing a correlation technique, emphasis was placed on simplicity and speed, with more elaborate methods being rejected as taking too long to perform. Possible solutions to correlation problems that seemed too time consuming to pursue in this study, were referenced and concisely summarized.

### Approach

The investigation into range imaging and image correlation described in this thesis was divided into five major parts:

1. Modeling the laser scanner of the air-to-ground missile. A computer program was written which forms range images in a manner that models the scanning of an air-to-ground missile.



2. Recognizing targets from range images. Different techniques of target recognition, all of which utilize range images, were explored. The main emphasis was on correlation and the preprocessing that must be performed on range images before the correlation process is used.

3. Recognizing a tank from a range scene. Factors and problems involved with recognizing an object from a range scene were explored. Some of the problems considered were scene clutter and object rotation. A threshold correlation coefficient was also searched for in this section.

4. Other factors affecting the correlation coefficient of a range scene. Effects on correlation coefficients such as the laser's "on target" beam spot and a range image's pixel dropouts were considered.

5. Scanning and target recognition for an actual air-to-ground missile. The actual implementation of range imaging and image correlation into an air-to-ground missile was studied.

## II. Modeling the Laser Scanner

To give an air-to-ground missile a target acquisition ability, some type of imaging system must be placed on board the missile. The type of imaging system that will be considered here is a laser scanner. The laser scanner provides the missile with time-of-flight range information for each point it scans in a scene. Since laser scanners are typically raster-scanned in azimuth and elevation, the range matrix, which results from the scan, has the form of  $R(\theta, \phi)$ . This range matrix is then mapped to intensity to form a two-dimensional range image. After mapping to intensity, the range matrix can be transformed into a Cartesian form  $Z = F(x, y)$  where  $Z$  corresponds to intensity, i.e. range. This range matrix is a perspective view of the original scene which depends only on the geometry in the scene, and thus can be used for target identification (Butler, 1985a:1). Such range imaging has previously appeared in the literature in works by Jarvis (Jarvis, 1983:505-511), Nitzan (Nitzan and others, 1977:206-219) and Shirai (Shirai and others, 1971:80-87).

This analysis will model the scanning of an air-to-ground missile as closely as possible without introducing too many complications. A computer program will result from this analysis, which will form range images that duplicate as closely as possible the images formed by an actual laser

scanner. The first step in this modeling process is to determine the scenario in which the air-to-ground missile will operate.

#### Determining the Scenario

The operational scenario of the air-to-ground missile modeled in this paper will be a simplified version of the real operational scenario of the missile. This analysis will assume the missile is traveling at a constant altitude, with a constant velocity, and in a straight line. The assumption that the ground is flat with no hills or valleys will also be made. The missile's laser scanner will be raster scanned back and forth in the horizontal direction at a constant declination angle,  $\phi$ . The speed of the missile will push the scan forward in a push-broom manner. Figure 1. portrays such a scan where  $\phi$  represents the declination angle,  $\theta$  the rastering angle,  $h$  the altitude of the missile,  $v$  the speed of the missile,  $t$  some initial time,  $t'$  some later time, and the  $x$ - $z$  plane represents the ground. The missile will obtain its range information by measuring the time of flight between the time the laser pulse leaves the missile and the time it returns to the sensor and is detected. The distance that the missile moves during this time of flight will be assumed to be negligible. This type of scanning scenario is the kind with which the Electro-Optical Terminal Guidance Branch at Eglin AFB is presently conducting its experiments.

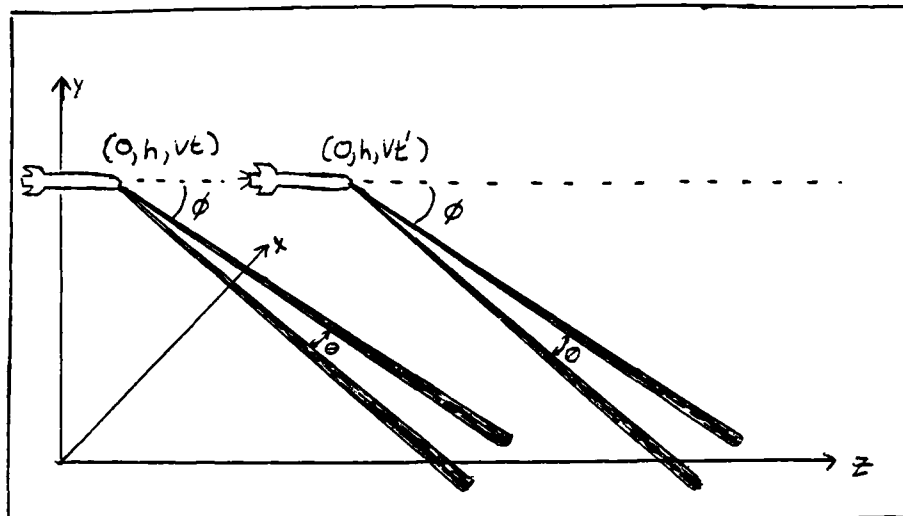


Fig. 1. An Air-to-Ground Missile Raster Scanning with a Laser.

In modeling the scanning of an air-to-ground missile, a paraxial approximation will be used. With the paraxial approximation, all objects of interest are assumed to be near the ground, close to the bore sight of the sensor (which is coaxial with the laser scanner), and to have dimensions that are small compared to the distance to the missile. In mathematical terms, the paraxial case is expressed by the fact that, using the coordinate system of Figure 1, the range depends only on the  $y$  and  $z$  coordinates of the missile and the  $y$  and  $z$  coordinates of the points on the target, not on the  $x$  coordinates.

The paraxial approximation is reasonable in that to give the missile time enough to complete a scan and deter-

mine if the scanned scene contains the target or not, the scanning must not take place at distances much less than 1 km in front of the missile. The width of a typical target, say that of a tank, is less than 10 m, which makes its dimensions much less than the distance, about 1 km, at which the missile is performing its scan. Thus, the paraxial approximation can definitely be used with target sizes on the order of a tank. A scanning distance of 1 km would give a missile traveling at 200 m/sec, 5 sec to form a range scene, detect the target, and drop its submunition on the target. Scanning distances of much less than 1 km would put large demands on the speed of the missile's processor.

#### Formulation of the Mathematics of the Scan

To model the laser scanning of an air-to-ground missile mathematically, one must have a way of representing objects. One can represent a general quadric surface, such as spheres, ellipsoids, paraboloids, hyperboloids, and elliptic cones, with the equation (Protter and Morrey, 1975:230-236):

$$Ax^2 + By^2 + Cz^2 + Dxy + Exz + Fyz + Gx + Hy + Kz + L = 0 \quad (1)$$

The symbols x, y, and z in equation (1) are spatial coordinates of a Cartesian coordinate system, and the coefficients in front of the coordinates are constants determined by the particular quadric surface. Cylinders, cones, and rectangular boxes can also be constructed from one or more of combi-

nations of equation (1), along with appropriate boundary conditions.

The scanning laser beam will be represented by a three dimensional line in what is called the two-point parametric form:

$$x = x_0 + (x_1 - x_0)s \quad (2)$$

$$y = y_0 + (y_1 - y_0)s \quad (3)$$

$$z = z_0 + (z_1 - z_0)s \quad (4)$$

where  $(x,y,z)$  are dependent variables of a Cartesian coordinate system,  $(x_0,y_0,z_0)$  represent the Cartesian coordinates of a point through which the line passes,  $(x_1,y_1,z_1)$  represent the Cartesian coordinates of another point through which the line passes, and  $s$  is the parameter for the equations. The coordinates  $(x_1,y_1,z_1)$  will represent the coordinates of the laser/sensor throughout this paper. The coordinate  $y_1$  will always be the altitude  $h$  of the missile,  $x_1$  will always be equal to  $x_0$  to incorporate the paraxial condition, and  $z_1$  will be determined by the velocity of the missile and the time that it has been traveling. The coordinates  $(x_0,y_0,z_0)$  will represent a point on the ground toward which the scanning laser beam is aimed. Since this is the case,  $x_0$  will equal  $x_1$ ;  $y_0$  will equal zero; and  $z_0$  will be determined by  $z_1$ ,  $h$  and the declination angle,  $\phi$ .

With the specifics of the coordinates of the points  $(x_0,y_0,z_0)$  and  $(x_1,y_1,z_1)$  determined, equations (2) through

(4) reduce to the following equations:

$$x = x_0 \quad (5)$$

$$y = hs \quad (6)$$

$$z = z_0 - hs/\tan(\phi) \quad (7)$$

where  $(x,y,z)$  are dependent spatial variables of the Cartesian coordinate system used,  $x_0$  and  $z_0$  are two of the coordinates defining the scan point on the ground,  $h$  is the altitude of the missile,  $\phi$  is the declination angle, and  $s$  is the parameter for the equations. Figure 2. depicts the geometry used to determine equations (5)-(7).

The scanning line, which represents the scanning laser beam, is swept in the horizontal direction by varying  $x_0$ , and is swept in the forward ( $z$ ) direction by varying  $z_0$ . The ranges of each horizontally swept row of points are placed in a single row of a 256 x 256 range matrix. Each time one of the rows of the matrix is filled, the coordinate  $z_0$  is increased by a set amount and the next matrix row is filled. This procedure is continued until the entire 256 x 256 range matrix is filled. In this manner, the two-dimensional range matrix is formed which holds three-dimensional information about a scanned scene -- the third dimension being stored as range in each of the elements of the matrix.

The point of intersection of the scanning line represented by equations (5)-(7) and an object represented by one or more combinations of equation (1), is determined by

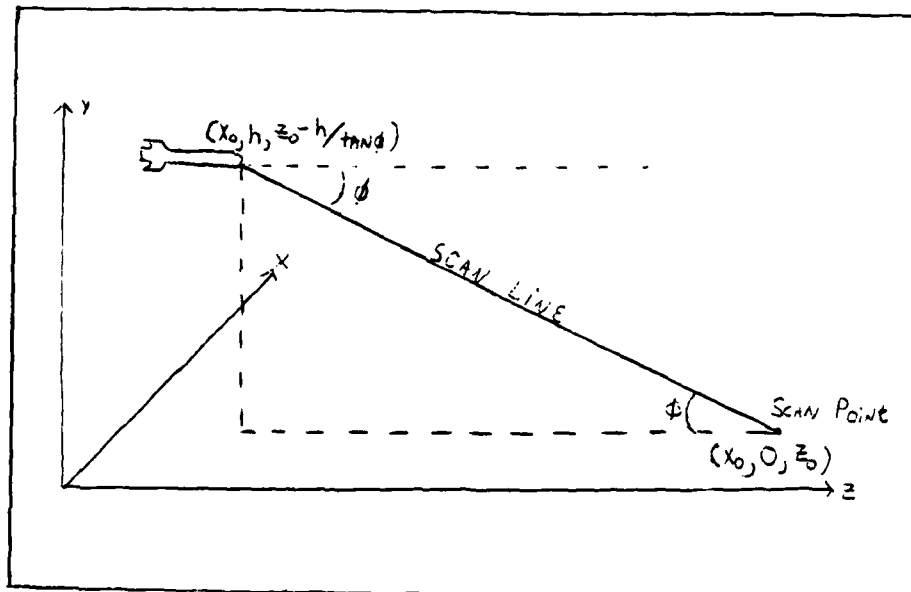


Fig. 2. The Geometric Relationship between the Sensor's Position and the Scan Point.

solving these same equations simultaneously for s. Upon solving for s, the following equation was obtained

$$s = [-Q \pm \sqrt{Q^2 - 4PS}] / (2P) \quad (8)$$

where

$$P = Bh^2 + Ch^2/\tan^2(\phi) - Fh^2/\tan(\phi)$$

$$Q = -2Cz_0h/\tan(\phi) + Dx_0h - Ex_0h/\tan(\phi) + Fz_0h + Hh - Kh/\tan(\phi)$$

$$S = Ax_0^2 + Cz_0^2 + Ex_0z_0 + Gx_0 + Kz_0 + L$$

- A...L = constant coefficients of equation (1)
- $x_0$  = same coordinate used in equation (5)
- $z_0$  = same coordinate used in equation (7)
- h = altitude of the missile
- $\phi$  = declination angle



Once  $s$  is found, it can be substituted back into equations (5)-(7) to determine the coordinates of the intersection point,  $(x,y,z)$ . If the scanning line does not intersect the object, then  $s$  will be imaginary. Equation (8) gives two values for  $s$  which takes into account the fact that, except for tangent points, the scanned line will intersect an object represented by equation (1) at two points. Of course, only one intersection point is realistic and the point with the smallest range to the missile is used.

The intersection point is not, by itself, all that important since it is the range that is stored in each element of the two-dimensional matrix. The range, though, is determined from the intersection coordinates. Using the equations for the intersection coordinates one can obtain the following form for the range:

$$R = h(1 - s)/\sin(\phi) \quad (9)$$

where

$R$  = range  
 $h$  = altitude of the missile  
 $\phi$  = declination angle  
 $t$  = parameter variable

Solving for the intersection coordinates has now been bypassed altogether. If the scanning line misses the object, then the range from the missile to the scan point on the ground will be placed in the range matrix. This "object missed" range value is determined by setting  $t$  to zero in equation (9). This value will always be constant since the

altitude of the missile is constant,  $\phi$  is constant, and the ground is assumed to be flat.

#### The Images That Can Be Formed by the Computer Program

The computer program developed in this research can generate the image of any quadric surface when the coefficients of the surface are entered. In particular, it can generate any size sphere at any position in a Cartesian coordinate system, when given the radius of the sphere and the position of the center of the sphere. The program can also generate cylinders of arbitrary lengths, positions, radii, and angular orientation when these parameters are entered. Besides spheres and cylinders, this program can generate rectangular boxes of arbitrary dimensions and positions. The program can also rotate these boxes through any arbitrary angle in the x-z plane and the y-z plane of the coordinate system depicted in Figure 2.

This computer program can combine any number of these quadric or quasi-quadric surfaces together in one range scene. Thus, one can form a simple model of a tank at any orientation with just four rectangular boxes and a cylinder as is shown in Figure 3. The model tank shown in Figure 3. has the dimensions, obtained from Jane's Armour and Artillery 1983-1984 (Foss, 1984:60-64), of a Russian T-72 tank.

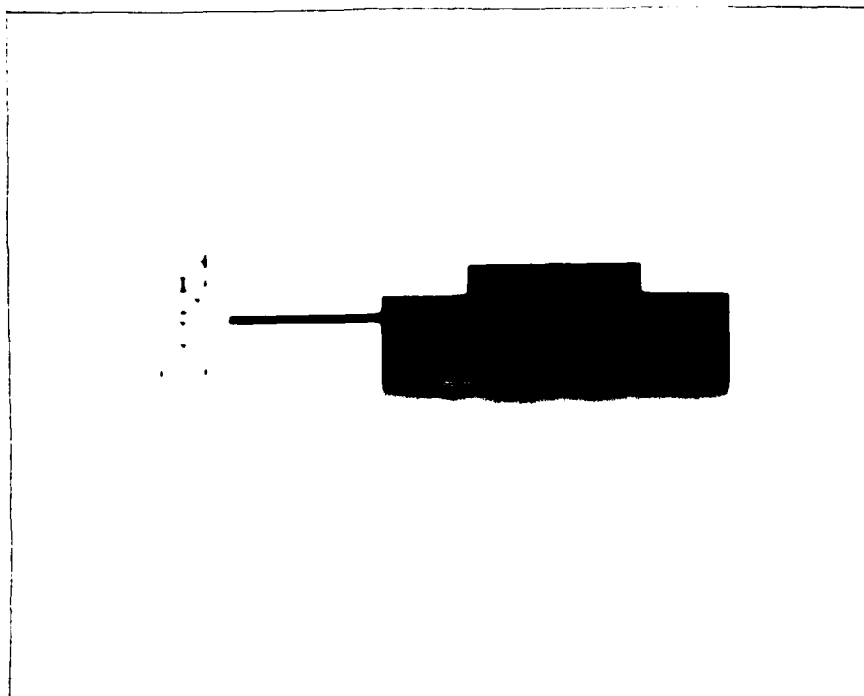


Fig. 3. Range Image of a Model Russian T-72 Tank.

#### Investigating the Physical Parameters of a Range Scan

This same computer program can perform scans, and thereby create range images, of objects at different declination angles and missile heights. Figure 3 was scanned from a missile height of 300 m and a declination angle of  $20^\circ$ . This particular height and declination angle are parameters with which the electro-optical branch at Eglin AFB is currently running its experiments. The  $20^\circ$  declination angle and 300 m missile height would put the range scan about 0.82 km in front of the missile.

This computer program performs a  $256 \times 256$  scan in the x-z plane of Figure 2. The area to which this scan corresponds is variable and is determined by the scaling of the objects in the scan scene and the units in which the objects' dimensions are entered into the program. If the objects are not scaled and their dimensions are entered into the program in meters (m), then the program will perform a  $256 \times 256 \text{ m}^2$  scan in the x-z plane of Figure 2, ranging from  $z = 1 \text{ m}$  to  $z = 256 \text{ m}$  and  $x = -127 \text{ m}$  to  $x = 128 \text{ m}$ . The increment between sampling points in both the x and z directions is 1 m, but the corresponding increment in the x-y plane is  $\tan(\phi)$  meters where, again,  $\phi$  is the declination angle of the scan. The general form for the increment in the y direction, i.e. vertical direction, is given by

$$\delta y = \delta z \tan(\phi) \quad (10)$$

where

$\delta y$  = the increment between sampling points in the y direction  
 $\delta z$  = the increment between sampling points in the x direction  
 $\phi$  = the declination angle of the scan

The tangent factor of equation (10) elongates all vertical components of an object so that when the scanned object is stored in the range matrix  $R(x,y)$ , it is out of proportion with the real object. This could have serious consequences for target recognition if the reference object, by which the scanned object is going to be compared, has not been scaled in like manner. This problem can be solved by scaling the reference object's y components by the same tangent factor that will scale the scanned object's y components. If this scaling is performed, then both the scanned image and the reference object will be distorted. As long as both the scanned object and the reference object are scaled in the same manner, this distortion will not matter.

For this research, all of the scanned objects were also scaled in the directions perpendicular to the vertical direction. With this scaling, all of the distortions caused by the tangent factor of equation (10) were eliminated. Since the reference objects were scaled in the same manner as the other scanned objects, there were no scaling differences between the two groups. Correlating these two groups of images thus produced accurate results.

The first increment size used in this paper was chosen so that the model T-72 tank would fill a large part of the scan matrix yet still be within the boundaries of the matrix. The filling of the scan matrix was desired so that the image would be large enough to display detail on an image processor. This choice of increment size resulted in images like Figure 3. The increment sizes used to form the tank in Figure 3 were, using the coordinate system of Figure 2: 20 cm for the z direction, 7.3 cm for the x direction, and 7.3 cm for the y direction. One can interpret the x and y increment sizes as modeling a laser beam spot of 7.3 cm in diameter. If one interprets the increments in this manner, then the laser scanner would be successively sampling portions of the tank, 7.3 cm in diameter, both in the x direction and the y direction.

The 7.3 cm beam diameter used to form the tank in Figure 3, meant that the vertical part of the hull of the tank was sampled 95 times in the x direction and 32 times in the y direction. In addition to the hull, the top of the turret was sampled 17 times in the z direction. As one can see from Figure 3, this beam diameter size produced a well defined range image.

#### Improving the Modeling of the Laser Scanner

In a real laser scanner, the beam spot from the laser has a Gaussian profile and will average over the area it covers. The range that the beam returns will thus be a

weighted average for that finite area. In modeling this averaging process, another version of the previous program was created. This version still scans in the same manner as before, but now it averages the range values of each of the adjacent four pixels and places the result back into the same four pixels. This modification not only more accurately models the scanning process, but has doubled the effective spot size on the target. Thus, for the case of the beam diameter of 7.3 cm, which was dealt with before, the beam diameter is now 14.6 cm. Figure 4 is a range image of the same model tank shown in Figure 3, but with the averaging process used. One can see from Figure 4 what can be called "ghost" edges on the tank. These ghost edges are caused by the averaging over pixels which belong to both the tank and the background. The result of the averaging, are pixels whose intensity levels are half way between those of the tank and those of the ground. Ghost edges do not occur in actual range images though. To understand the reason for this absence, one needs to understand more of the details of the scan detector.

#### Operation of the Scan Detector.

The scan detector used by the Electro-Optical Terminal Guidance Branch at Eglin AFB, registers a return pulse when the amplitude of the radiation entering it crosses a certain threshold level. Once the detector has been triggered, it stops a digital timer in the missile's processor and from

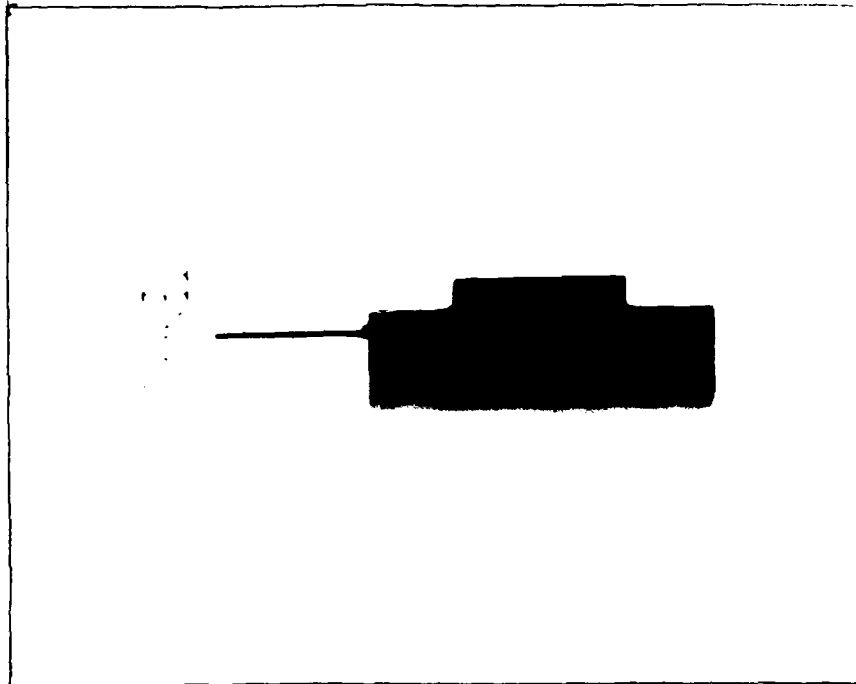


Fig. 4. Range Image of a Model T-72 Tank  
with "Ghost" Edges.



this measured time the range is computed. The timer is not reset until the next laser pulse is fired. Let's say that the beam spot that the laser pulse forms on the target covers an area that has different depth levels. The differing depth levels cause the laser pulse to essentially split into a number of smaller laser pulses, which will enter the detector at different times due to the different distances traveled. If the depth levels do not differ from each other by very much, then the "mini" laser pulses will not be lagging each other by very much upon entering the detector. The amplitude of the first pulse entering the detector might not be enough to trigger the detector. Since the next pulse is immediately behind though, it can build on the amplitude registered in the detector by the first pulse and trigger the detector.

Though the second pulse triggered the detector, the triggering point would have most likely been at an earlier time than if the second pulse had entered the detector by itself. Thus, the time recorded for the whole beam pulse would have been some kind of average between the time the first pulse entered the detector and the time the second pulse entered the detector. Since the measured time is converted into range, the range set for the pixel corresponding to this laser pulse will also be some kind of weighted average.

Of course in discussing the above, the first pulse might have had enough amplitude to trigger the detector and that range value would have represented the range of the pixel. On the other hand, it might have taken three or more of the mini pulses to trigger the detector, and one would have had even more of an averaging of the range. Everything depends on the strength of the reflections, the difference in the levels of depth covered by the pulse spot, and the part of the pulse spot that gets reflected. The latter dependence originates from the fact that at best the beam spot is Gaussian in profile, and thus the center of the spot would have a larger amplitude than at the edge of the spot.

The whole averaging process of the actual laser scanner is very statistical in nature and the part of the computer program developed to model it, models it in the very simplistic manner described in the preceding paragraphs. To model this process any more closely would be very complicated indeed. Now, that the operation of the detector has been discussed the absence of the ghost edges can be treated.

#### Explaining the Absence of the Ghost Edges.

If the area of the target that the laser beam spot covers has depth levels that differ by a large amount, e.g. an edge of a tank, then the so called mini laser pulses will lag behind each other by a large amount. Therefore, if the first mini pulse that enters the detector doesn't trigger it, then by the time the second pulse enters the detector,

most of the signal from the first pulse would have decayed away. This means that the second laser pulse would have nothing upon which to build. Thus, if the second pulse does not have enough amplitude to trigger the detector by itself, then the detector will not be triggered for that whole laser pulse -- unless of course there are more mini pulses entering the detector with large amplitudes. If the detector is not triggered for the whole laser pulse then the corresponding pixel is called a drop out pixel. This will be covered in more detail later.

Usually though, the first mini pulse is the one that will trigger the detector. This explains the absence of ghost edges in actual range images; the range difference between the tank and the background is too large for averaging to take place, and the range value for the tank is the value recorded for that pixel. Again though, the reflectivity of the surfaces that the laser spot strikes and the portion of laser spot that strikes the surfaces will determine whether the range value for the tank or the background is recorded for the pixel.

The major factor determining the point when range averaging ends is the decay time of the detector. This decay time controls the length of time that a signal will stay registered in the detector and thus available for the next mini pulse to build upon. The longer the decay time

the larger the difference in depth levels that will be averaged.

Summarizing, if the levels of depth covered by the laser spot differ by a large amount, then there will not be any averaging over the range values for those levels; only those levels that differ by a relatively small amount will be averaged. If all of the depth levels covered by the beam spot differ by a large amount, then only one, if any, range value for one particular depth level will be recorded. The amount by which depth levels can differ and still be averaged is determined primarily by the decay time of the detector.

#### Eliminating the Ghost Edges.

To reduce the ghost edges as much as possible without eliminating the averaging process altogether, a threshold value was determined which controlled the number of pixels which were averaged. When averaging over the set number of pixels, the pixel set would be placed into another array and ranked ordered from the pixel with the smallest range value to the pixel with the largest range value. This array would then be searched and only the pixels that differed in range from the first pixel in the array, i.e. the pixel with the smallest range, by less than a determined amount would be averaged over. This average range value would then go into all the pixels of the set.

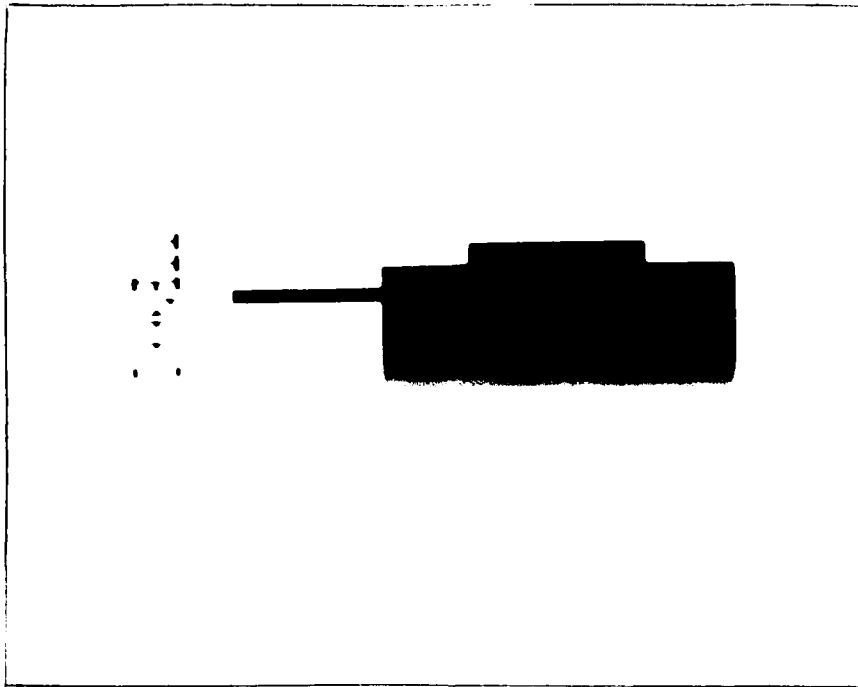


Fig. 5. Range Image of a Model T-72 Tank  
Without "Ghost" Edges.

Averaging in the manner described above, reduced the ghost edges tremendously, but still retained the averaging process. Figure 5 is a range image of a tank formed using the new averaging procedure. The tank in the range image is the same model T-72 tank shown in Figure 4, formed at the same scanning altitude and declination angle. The only major difference between the two figures is the absence of the ghost edges in Figure 5.

#### Increasing the Spot Size on the Target

This averaging over four pixels can be extended to sixteen pixels, thereby increasing the spot size on target by a factor of two. Figure 6 is an example of averaging over sixteen pixels; it is a range image of a slightly improved model of the T-72 tank. This model of the tank was used, because it showed more of the difference that the beam spot makes in the detail of a range image.

The size of the beam spot (on a vertical surface) which was modeled when Figure 6 was formed was 29.1 cm (diameter). This spot size along with the scan altitude and the declination angle, meant that the hull of the T-72 tank was being sampled 48 times in the x direction (using the coordinate system of Figure 2); the vertical side of the tank was being sampled 16 times in the y direction; and that the top of the turret was being sampled 9 times in the z direction.

One can compare Figure 6 with Figure 7, which is a range image of the same model T-72 tank, but which was formed with

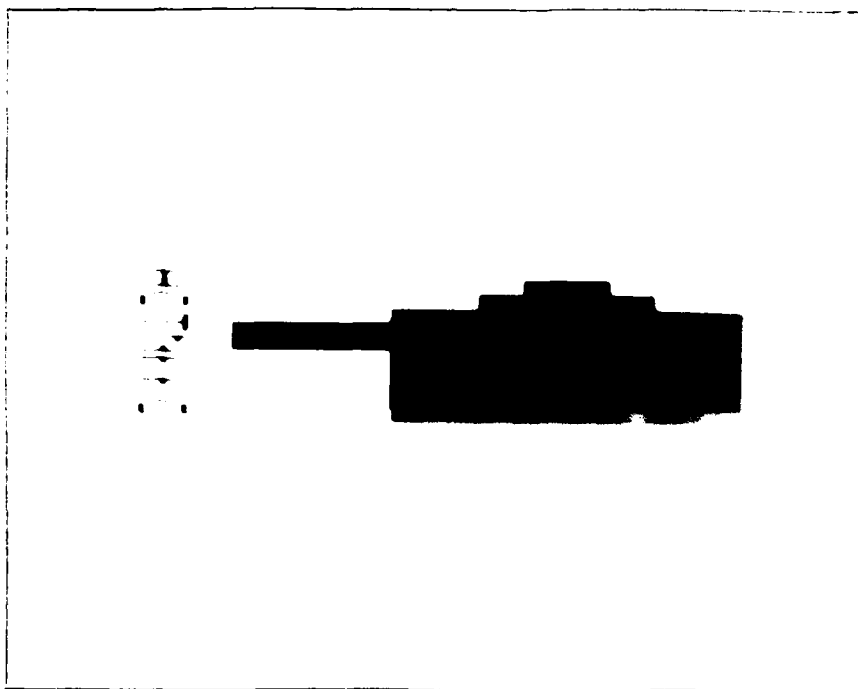


Fig. 6. Range Image of a Model T-72 Tank Formed  
with a Beam Diameter of 29.1 cm.

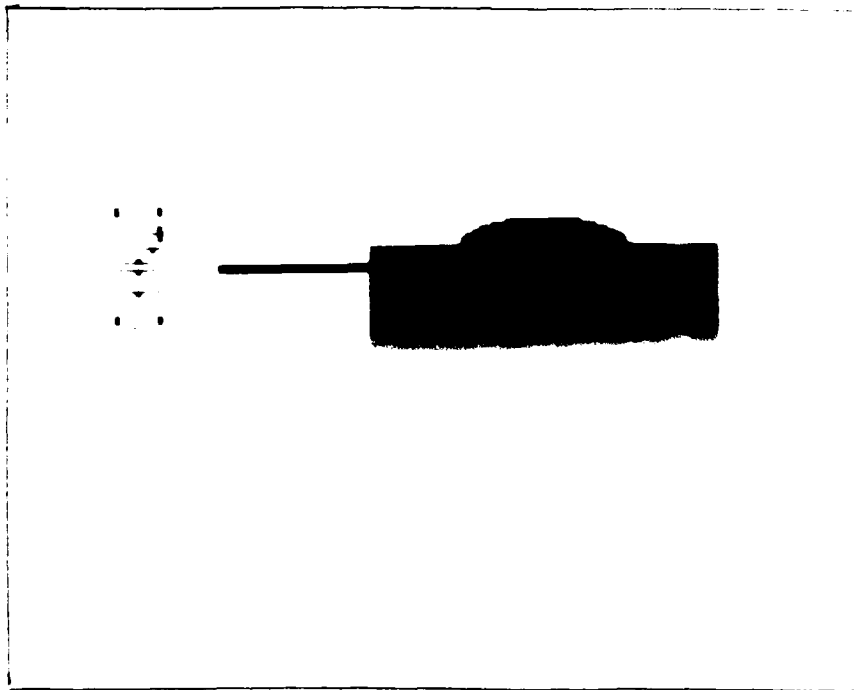


Fig. 7. Range Image of a Model T-72 Tank Formed with a Beam Diameter of 7.3 cm.



a beam diameter of 7.3 cm. The same scan altitude and declination angle were used to form both figures. One can see that by using this larger spot size, one obtains less resolution on the edges of the turret and that the gun barrel's size has been distorted. If the tank had been modeled with surfaces more complicated than planar rectangles and cylinders, one would have also noticed a lack of minute detail on these surfaces, which would have been visible with a smaller beam spot.

Loss of detail in a range scan might not be so bad, since tanks, even of the same model, will have small differences among themselves. These small differences make it harder for the tanks to be recognized. Scanning with a larger beam spot, would hide many of these small differences among tanks and thereby help the missile to recognize them. On the other hand, too large of a beam spot would cause a missile to recognize spurious objects as tanks. Thus, a fine line exists between gathering too much geometric information about a tank and not gathering enough. This subject will be discussed later in more detail.

#### Modeling the Dropout in Range Images

Actual range images formed by laser scanners will not be as perfect as Figures 3 and 7 portray them to be, there will be dropout pixels in the range scenes. These dropout pixels are due to returns that do not have enough amplitude to trigger the detector and to specular reflections that

return amplitudes that are much higher than normal. The specular returns cannot be trusted because the part of the laser beam that is specularly reflected, is weighted much more than the other parts of the returning beam. As a result, the averaging process of the beam spot will not take place and a spurious range value could be placed into the range matrix. This would be especially true, if the beam spot hits an edge of a tank and also specularly reflects from some background object.

The detector for the electro-optical branch at Eglin AFB is set up so that any return above a certain threshold level and below another level are ignored, and some preset range value that can never be realized is put in its place. This preset value is chosen so that every dropout pixel in the range image can be later found when, if any, postprocessing is done. The computer program developed in this research also models this pixel dropout.

The computer program used in this research will randomly degrade, by dropping out pixels, an image of an object by any percentage entered into the program. Logically, what one would do to degrade an image is to select randomly the pixels that are to become dropouts and set the range value in those pixels to a value that can never be realized. Immediately, a range value that is negative or even zero comes to mind as logical value for the dropout pixels. This though,

was only done when the degraded image was going to be repaired.

Since it was desired to view these degraded images, the dropout pixels' ranges were set to the background range, a range value that could be realized. The reason for setting the dropout pixels to the background range value is on account of having to normalize the range values to numbers between 0 and 255. Numbers between 0 and 255 are the only values that the image processor used in this research could handle.

If the dropout pixels had been set to a range value of 0 meters (m), then range values all the way from 0 m to 824 m would have had to been normalized to values between 0 and 255. This would have been acceptable, except for the fact that for a scanned tank, the range values that would be returned would be between about 817 m to 824 m. Thus, when normalized to the 0 to 255 range, the values representing the tank, excluding dropouts, would be between 253 and 255. This would have not allowed much information to be recorded about the tank in the range scene!

If on the other hand the dropouts are represented by the background range value of 824 m, then the whole scanned scene, if there are no more objects in the scene beside the tank, would have range values between 817 m and 824 m. For this case, the tank would be represented by the entire 0 to 255 range, and greater detail would be recorded about the

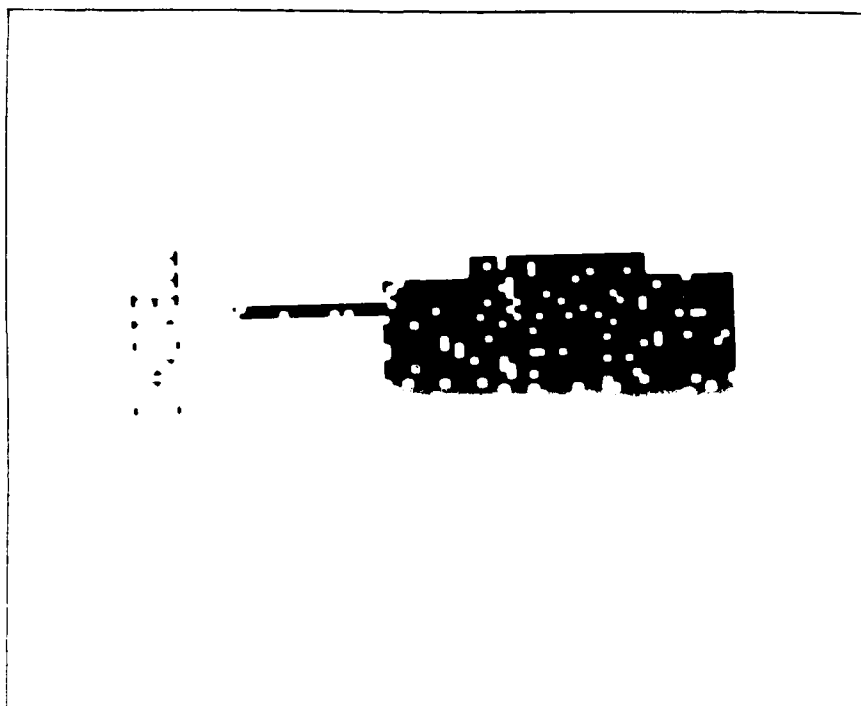


Fig. 8. Range Image of a Model T-72 Tank That Has Been Degraded by 10%.

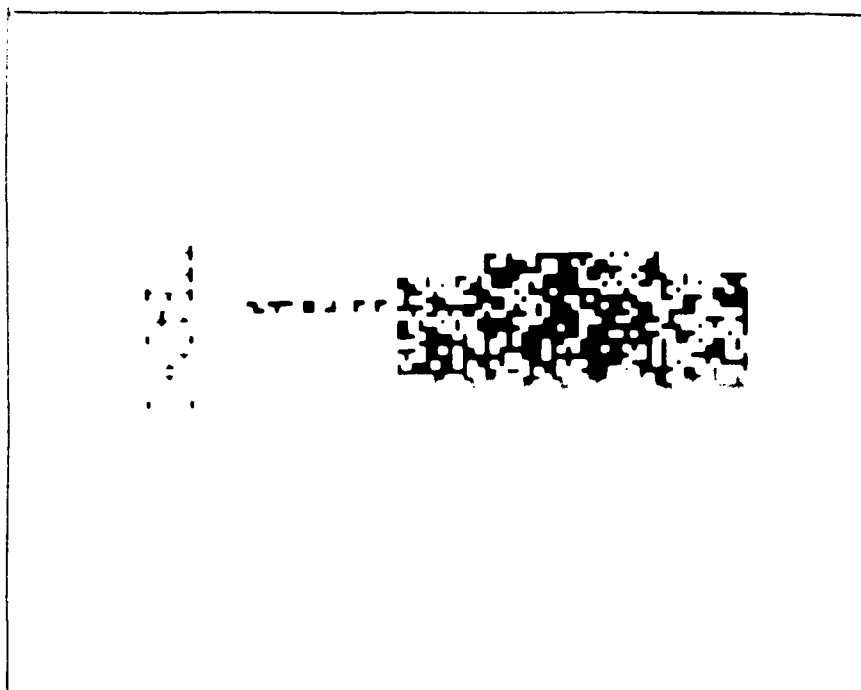


Fig. 9. Range Image of a Model T-72 Tank That Has Been Degraded by 40%.

tank. Figure 8 is an example of a 10% pixel dropout in a range image of a model T-72 tank, and Figure 9 is an example of a 40% pixel dropout in a range image of the same model tank. Both tanks were scanned at an altitude of 300 m, with a declination angle of 20 deg, and a beam diameter, on a vertical surface, of 14.6 cm. As one can imagine from these figures, an automated system designed to recognize tanks out of range scenes, might have a hard time recognizing the degraded tanks as tanks. Thus, a method of repairing the pixel dropouts in range images is needed. This will be especially true when the information in Chapter V is presented.

#### Repairing the Pixel Dropouts

If one is going to repair the pixel dropouts, one does not have to worry about not setting the dropouts' ranges to zero or a negative number, because one's repair algorithm should replace all of these preset numbers with non-zero, non-negative numbers. In fact, the dropouts have to be represented by some range value that can never be realized, if only the dropouts are going to be replaced and not non-dropouts also. The computer program in this research sets the dropouts' range values to 0 when the dropouts are going to be repaired, and to the background range value when it isn't going to be repaired.

The method that this computer program uses to repair the dropouts, i.e. object degradation, is called the median

replacement method. The way this method works is that once the range image of the object(s) is formed, the range matrix is searched for zero range values. Once one of these zero range values is found, the program takes the eight pixels surrounding it and places their range values in a 1 x 8 array. It then ranks orders the array from the smallest range value to the largest. Once the ordering has taken place, the program takes the range value of the fourth element of the array and replaces the dropout pixel's range value with it.

The reason that the median range value is used and not the average is because using the average range value to replace the dropouts would degrade the edges of the object. Edges are degraded by having the dropout pixels replaced with the range value of the ground and not of the tank. This median replacement method will not degrade edges, it will though, if not modified, degrade corners. The replacement procedure was modified slightly, so that the ground's range value would only be accepted as the median value, if all the other range values in the matrix also corresponded to the ground or corresponded to dropouts. If the median value was zero, corresponding to a dropout, the situation was handled in a similar manner.

Every effort is thus made to repair the dropout pixels as best as possible and still preserve edges and corners. Figures 10 and 11 show range images of a tank that have been

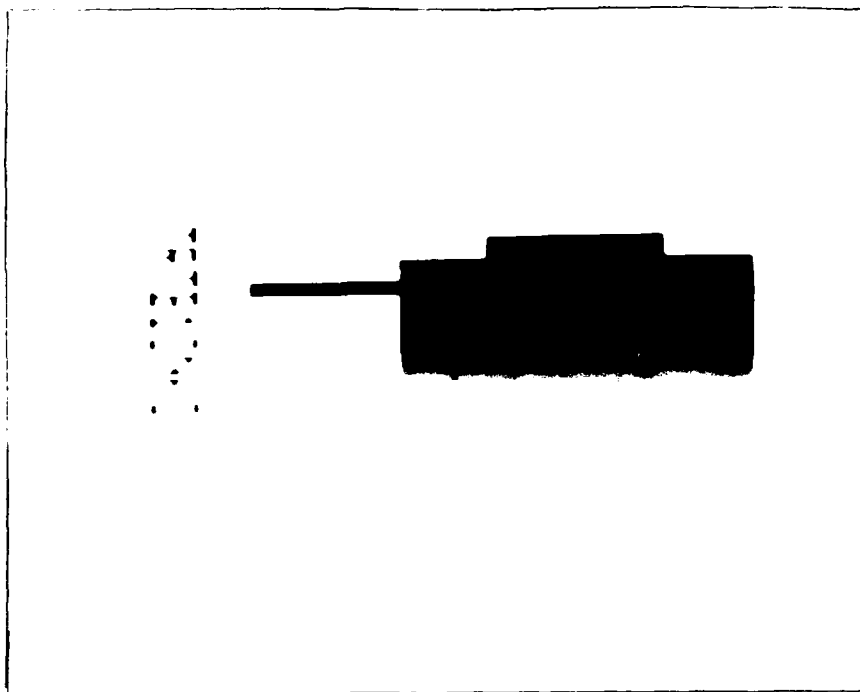


Fig. 10. Range Image of a Model T-72 Tank That  
Has Been Degraded by 10% and Then Repaired.



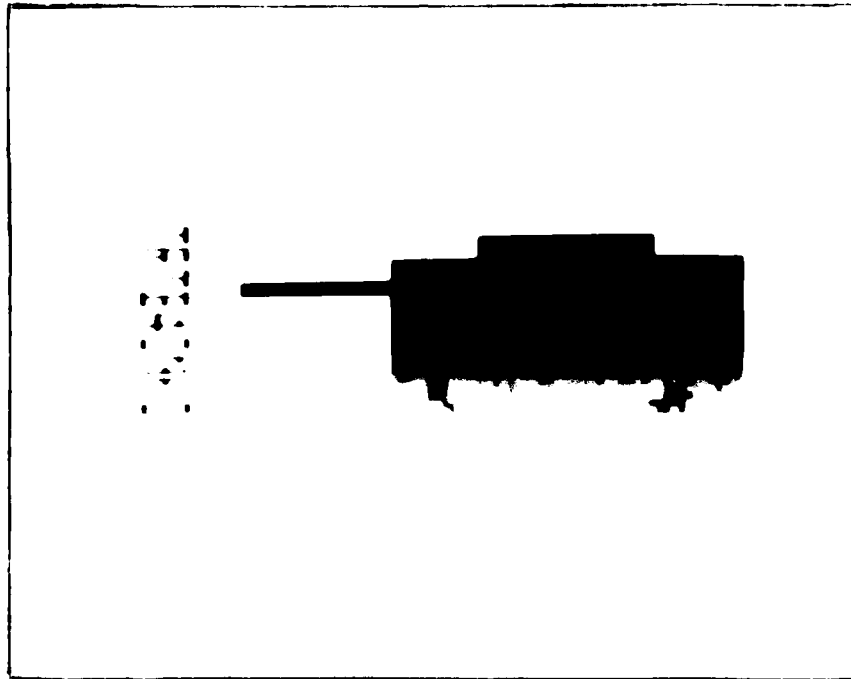


Fig. 11. Range Image of a Model T-72 Tank That Has Been Degraded 40% and Then Repaired.

degraded by 10% and 40% respectively, and then both repaired using the modified median replacement procedure described beforehand. The tanks in these figures were formed with the same parameters used to form the degraded images of Figures 8 and 9. If Figures 10 and 11 are compared with Figures 8 and 9, one can see what a good job the median replacement method performs in repairing the degradations. Only a few pixels in Figure 10 are out of place, and even in Figure 11 only a relative few pixels are out of place. One also can see from Figures 14 and 15 that all the edges have been preserved. Repairing the degraded images will be shown to be very important in Chapter V.

### III. Recognizing Objects from Range Scenes

Now that synthetic range images can be formed, the problem of recognizing objects from those range images must be addressed. One advantage that range images have over other images, e.g. radar, infrared, and intensity images, is that they preserve the three dimensional geometry of the objects in a scanned scene. Many researchers have used this fact in recognizing objects in a range image.

#### Using Range Geometry for Scene Analysis

The main task of geometric recognition techniques is characterizing an object by its geometry and extracting this geometry from a range scene. Many of the researchers in the past have used planes to characterize objects, e.g. Rocker and Kiessling (Rocker and Kiessling, 1975:669-673), and Duda (Duda and others, 1979: 259-271); while others have used cylinders and planes to characterize objects, e.g. Popplestone (Popplestone and others, 1975:664-668); and yet others have used general polyhedra to characterize objects, e.g. Shirai (Shirai, 1973:298-307). The exact type of geometric figure that one uses to characterize an object, depends of course on its general geometric shape, that is whether it is generally planar or curved or both.

The main problem that these researchers have to overcome is one that all researchers in object recognition must

overcome, and that is multiple object orientations. Depending on the orientation of the object, planes will appear to have different dimensions and cylinders different lengths and diameters. Duda (Duda and others, 1979:259-271) has developed a technique of extracting normal views of planes; extracting the relative positions of these planes with respect to one another; and also grouping the planes according to whether they are horizontal, vertical or slanted. As of now, Duda has not tried to use this method for object recognition, nevertheless, the potential is there.

Bjorklund and Loe (Bjorklund and Loe, 1982:46-56) used invariant moments to characterize objects. These moments are invariant with the respect to orientation, scale, and translation in the analytic domain. Using synthetic range images of rectangular boxes, these researchers found that the 3-D invariant moments changed only slightly with orientations ranging from  $0^{\circ}$  to  $105^{\circ}$ . The slight change in the moments were mainly due to quantization error. The two invariant moments that the researchers used though, still differed enough between the two different sized rectangular boxes to allow for discrimination. Using these invariant moments along with other object parameters which can be derived from them, e.g. volume, center of mass etc., the researchers were able to discriminate between one type of object from a background of other objects.

Discriminating between different sizes of rectangular boxes though, is still a long way from distinguishing tanks from background clutter. This brings out one large drawback to all these methods that characterize objects with simple geometric figures and parameters, and that is that they are really only effective in man-made environments. In man-made environments, there are many planar surfaces and simple geometric shapes that can be extracted, but say in a forest there are not. It would not be easy for example to characterize the top of a tree in full bloom with cylinders. There are a lot of potential targets in man-made environments though, so these methods do deserve further attention.

There is also one measure of merit for these geometric scene classification methods, that this researcher could not find -- time of computation. The time that it takes to analyze a range scene and to classify the objects in that scene as targets or non-targets, is very important when one has only about 5 sec to complete the scene analysis. Thus, the computation intensities of these methods need to be analyzed, so that their potential application for use in air-to-ground missiles can be more fully evaluated.

#### Using Correlation for Object Recognition

The method of object recognition that will be used in this paper is that of correlation. The two dimensional correlation of the function  $f(x,y)$  with another function  $g(x,y)$  is indicated by  $*$  and defined by the equation

$$f(x,y) * g(x,y) = \iint_{-\infty}^{\infty} f(a+x, b+y)g(a,b)da db \quad (11)$$

where  $a$  and  $b$  are dummy variables of integration and  $x$  and  $y$  are spatial variables. The correlation process is very similar to convolution except that there is no folding of the function  $g(x,y)$  about the axis (Gaskill, 1978: 172). In this manner, a correlation gives the area of the product of the two functions  $f(x,y)$  and  $g(x,y)$  at each point  $(x,y)$ , as the function  $f(x,y)$  is moved in the  $x$ - $y$  domain. For the case of range images,  $g(x,y)$  would represent the range scene, and  $f(x,y)$  would represent the reference target that one is looking for in the range scene.

If the two functions  $f(x,y)$  and  $g(x,y)$  are very similar, then one will obtain a very large peak at the point where  $g(x,y)$  is centered. If the two functions are very dissimilar, then the opposite is true -- there will not be any pronounced peak in the correlation plane. Since a very fast recognition method is needed in air-to-ground missiles, it would be very advantageous to use the peak correlation value as a measure of "goodness" of the correlation, i.e. how well an object in the range scene is similar to the reference object. Of course goodness is relative, and each range scene's peak correlation value should be compared to that of the reference object's autocorrelation, i.e correlation with itself. The closer the peak value is to that of the autocorrelation, the more similar the object in the range image is to the reference target.

### Implementing the Correlation Digitally.

One of the advantages of using correlation as a method of object recognition, is that it can be performed both optically (Goodman, 1968:171-184) and digitally. In this research all of the correlations were performed digitally with a Fast Fourier Transform (FFT). An FFT is a computer algorithm which digitally performs a Discrete Fourier Transform (DFT) very quickly. With a DFT, a Fourier transform in one dimension, described mathematically by the following equation:

$$F(f_x) = \int_{-\infty}^{\infty} f(x) \exp(-i2\pi f_x x) dx \quad (12)$$

where

$f(x)$  = some function of the spatial variable  $x$   
 $i = \sqrt{-1}$   
 $F(f_x)$  = the Fourier transform of  $f(x)$  which is now a function of the frequency variable  $f_x$

becomes a DFT with the following form (Brigham, 1974:98):

$$F(n/(NT)) = \sum_{k=0}^{N-1} f(kT) \exp(-i2\pi nk/N) \quad (13)$$

where

$F(n/(NT))$  = the discrete Fourier transform of  $f(kT)$  and is a function of the spatial frequency  $n/(NT)$   
 $f(kT)$  = the function sampled at  $kT$   
 $k$  = the dummy summation variable  
 $N$  = the total number of times that the function  $f(x)$  is sampled  
 $T$  = the period at which the sampling takes place  
 $n$  = the frequency counting variable which covers the range  $n = 0, 1, \dots, N-1$

The discrete inverse Fourier transform is analogous to equation (13). The particular FFT algorithm used in this research to implement the DFT was one developed by Cooley and Tukey (Cooley and Tukey, 1965:297).

The correlation can also be performed with Fourier transforms by using the correlation theorem (Brigham, 1974: 66-68), which can be stated mathematically as the following:

$$z(x,y) = FT^{-1}[G(f_x,f_y)F^*(f_x,f_y)] \quad (14)$$

where

$z(x,y)$  = the 2-D correlation  
 $FT^{-1}$  = the inverse Fourier transform operation  
 $G(f_x,f_y)$  = the Fourier transform of the function  $g(x,y)$   
 $F(f_x,f_y)$  = the Fourier transform of the function  $f(x,y)$   
 $F^*(f_x,f_y)$  = the complex conjugate of  $F(f_x,f_y)$

A discrete correlation has the same form as equation (14), one just replaces the continuous transforms by their discrete counterparts, and the functions by matrices containing sampled points of the functions. Thus, a correlation can be performed digitally by performing an FFT on  $f(x,y)$  and  $g(x,y)$ , multiplying the resulting arrays element by element, and then performing an inverse FFT on the result. Although three FFTs and an array multiplication have to be performed, this is usually a lot faster, due to the speed and efficiency of the FFT, than computing the correlation directly (Brigham, 1974:119).

There is a problem with using equation (14) or its discrete counterpart for object recognition; it does not take



into account the energies of the two functions being correlated. The functions that will be correlated in this paper are range images, so the energy of a range image will be defined to be

$$\text{energy} = \sum_{i=1}^{256} \sum_{j=1}^{256} R(i,j) \quad (15)$$

where  $R(i,j)$  is the "i"th, "j"th element of the range matrix which contains the range value for each scanned point in a range image. To account for the differing energies of range images, each correlation in this paper will be divided by the product of the energies of the range images being correlated. In this manner, the sizes of the objects in the range images will not have an effect on the correlation's peak value. This is important since the correlation peak will be used for recognition.

#### Testing the FFT.

In order to test the FFT, range images of two simple functions were formed by the range imaging program. The first range image formed was of a 2-D rectangle function (Gaskill, 1978:67) with a height of 1 unit and sides of 20 units. The second range image formed was of a cylinder function (Gaskill, 1978:71-72) with a height of 1 unit and a radius of 10 units. Since these two functions were scanned with an angle of 20 deg, their range images were not true rectangle and cylinder functions, but they were close. Also since these objects were not sampled continuously but dis-

cretely, the range image of the cylinder function was not perfectly cylindrical. It should be close enough for the testing of the FFT though. Figures 12 and 13 are range images of the rectangle function and the cylinder function respectively. From these figures one can see the effect of scanning with the  $20^\circ$  declination angle -- the front edges are not as sharply defined as the other edges. The finite sampling of the cylinder function is also clearly shown in Figure 13.

The log-magnitudes of the FFTs of the the rectangle function and the cylinder functions are shown in Figures 14 and 15 respectively. The highest peaks in both of the graphs shown in Figures 14 and 15 have been normalized to one. These figures show clearly that the computer program's FFT routine is working correctly, for Figure 14 is that of 2-D sinc function (Gaskill, 1978:68-69) which results when a Fourier transform is performed on a 2-D rectangle function; and Figure 15 is that of sombrero function (Gaskill, 1978: 72-73) which results when a Fourier transform is performed on a cylinder function.

Figure 16 is evidence of the usefulness of the FFT, for it displays the Fourier transform of an elongated cylinder function, or what could be called an ellipse function. The Fourier transform of this "ellipse" function would prove very hard to compute analytically, even though something like the result shown in Figure 16 would be

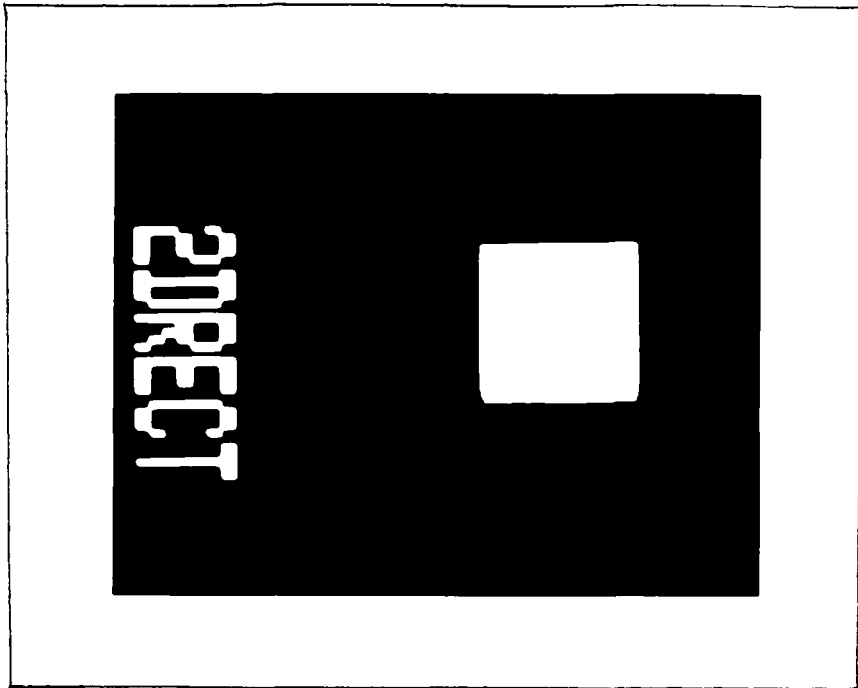


Fig. 12. Range Image of a 2-D Rectangle Function.

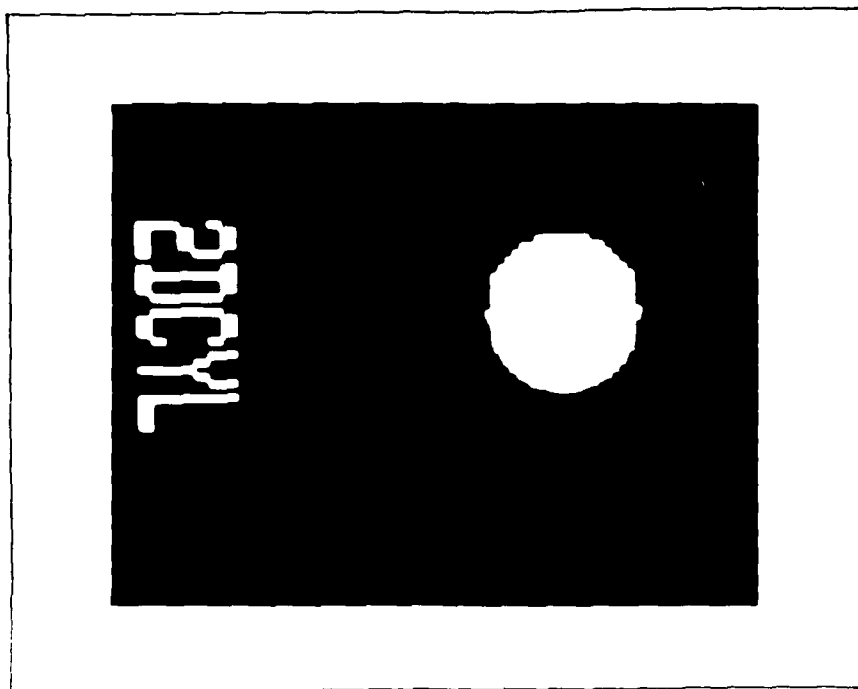


Fig. 13. Range Image of a 2-D Cylinder Function.

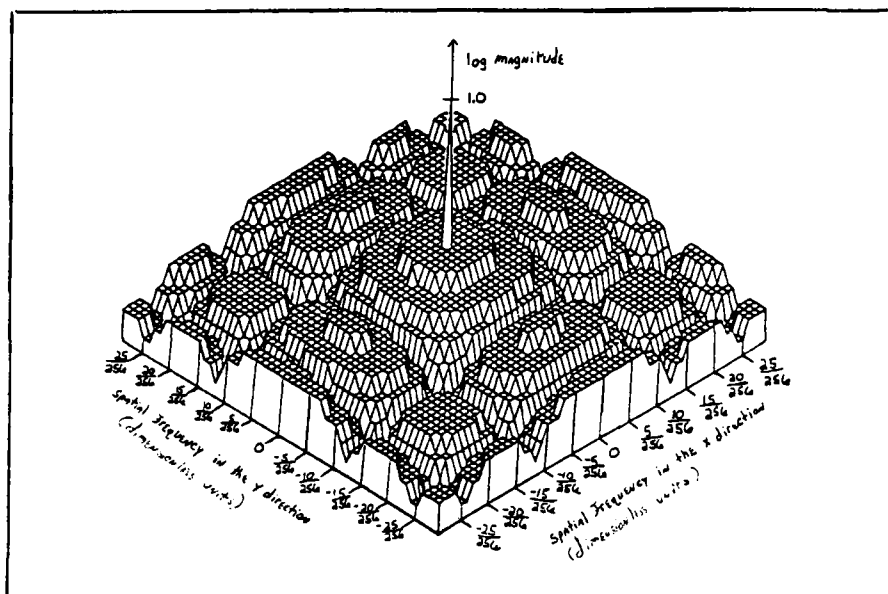


Fig. 14. FFT Log-Magnitude of the Rectangle Function.

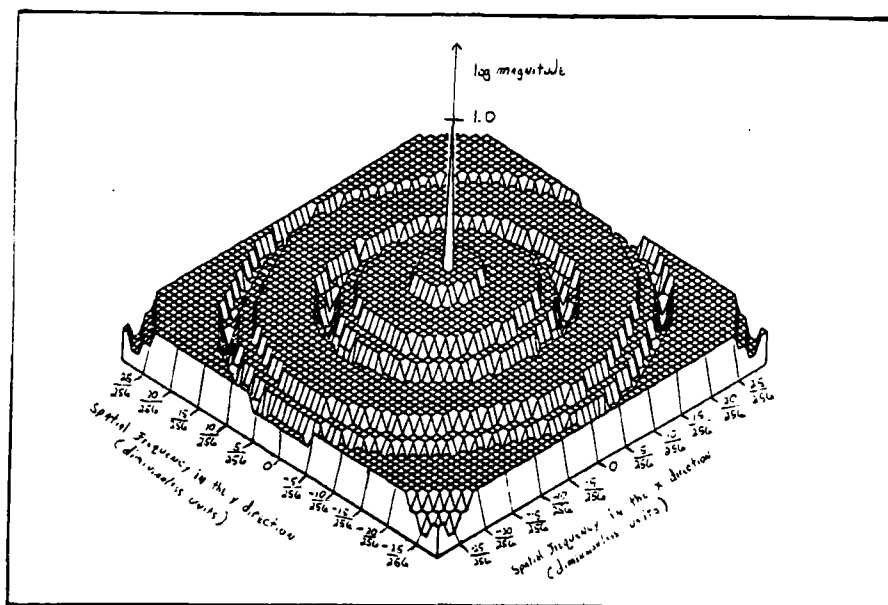


Fig. 15. FFT Log-Magnitude of a Cylinder Function.

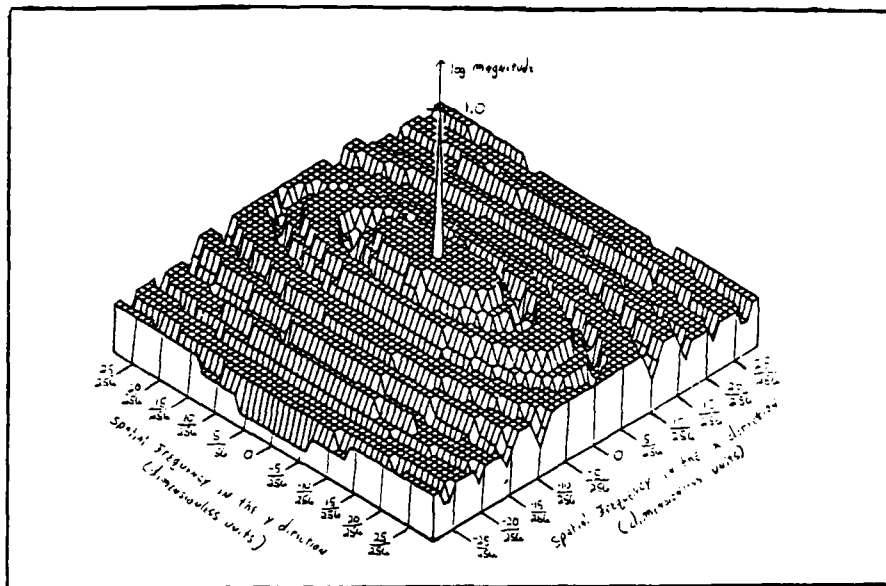


Fig. 16. FFT Log-Magnitude of an Ellipse Function.

expected. The FFT routine, on the other hand, makes calculating the Fourier transform of this ellipse function and other much more complex objects, relatively simple. On top of the ease with which the FFT can calculate Fourier transforms, it can calculate them in a matter of a few seconds. Considering just these two aspects of the FFT, makes it a very useful and worthwhile tool.

#### Testing the Correlation Routine of the Computer Program.

To test the computer correlation routine, the 2-D rectangle function of Figure 12 was correlated with itself. The result of the correlation is shown in Figure 17 with

the peak normalized to a value of one. Figure 17 can be compared with the form of an Optical Transfer Function (OTF) of a square exit pupil, which Goodman (Goodman, 1968:117-119) computes in his book on Fourier optics. The reason that the OTF of this pupil function has the same form as the correlation of the 2-D rectangle function, is because the OTF can be geometrically interpreted as the area of overlap between two displaced pupil functions, divided by the total area of the pupil function (Goodman, 1968:116-117). Figure 18 displays the graph that Goodman has of the OTF of a square exit pupil. Except for the finite number of amplitude levels displayed in Figure 17, Figures 17 and 18 have close to identical forms. The degree of similarity between these two figures gives credence to the computer program's ability to perform correlations.

To further test the correlation routine of the computer program, the cylinder function of Figure 13 was correlated with itself. The graph of the correlation turned out very similar to the graph of the rectangle's autocorrelation, even though the functions were very different in shape. This graph was also almost identical to the OTF that Goodman obtains for a circular pupil function (Goodman, 1968:110-120). Thus, this added proof confirms that the program's correlation routine is performing correctly. The next step is to see how the correlation performs as an recognition routine.

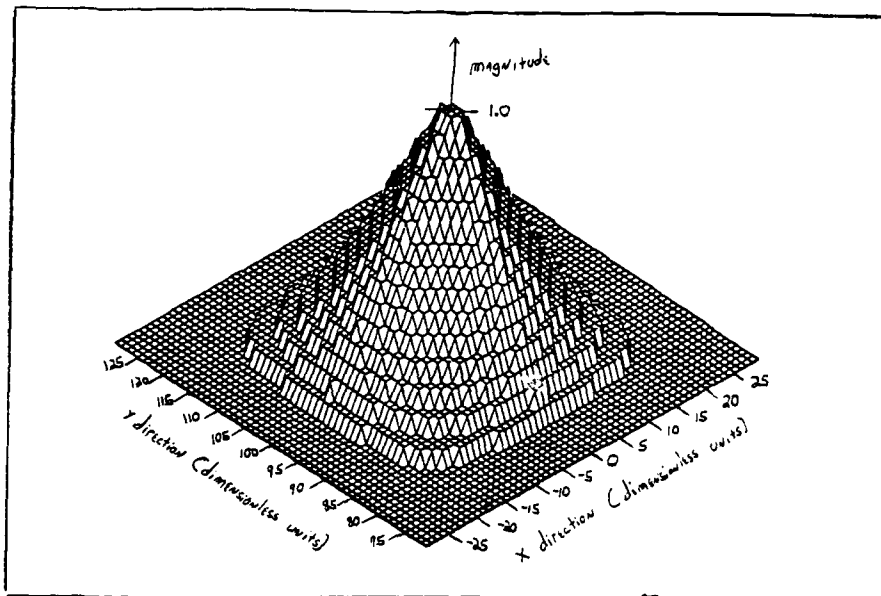


Fig. 17. Autocorrelation of the Rectangle Function.

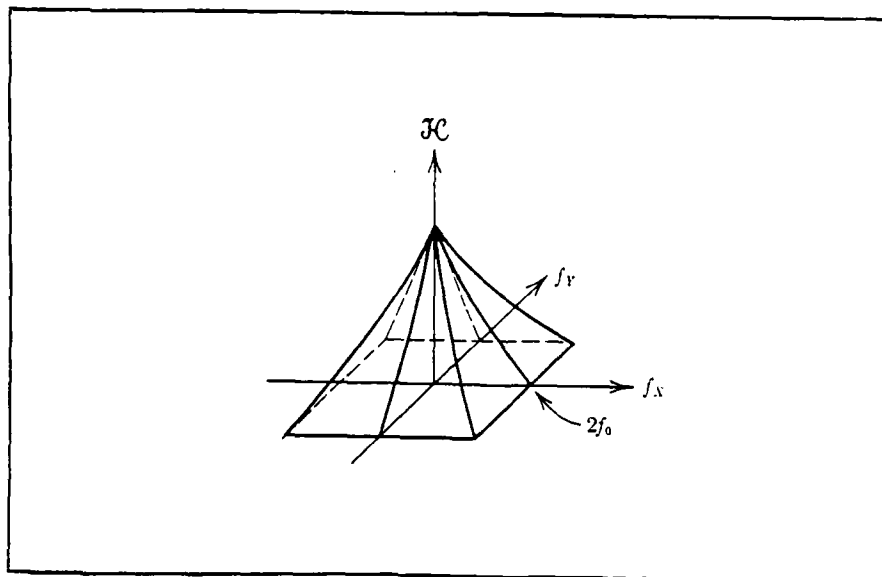


Fig. 18. OTF for a Square Exit Pupil.



#### Correlating the Rectangle and the Cylinder Functions.

The 2-D rectangle function and the cylinder function have very different shapes and thus should test the distinguishing ability of the correlation adequately. Using the rectangle function as the reference object, the range images of the cylinder function and the rectangle function were cross correlated. The result is displayed in Figure 19, where the entire correlation has been divided by the normalization factor that was used when the rectangle function was correlated with itself. With the division, the best result that the correlation can now produce is one, i.e. if the rectangle function were to be identical in form with the cylinder function. The worst result that the correlation can produce is zero which would be the case if the cylinder function and the rectangle function had no similarity at all (impossible).

The correlation peak of Figure 19 has an amplitude of 0.8317. One can also see from Figure 19 that this correlation has a form very similar to the rectangle function's autocorrelation depicted in Figure 17. The autocorrelation of the rectangle function, the autocorrelation of the cylinder function, and the correlation of cylinder function with rectangle function all have very similar forms. The form, though, of the correlation is not being used in this research as a measure of similarity, the peak correlation value (correlation coefficient) is. The value 0.8317 is a very high

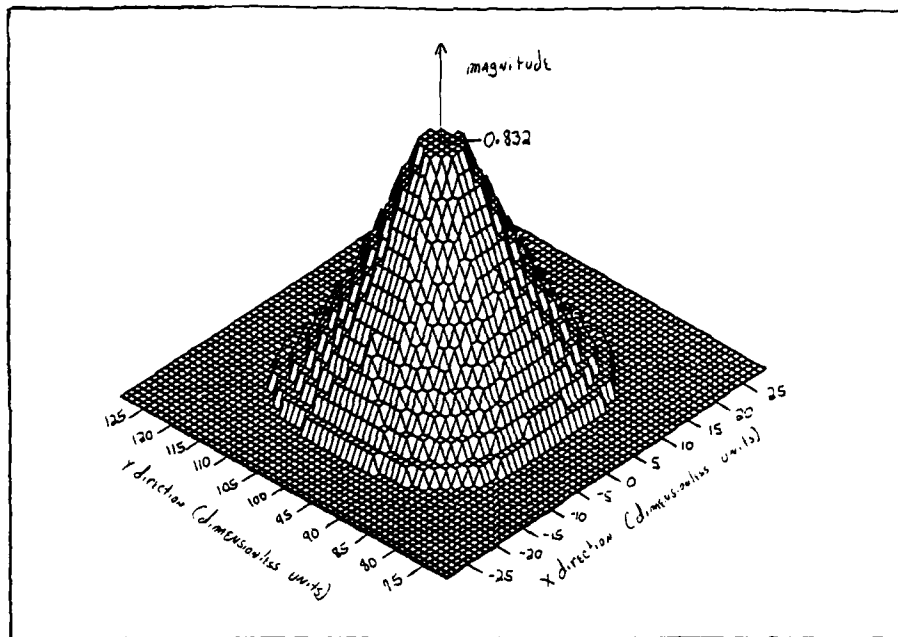


Fig. 19. Correlation of the Cylinder Function with the Rectangle Function.

correlation coefficient, yet the rectangle function and the cylinder function have very different shapes. These two functions do have, though, similar areas distributed in similar manners. As was stated in the beginning of this chapter, a correlation produces both area and shape information about the functions being correlated. It is this area of the product that is producing the high correlation -- even though the two functions have quite different shapes. If there was some way of retaining the functions' shape information without retaining their area information, this "too high of a

correlation" problem could be solved. Fortunately, there is a way to accomplish this very feat.

#### The Advantages of Edge Enhancement.

Many times one wants to simplify an image as much as possible but still retain its distinguishing characteristics. One way of emphasizing an object's important features is edge enhancement. Edge enhancement preserves an object's shape while eliminating much of its area information. This greatly simplifies the object while still retaining its most distinctive feature, i.e. its shape. A gradient filter was implemented in this research to perform the edge enhancement on the range images.

The magnitude of the gradient of a function gives the magnitude of the greatest change in the function, at the point where the gradient is taken. Thus, when a gradient filter is performed on an image, the filter emphasises all points in the image where there are changes in the intensity. At the same time, the filter sets all of the points to zero where there is no change in the intensity. As a result of the gradient filter, edges are emphasized and most of the area of the object is eliminated. This gradient filter was implemented in the frequency domain after the Fourier transform had been performed on the range image. The manner in which the filter was put into effect, was by multiplying every spatial frequency component of the image by its own x and y frequency.

The reason that this procedure serves as a gradient operator can be explained via the discrete inverse Fourier transform. The 1-D inverse Fourier transform is represented digitally by the following discrete inverse Fourier transform:

$$f(k) = 1/N \sum_{n=0}^{N-1} F(n/N) [\exp(i2\pi nk/N)] \quad (16)$$

where

$f(k)$  = the function in the spatial domain  
 $F(n/N)$  = the Fourier transform of  $f(k)$   
 $k$  = the digital equivalent of the spatial variable  
 $i = \sqrt{-1}$   
 $n$  = the counting variable which for our case serves as the spatial frequency  
 $N$  = the total number of sample points taken of the function

If one takes the derivative of equation (16) with respect to  $k$ , i.e. the digital equivalent of taking the derivative of the inverse Fourier transform with respect to  $x$ , then one will obtain the following equation:

$$f'(k) = 2\pi i / N^2 \sum_{n=0}^{N-1} n F(n/N) [\exp(i2\pi nk/N)] \quad (17)$$

where  $f'(k)$  is the derivative of  $f(k)$  with respect to  $k$ , and all of the other variables are defined in the same manner as in equation (16). From equation (17) one notices that every frequency component has been weighted by " $n$ ". Since " $n$ " can be interpreted as the spatial frequency, multiplying each frequency component by its own frequency is equivalent, within a constant factor, to taking the spatial derivative of the function.

Correlating the Edge Enhanced Rectangle and Cylinder Functions.

Figures 20 and 21 are range images of the edge enhanced 2-D rectangle and cylinder functions respectively. In these two figures the back edges of the functions are emphasized more than the front edges, and the corners are emphasized most of all. The reason for the existence of the first phenomenon is because of the  $20^\circ$  declination angle with which the functions were scanned. Scanning with a declination angle other than  $0^\circ$  and  $90^\circ$  creates a greater discontinuity in the range for the back edges of functions than the front edges. Since large discontinuities in the intensity, i.e. range, of an image are emphasized more when edge enhanced than smaller discontinuities, the back edges are emphasized more than the front edges. In the case of corners, the intensity is changing drastically in two directions, whereas for an edge the change in intensity is only in a single direction. Thus, when edge enhanced, the corners will be emphasized roughly  $\sqrt{2}$  times as much as an edge.

The effect of edge enhancing on the graph of an FFT is shown in Figure 22, where the log-magnitude of the rectangle's enhanced FFT has been plotted. The highest peak in this figure has been normalized to one. Upon comparison of Figures 22 and 14, the most noticeable difference between the two figures is the absence of the dc component in Figure 22. This absence is logical since the dc component has a fre-

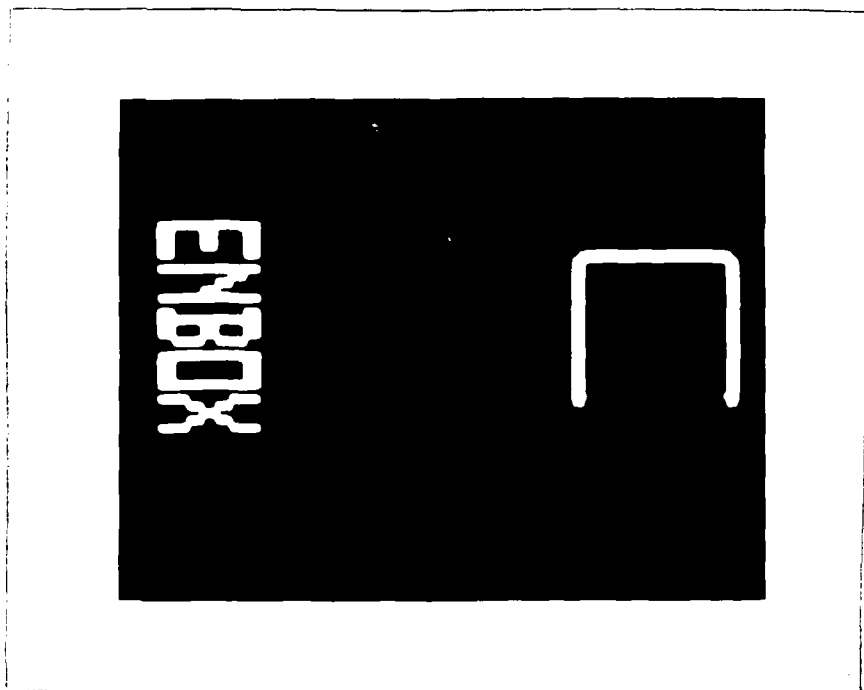


Fig. 20. Enhanced Range Image of the Rectangle Function.

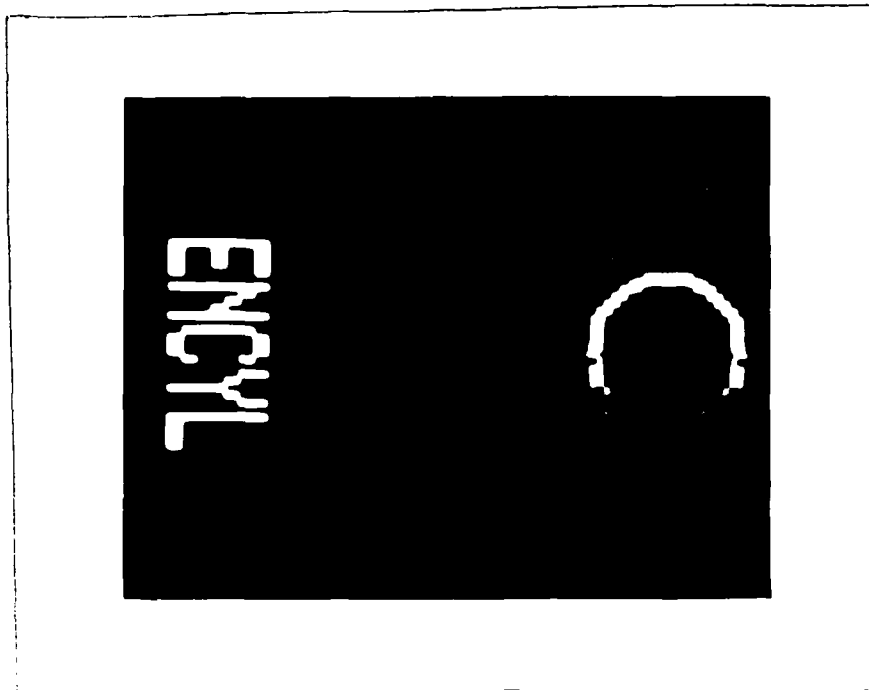


Fig. 21. Enhanced Range Image of the Cylinder Function.

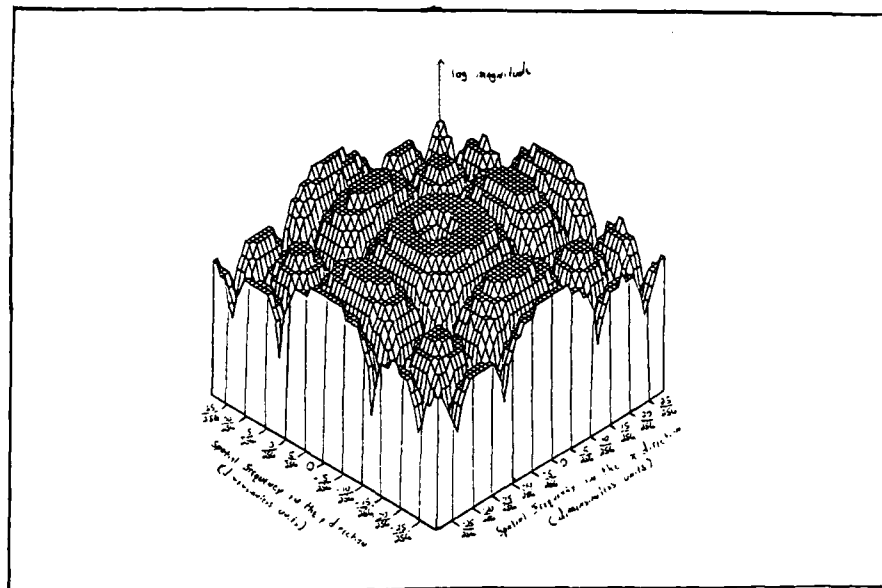


Fig. 22. Log-Magnitude of the Enhanced FFT of a Rectangle Function.

quency of zero, and every frequency component is being weighted by its own frequency. It is hard to distinguish any more differences between the two graphs, except the difference that the normalization causes. There are major differences though, as Figures 20 and 21 attest.

Figures 20 and 21 show that the shapes of the two functions have been preserved but that much of their area information has been eliminated. Thus, these two edge enhanced functions should prove to be very adequate in testing the theory, that edge enhancing should improve a correlation's "object distinguishing ability". Figure 23 is a graph of the autocorrelation of the edge enhanced 2-D rec-



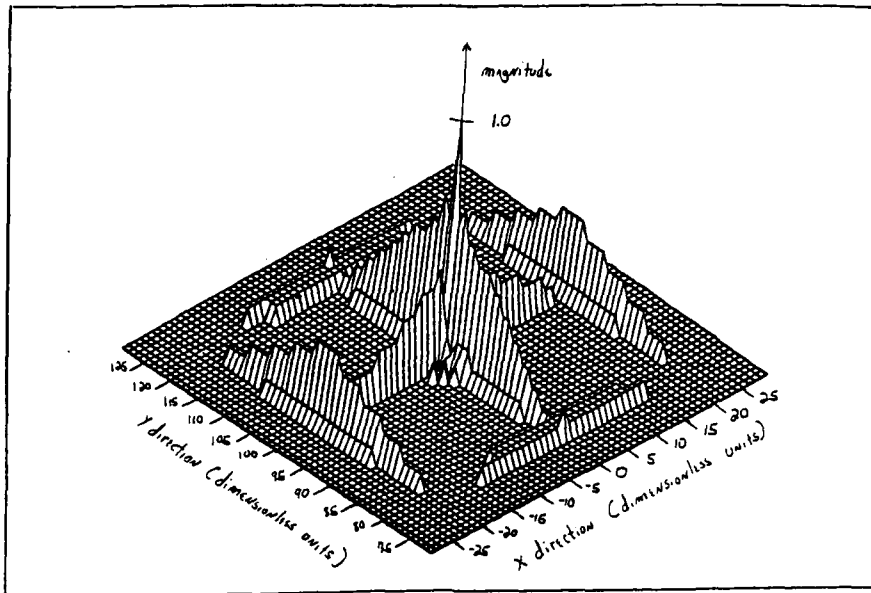


Fig. 23. Autocorrelation of the Enhanced Rectangle Function.

tangle function of Figure 20. Again, the largest peak in the correlation has been normalized to one. In Figure 23 the outline of the rectangle function itself is easily seen, proving that with edge enhancement a correlation emphasizes an object's shape more than its area. One can see upon comparing Figure 23 with Figure 17, that much of the area information has indeed been eliminated with edge enhancing. Similar results were found for the autocorrelation of the enhanced cylinder function. It can therefore be concluded that a correlation of edge enhanced objects utilizes the objects' shapes more than their area information.

The last step in analyzing the effect of edge enhancement on the correlation process, was to correlate the edge enhanced rectangle and cylinder functions of Figures 20 and 21 respectively. For the correlation, the rectangle function was used as the reference function, and the entire correlation was divided by the factor used to normalize its autocorrelation. The result of the correlation is shown in Figure 24. Upon examining Figure 24 one can see that a combination of the two functions' shapes have been recorded, without including most of their area information. The most important aspect, though, about the correlation of Figure 24 is that its correlation peak has a magnitude of 0.1730. Before edge enhancing the two objects, the correlation of the rectangle and cylinder functions produced a peak magnitude of 0.8317. Thus, edge enhancing produces a significant improvement in the correlation's distinguishing ability. All range images used in future correlations will be, from this point on, edge enhanced.

#### Mapping Intensity to Height.

Now that the utility of edge enhancement has been established, its mapping to intensity needs to be more thoroughly explored. To find just exactly how the pixels of vertical and horizontal enhanced edges map to intensity, a rectangular box was scanned using the range imaging program. The box had a width (along the x axis of Figure 2) of 2 m, a depth (along the z axis) of 4 m, and a height of 4m. Once

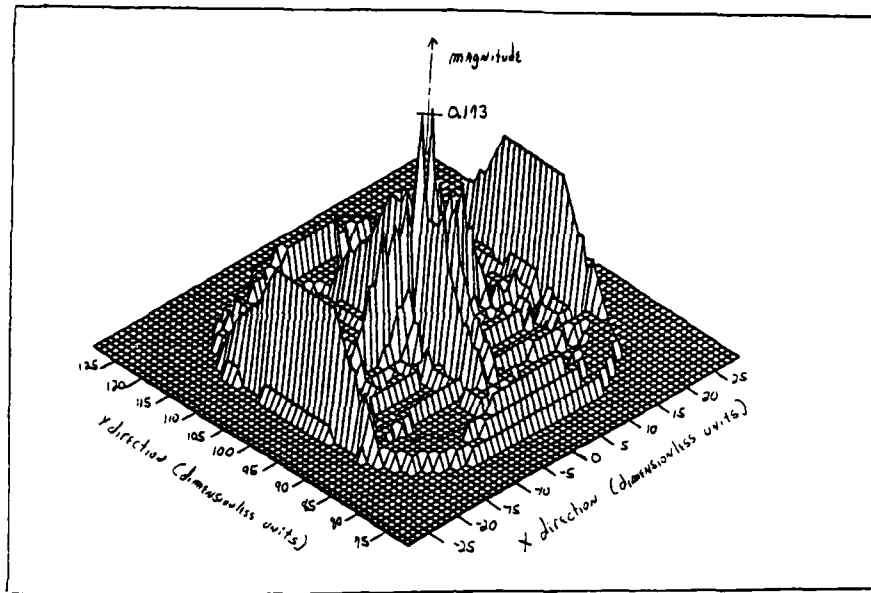


Fig. 24. Correlation of the Edge-Enhanced Cylinder Function with the Edge-Enhanced Rectangle Function.

the box had been scanned and its range image edge enhanced, the pixel levels of the right vertical edge of the enhanced box were plotted versus their corresponding heights. The result of this plot is shown in Figure 25. A pixel level of 0 corresponds to the lowest intensity in the edge enhanced image and 255 corresponds to the highest.

As one can see from Figure 25, the relationship between pixel level, which is an indicator of the intensity of the pixel, and height is linear. The graph in Figure 25 is only valid for edges though, -- for corners, the change in excitation is in two directions so that they will map to pixel levels roughly  $\sqrt{2}$  times as large as edges located at the

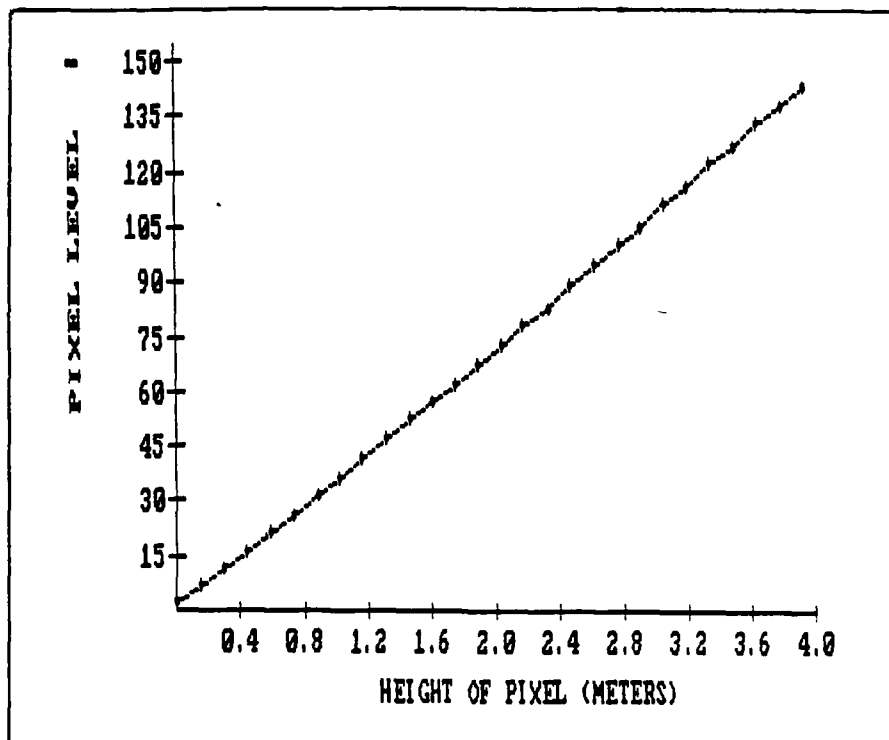


Fig. 25. Pixel Level vs. Pixel Height for Bidirectional Edge Enhancement.

same height. As an example, at a height of 4 m the front right edge of the scanned box has a pixel value of 148, but the back right hand corner of the box, which is also at a height of 4 m, has a pixel value of 255. Thus, this corner pixel value was mapped to a value 1.7 times the pixel value of the edge, both of which were at the same height.

The pixel levels used in Figure 25 were normalized to the range of 0 to 255 so that the enhanced image could be viewed on an image processor. The actual values that 0 and

255 correspond to are  $3.443 \times 10^{-3}$  and  $3.282 \times 10^3$  respectively. This means that the pixel belonging to the edge at the height of 4 m has an actual pixel level of  $1.905 \times 10^3$ . Now, the 4 meter height of the edge pixel is not what causes it to map to this particular pixel level. On the contrary, it is the intensity, i.e. range, changing abruptly by a fixed amount at this edge pixel that causes it to map to this pixel level. Using the geometry, this height of 4 m is found to correspond to a change in the range of 58.5 m at the edge pixel. Thus, every time there is an abrupt change in range of 58.5 m in one direction, a non-normalized pixel level of  $1.905 \times 10^3$  should be mapped to that pixel. This is also true for horizontal edges. As proof, the back horizontal edge of the box is at a height of 4 m and all of the pixels, except for the ones close to the corners, have pixel levels ranging from  $1.893 \times 10^3$  to  $1.905 \times 10^3$ .

The trouble with trying to predict the pixel level to which an edge will map, is that the height of the edge is really not what determines the mapping. It is the range discontinuity that determines the mapping. Thus, the enhanced, horizontal back edge of a tank's turret will map to different pixel levels depending on whether it is tilted or other objects are behind it. One must therefore really know the range discontinuity corresponding to an edge, to predict the pixel level to which it will map.

#### IV. Recognizing a Tank from a Range Scene

The task that must be accomplished in this chapter, is that of investigating the factors and the problems which are involved in recognizing a model T-72 tank from a scanned scene. Some of the problems that will be addressed are scene clutter and object rotation. A threshold correlation coefficient will also be searched for in this chapter, as well as other enhancement methods explored.

##### Establishing Correlation Coefficients for a Tank

The first step in this investigation into tank recognition is establishing a threshold correlation coefficient for the model T-72 tank. A correlation coefficient will be defined in this paper to be the magnitude of the highest peak in the correlation. By threshold, it is meant that for coefficients above the threshold the tank will be considered to be contained in the range scene, and for coefficients below or equal to the threshold the tank will be considered to be absent from the range scene.

Since it was shown in Chapter III that edge enhancement is vital to the correlation technique of object recognition, all future correlations will be performed with edge enhanced images. Figure 26 is an edge enhanced image of the same T-72 tank shown in Figure 5. The tank in Figure 5 was formed with a beam diameter, on a vertical surface of the tank, of

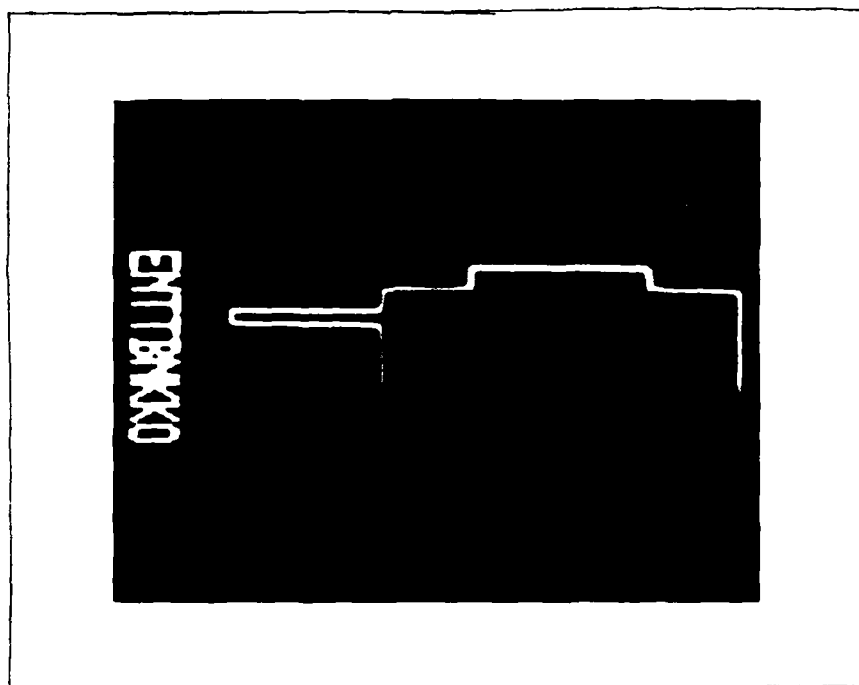


Fig. 26. Enhanced Range Image of the Model T-72 Tank.

14.6 cm. From Figure 26 one can see that the shape of the tank has been preserved while most of its area information has been eliminated. Figure 26 also supports the graph in Figure 25, for the higher pixels on the tank's outer edges are enhanced more than the lower pixels.

To begin the search for this threshold correlation coefficient, the edge enhanced image of the T-72 tank was autocorrelated, and a normalization factor was found which normalized the correlation peak to one. This normalization factor was used to divide all of the future cross correlations, when the reference object was this model tank. The autocorrelation is plotted in Figure 27. No dimensions are given on this graph's axes since in creating a range image, an actual 3-D scene is transformed into a 2-D image. In the transformation, the z-direction and the y-direction (see Figure 2) of the scene are combined into the single y-direction of the range image. Only the x-direction is transformed directly. Thus, placing dimensions on the axes of the correlation graph would be meaningless. The graph shown in Figure 27 is 58 x 58 section, centered on the row, column coordinates of (129,129), of a 256 x 256 matrix containing the entire correlation. The coordinates labeled (0,0) corresponds to the matrix's row, column coordinates of (129,129). Each increment of one on the axes of the graph, corresponds to an increment of one in the correlation matrix. All of the correlation graphs displayed in this paper will



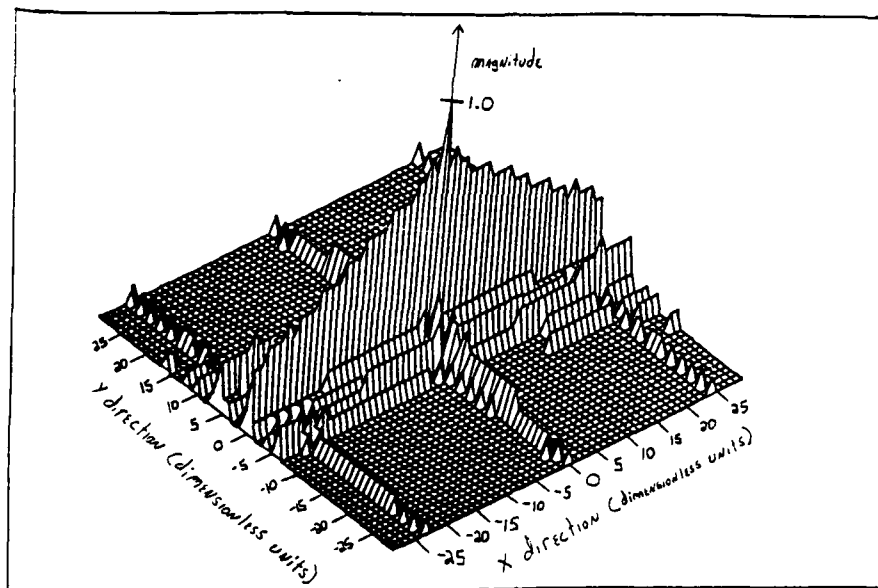


Fig. 27. AutoCorrelation of the Edge Enhanced Model T-72 Tank.

follow the same format as the one in Figure 27.

Table I lists the values of the correlation peaks of several different objects when they were correlated with the reference T-72 tank. A value of one for a correlation coefficient indicates a perfect match to the tank, and the closer the value is to zero, the less the object is similar to the tank. The range images that were correlated with the reference tank were of single objects which are listed in the table. The dimensions listed in the table for the T-72 tank are for its overall dimensions, i.e. the width of the hull of the tank, the depth of the hull of the tank, and the total height of the tank from the bottom of the hull to the top of

TABLE I

Correlation Coefficients Resulting from the Correlation  
of Different Objects with a Model of a T-72 Tank

| Object                     | Correlation<br>Coefficient | Width<br>(meters) | Depth<br>(meters) | Height<br>(meters) | Radius<br>(meters) |
|----------------------------|----------------------------|-------------------|-------------------|--------------------|--------------------|
| T-72<br>Tank               | 1.000                      | 6.95              | 4.75              | 2.37               | ---                |
| Sphere                     | 0.113                      | ---               | ---               | ---                | 3.47               |
| Vertical<br>Cylinder<br>#1 | 0.259                      | ---               | ---               | 2.37               | 3.47               |
| Vertical<br>Cylinder<br>#2 | 0.180                      | ---               | ---               | 10.0               | 0.30               |
| Horizontal<br>Cylinder     | 0.630                      | 4.80              | ---               | ---                | 0.11               |
| Box #1                     | 0.674                      | 6.95              | 4.75              | 2.37               | ---                |
| Box #2                     | 0.529                      | 6.00              | 4.00              | 2.0                | ---                |

the turret. The width listed in the table for the horizontal cylinder corresponds to its length. This horizontal cylinder has the same length, radius and orientation as the barrel of the model T-72 tank.

The sphere, box #1, box #2, and vertical cylinder #1 are models of possible decoys that could be set up to fool the air-to-ground missile. From their correlation coefficients with the tank, it looks like both of the boxes would be good decoys. The most probable reason for these two

objects' high correlation coefficients is that the T-72 tank model was primarily formed with rectangular boxes. A better model of the T-72 tank would probably not correlate as highly with the boxes as the present model does. Since, though, a tank's primary shape is rectangular, the correlation will still probably be fairly high. Figure 28 is the magnitude of the correlation of box #1 with the T-72 tank. As can be seen, this correlation is somewhat similar to that of the autocorrelation of the T-72 tank displayed in Figure 27, yet it is easily seen as different from the autocorrelation. What is needed, though, is a recognition technique that is very fast, therefore the two correlations cannot be generally compared -- only their correlation peaks.

From Table I, it is seen that box #1, whose dimensions generally match those of the tank, correlates better with the tank than box #2 whose dimensions are slightly off from those of the tank. Thus, if a decoy is to be built for an air-to-ground missile, it should be built with the same general dimensions of the real target. This statement is not very astounding, since this is what logic would already mandate.

Vertical cylinder #2 was meant to model the trunk of a tree which the missile might scan across in its search for tanks. From the cylinder's correlation coefficient, it is obvious that a tree will not be mistaken for a tank. On the other hand, the horizontal cylinder listed in Table I has a

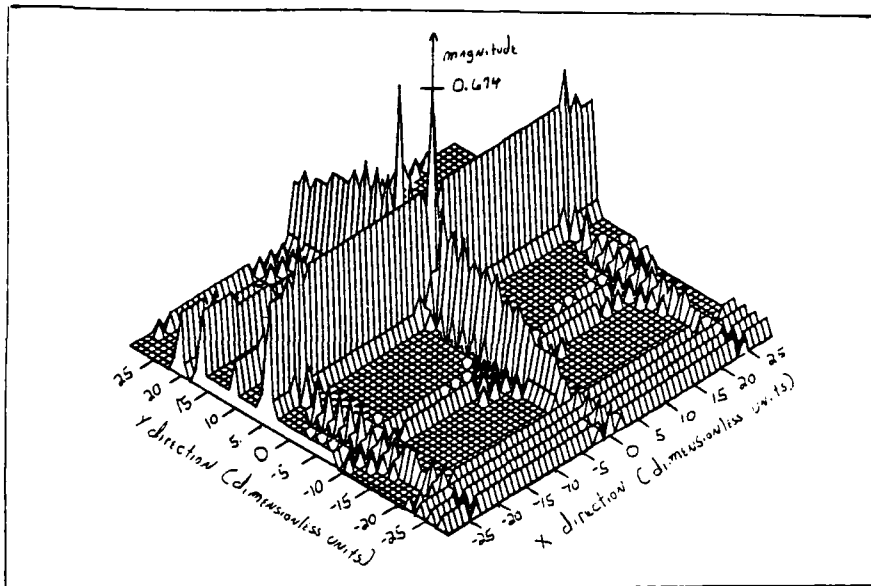


Fig. 28. Correlation of an Rectangular Box with the Model T-72 Tank (Both Edge Enhanced).

high correlation coefficient. This cylinder has the same dimensions, i.e. length, and radius as the tank's gun barrel. Since the tank's gun barrel is strongly edge enhanced and thus contains a lot of energy, it produces a high correlation coefficient when correlated with another gun barrel, i.e. the horizontal cylinder. Because of such a high correlation coefficient, one can conclude that the gun barrel is a distinguishing characteristic of the tank. It is probably the gun barrel that kept the correlation coefficient for box #1 from being higher than it was.

Now, the highest correlation coefficient that has been obtained for a non-tank object is 0.674. This means that

the threshold correlation coefficient for target recognition would have to be 0.675 or higher. A value of 0.680 would seem to be low enough to give the correlation technique some margin for error, yet still allow it to discern a tank from a simple decoy. There are other factors, though, that must also be considered before this value is fully accepted.

#### Modifying the Model Tank and the Range Scene

Now, a tank that is scanned in a real environment will not always be exactly like the reference tank in the scanning missile's memory. Neither will there be just a single tank by itself in the range scene, but also trees, rocks, decoys etc. Table II lists the correlation coefficients for some slightly modified model T-72 tanks, as well as for a T-72 tank in a range scene with other objects.

First, let's consider only the correlation coefficients for the modified T-72 tanks listed in Table II. Using a threshold correlation coefficient of 0.680, the results of Table II state that the T-72 tanks with tilted barrels and the T-72 tank that is tilted as a whole, would not be recognized as tanks. Also, if somehow in the missile's processing of the tank's image, it becomes enlarged by 10% or more, then the results listed in Table II state that the tank will not be recognized. These results would have serious consequences on the missile's effectiveness, since there are bound to be many tanks whose barrels will be angled at values other than  $90^{\circ}$ , as well as tanks tilted at various angles. For the

TABLE II

Correlation Coefficients for Modified T-72 Tanks and  
for Range Scenes Containing More Than the T-72 Tank

| Object                       | Correlation Coefficient | Description  |
|------------------------------|-------------------------|--|
| T-72 Tank with a Gas Tank    | 0.994                   | A rectangular box with a width of 0.5 m, a height of 0.5 m, and a depth of 2.0 m was placed on the hull of the tank.   |
| T-72 Tank with a Gas Tank    | 0.892                   | A rectangular box with the same dimensions as the above was also placed on the hull of the tank, but placed so that it changed the back enhanced edge of the tank. |
| T-72 Tank with a Machine Gun | 0.752                   | A cylinder of length 1.0 m and radius 0.03 m was placed on top of the tank's turret at 30°.  |
| T-72 Tank with Tilted barrel | 0.458                   | The barrel of the tank was tilted 5° upwards from its horizontal position.   |
| T-72 Tank with Tilted Barrel | 0.440                   | The barrel of the tank was tilted 10° upwards from its horizontal position.  |
| Tilted T-72 Tank             | 0.528                   | The entire tank was tilted 30° upwards from its horizontal position. This tilt was to model a tank sitting on a hill of positive slope.                            |
| Shifted T-72 Tank            | 0.970                   | The entire tank was shifted 2 m in the x direction (using the coordinate system of Figure 2.)  |
| Shifted T-72 Tank            | 1.00                    | The entire tank was shifted 1.456 m in the x direction.  |
| Enlarged T-72 Tank           | 0.572                   | All of the dimensions of the T-72 tank were enlarged by 10%.   |

TABLE II  
(continued)

Correlation Coefficients for Modified T-72 Tanks and  
for Range Scenes Containing More Than the T-72 Tank

| Object                                    | Correlation Coefficient | Description   |
|---|-------------------------|---|
| T-72 Tank with Tree                       | 0.311                   | A vertical cylinder of length 10 m and radius 0.3 m was placed behind the tank.   |
| T-72 Tank with Tree                       | 0.322                   | A vertical cylinder of length 10 m and radius 0.3 m was placed beside the tank where it would not affect the tank's edge enhancement.   |
| Two T-72 Tanks                            | 0.785                   | Two T-72 Tanks with a distance of 11.25 m separating them in the z direction (see Figure 2.) were contained in this range scene.  |
| Two T-72 Tanks                            | 0.731                   | Two T-72 Tanks with a distance of 0.45 m separating them in the z direction were also in this range scene, but one of the tanks was also shifted in the x direction by 4.0 m. |
| T-72 Tank with a Boulder                  | 0.981                   | A rectangular box with width 1.68 m, height 0.6 m, and depth 3.4 m was placed behind the tank so that it would affect the turret's edge enhancement.                          |
| T-72 Tank with a Boulder                  | 0.981                   | The same rectangular box as the above was placed behind the tank so that it would affect the hull's edge enhancement.   |
| T-72 Tank with Various Trees and Boulders | 0.181                   | Vertical cylinders with various sizes, a rectangle, and a sphere were contained in this range scene.  |

correlation technique to be applied to air-to-ground missiles, these problems will have to be solved.

Differing barrel orientations and the tilting of the tank are really multiple orientation problems that are still being researched by experts in the field of pattern recognition. This topic of multiple orientations will be discussed later. The amount of image enlargement in a range image should, on the other hand, be able to be determined and corrected for when the reference image is created. As long as the reference image is distorted in the same manner as the sensed image, then there should be no problem introduced with image distortion, i.e. image enlargement.

The problems become even worse when the range scenes containing more than the single T-72 tank are considered. If the threshold correlation coefficient, 0.680, is used again, then Table II states that the following range scenes would not be considered to contain tanks: the scene of the tank with the tree directly behind it; the scene of the tank with the tree beside it; and the scene of the tank with the multiple trees and boulders in the background. It appears that it is the trees that are causing such low correlation coefficients, for the coefficients for the range scenes with just a boulder in the background were very high. The trees in the range scenes were represented by tall and relatively thin cylinders and when edge enhanced, they contain a lot of energy. Even though a vertical cylinder correlates very



lowly with a tank by itself, a correlation coefficient of 0.180, the correlation peak of this cylinder is taking energy out of the tank's autocorrelation peak.

It indeed seems to be the energy of the trees that is doing the damage to the correlation coefficient, because adding a tree to a range scene containing a tank, really doesn't change the form of the correlation from that of the tank's autocorrelation. Figure 29 is a graph of the correlation of a range scene, containing a T-72 tank and a tree, with the reference T-72 tank. A comparison of this graph with the graph of the tank's autocorrelation (see Figure 27), shows that they are very similar. The only difference in the two graphs is the ridges in the back right hand side of the graph in Figure 29. It seems that if the trees were doing more to the correlation than taking energy away from the tank's autocorrelation peak, then there would be another major peak in the graph of Figure 29. The graph in Figure 29 doesn't have another correlation peak, so it must be the energy in the ridges that is causing the correlation coefficient to be so low.

For all the range scenes containing the T-72 tank along with background objects, the correlation peak belonging to the tank was always the highest peak in the correlation. It was mainly just the fact that the energy in the correlation was being spread around to other lower peaks, that was causing the tank's peak to be so much lower. The problem,

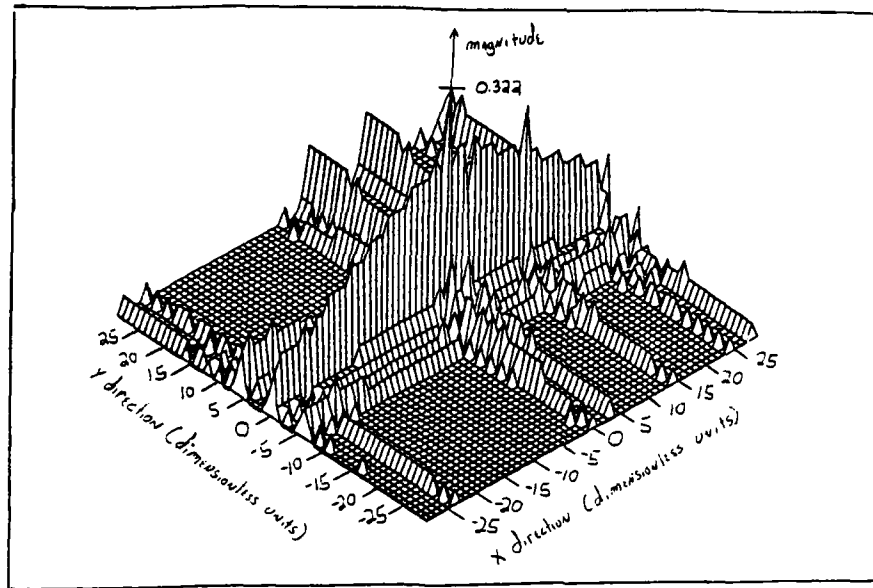


Fig. 29. Correlation of a Range Scene Containing a T-72 Tank and a Tree with the Reference T-72 Tank.

therefore, that has to be solved is that of restoring the energy of the tank's autocorrelation peak. This problem has been looked into by R. L. Mills in a Master's thesis (Mills, 1984).

To solve the problem of object clutter, Mills used a method of multiple correlations. The images that he used to test his correlation technique were 2-D visual images containing multiple targets and clutter. The first correlation pass that he performed on the images was used to locate the top correlation peaks. He then used the positions of these correlation peaks to extract  $64 \times 64$  sections from the original  $256 \times 256$  image, each section being centered around

one of the peaks. Next, he recorrelated each of the sections with a 64 x 64 image of the original reference object. Each of these correlations were scaled by the product of the energies of the 64 x 64 extracted section and the 64 x 64 image of the reference object. Thus, correlation coefficients for each of the objects in the image were established. These new correlation coefficients were then used to determine if any of the objects in the image were the same as the reference object.

Mills had good success in locating targets out of cluttered scenes with this procedure. The only problem was that after performing the first pass correlation, he had to manually locate the correlation peaks and compute their coordinates. Captain Cheryl Nostrand, a student at the Air Force Institute of Technology, is continuing Mills' work, and is working on having a computer automatically locate the correlation peaks of the first pass and compute their coordinates. Captain Nostrand's thesis should be finished by December 1985.

Obviously, the above technique will help with cluttered range scenes, but there is still the time constraint to consider. If there are a number of significant correlation peaks produced by the first pass correlation, then it might take a substantial amount of time to perform a correlation for each peak. For the application to an air-to-ground missile, there might only be time to recorrelate the section

of the range image corresponding to the largest correlation peak. If this were true, then only one tank in a range scene could be recognized. The time constraint might make one live with this result though. Another problem that this recorrelation technique might not be able to solve, is that of objects that are so close to the tank that they appear to be part of the tank. Correlating with the matrix section surrounding the tank in this case, will probably not help. Thus summarizing, this recorrelation technique looks promising, but probably will not solve the clutter problem totally.

Examining some more of the results listed in Table II, it appears that the correlation process is not always shift invariant. By shift invariant, it is meant that if the object that is being correlated is shifted from the coordinates of the reference object, then the correlation peak is shifted to the object's position, but without the magnitude and form of the peak changing. Cross-correlation is in fact always shift invariant, it is the scanning process that is not. Since the scanning process discretely samples an object, shifting the object might cause it to be sampled slightly more or less times than before. The result of this finite sampling is that an object that is contained in a range image might have a slightly larger or smaller size depending on its position. Thus, it is the change in the size of the scanned object that is making the correlation

coefficient lower, not the fact that the object is shifted. The effects of this "quasi" shift variance is not very great though; Table II shows that the correlation coefficient ranges only from 1.000 to 0.970 for a shifted tank.

Shift invariance is an important reason for using a correlation technique for target recognition. As was stated above, the form and magnitude of a correlation peak does not change when the input object is shifted with respect to the reference object, but the position of the peak does shift to the position of the input object. Thus, an air-to-ground missile can use the correlation peak's position to locate and destroy a target. The fact that this correlation technique was shown to be shift, or almost, shift invariant is therefore very important.

Another piece of information that Table II gives us is that, with a threshold correlation coefficient of 0.680, a tank can be recognized from a range scene containing two tanks. It doesn't matter if the two tanks appear to be separated in the range image or appear to be one object, the correlation coefficient is high enough for one of the tanks to be recognized either way. If one wants to recognize both of the tanks, then one will have to use a technique like Mills' method of multiple correlations.

#### The Effect of Rotation on the Correlation of a T-72 Tank

In establishing the threshold coefficient, all the tanks in the range scenes had the same orientation as that

of the reference tank. Clearly the orientation of a tank in the field cannot be predicted. Neither will all of the tanks in the field have the same the orientation. Thus in establishing the correlation coefficient, the effect of orientation needs to be taken into account. Figure 30 is a range image of the same model T-72 tank shown in Figure 5, but rotated by  $45^{\circ}$ . Figure 31 is also a range image of the T-72 tank shown in Figure 5, but rotated by  $90^{\circ}$ . Figure 32 and 33 are enhanced range images of the tanks shown in Figures 30 and 31 respectively.

Figure 34 is a graph of the correlation coefficients, i.e. correlation maximums, for the rotated T-72 tanks plotted versus degree of rotation. All correlations were with the T-72 tank depicted in Figure 5. The values in the first quadrant, i.e. 0 to  $90^{\circ}$ , should be fairly characteristic of those in the other three quadrants, and is the reason why only the first quadrant contains a large number of data points. The dashed curve in the second through fourth quadrants was drawn so as to parallel the curve in the first quadrant. One can see from this graph that rotation is going to cause severe problems for target recognition.

If the threshold coefficient, 0.680, that was established beforehand was to be used to establish target recognition, only the non-rotated tank would be recognized. Even the tank that is only rotated  $1^{\circ}$  would not be recognized. To give one an idea of the effect that rotation has on the

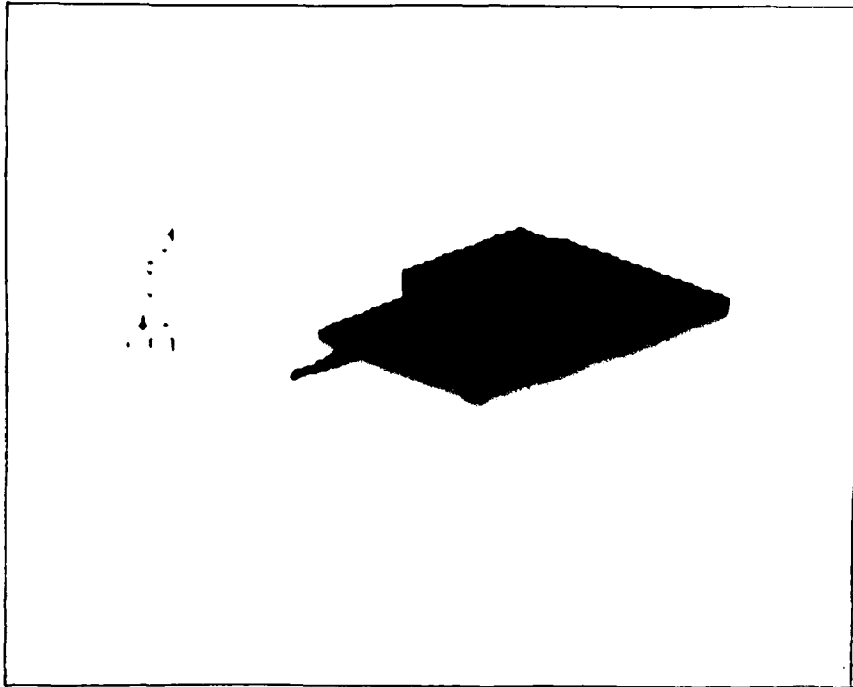


Fig. 30. Range Image of a Model T-72 Tank  
That Has Been Rotated 45 Degrees.

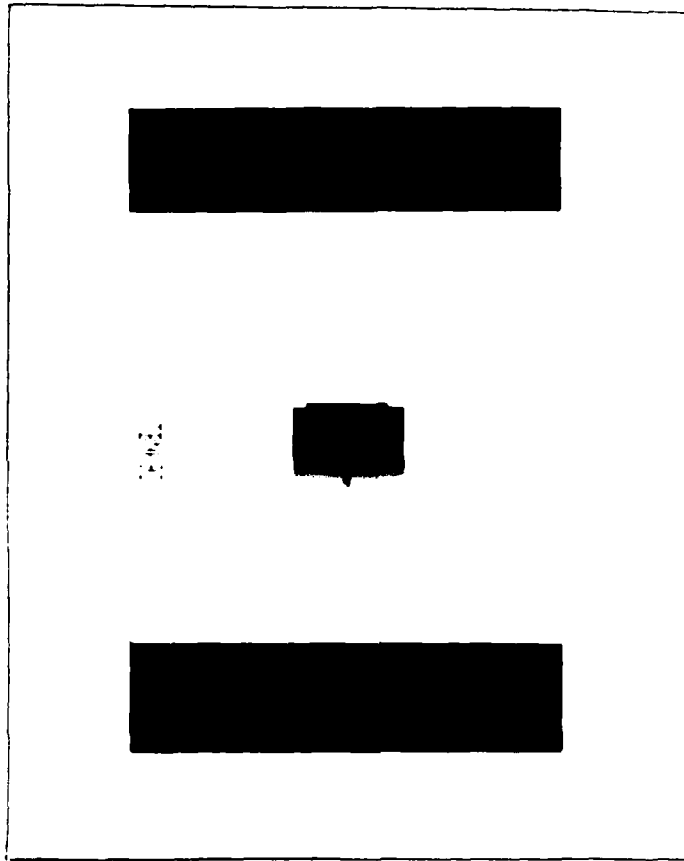


Fig. 31. Range Image of a Model T-72 Tank  
That Has Been Rotated 90 Degrees.



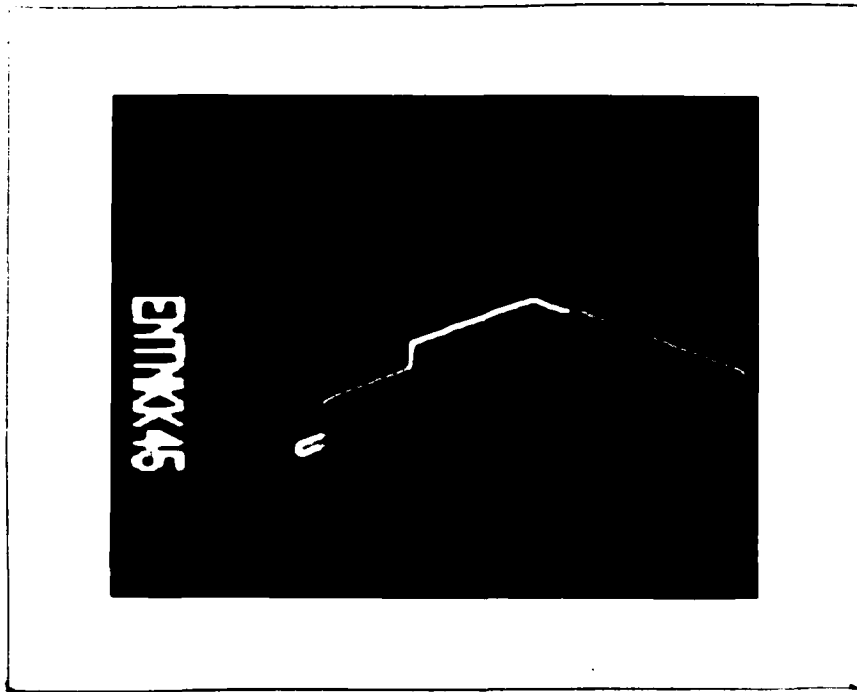


Fig. 32. Enhanced Range Image of the Model T-72 Tank That Has Been Rotated 45 Degrees.

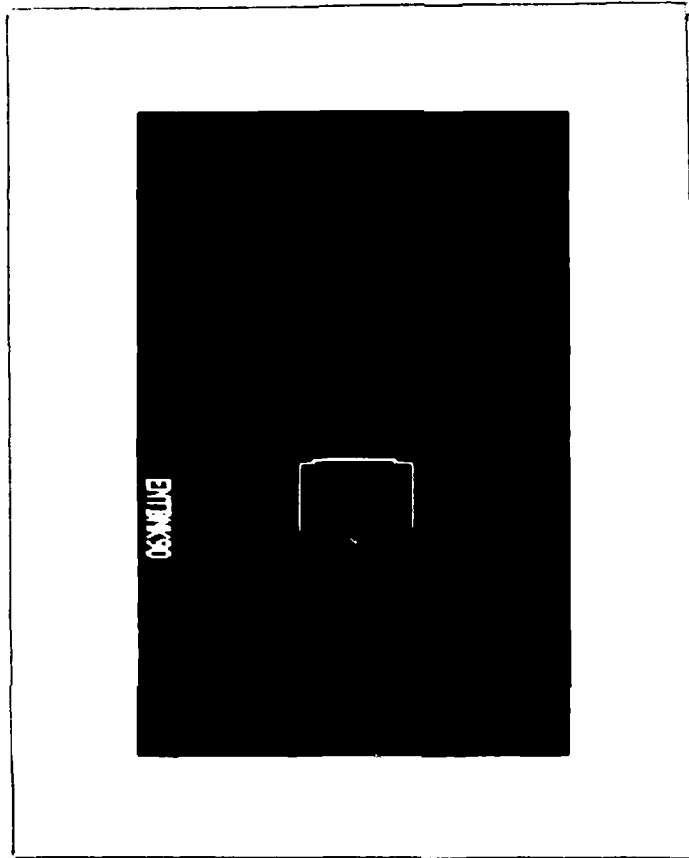


Fig. 33. Enhanced Range Image of a Model T-72 Tank That Has Been Rotated 90 Degrees.

AD-A167 148

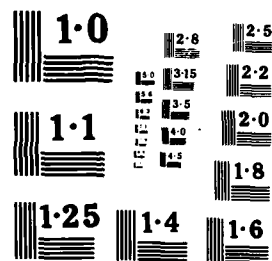
OBJECT RECONGNITION USING RANGE IMAGES(U) AIR FORCE  
INST OF TECH WRIGHT-PATTERSON AFB OH SCHOOL OF  
ENGINEERING J W GRANTHAM DEC 85 AFIT/CEP/ENG/85D-4  
F/C 17/8

2/2

UNCLASSIFIED

ML

END  
PAGE  
6-86  
107



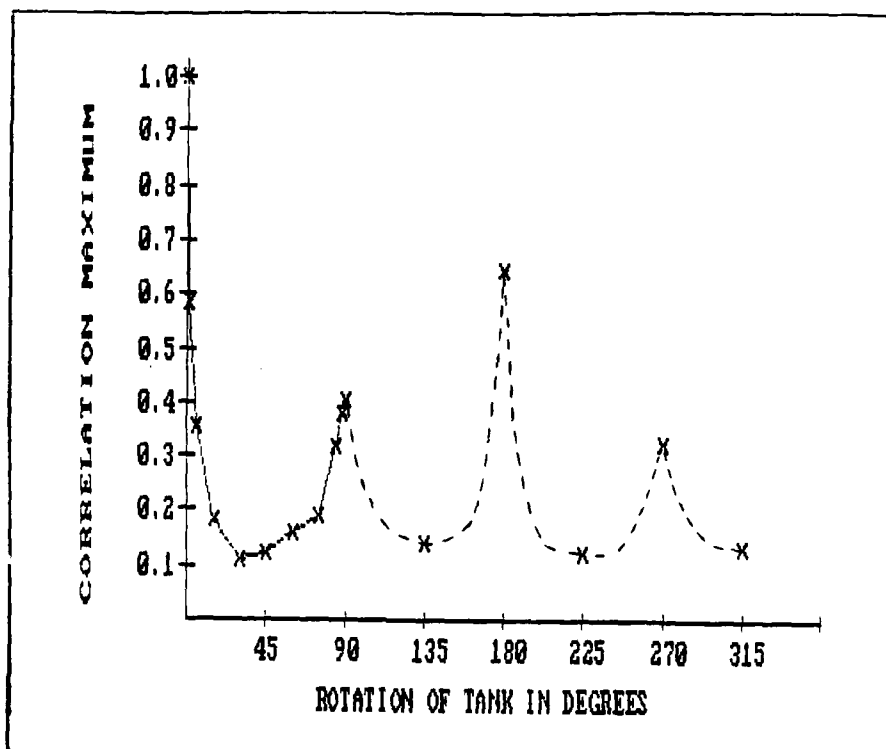


Fig. 34. Correlation Maximum vs. Degree of Tank Rotation.

graph of a correlation, the correlations of the T-72 tank rotated  $45^\circ$  and the T-72 tank rotated  $90^\circ$  with the non-rotated T-72 tank are shown in Figures 35 and 36 respectively. The correlations are somewhat similar to the autocorrelation of the T-72 tank shown in Figure 27, but there are many more "noise" peaks in the rotated correlations. These "noise" peaks are obviously taking energy away from the maximum peak, thereby lowering the correlation coefficient. The correlation with the  $90^\circ$  rotated T-72 tank is a

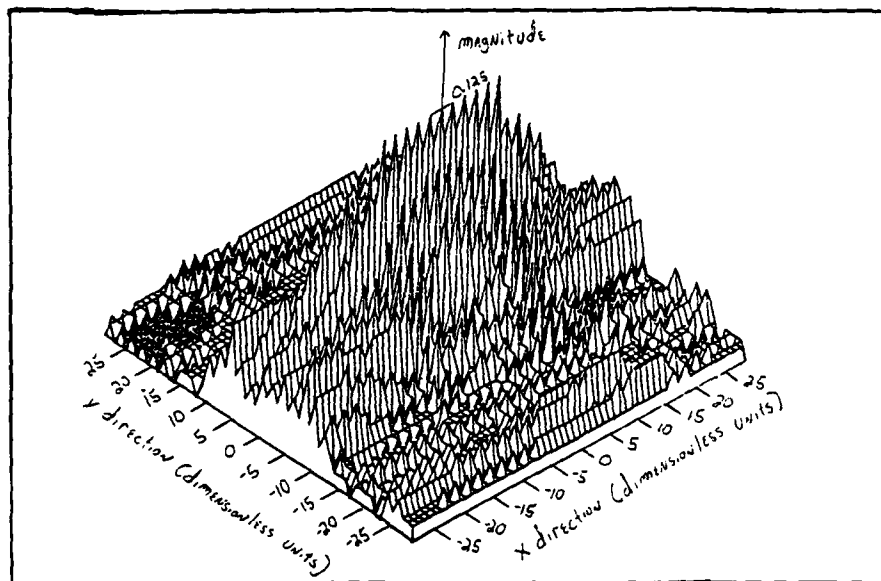


Fig. 35. Correlation of a Rotated (45 Degrees) Model T-72 Tank with a Non-Rotated Model T-72 Tank.

lot more similar to the autocorrelation of the non-rotated T-72 tank, than the corresponding correlation with  $45^\circ$  rotated T-72 tank. The correlation corresponding to the  $90^\circ$  tank rotation also has most of its energy contained along the line  $x = 0$ , whereas the correlation corresponding to the  $45^\circ$  tank rotation has its energy spread out more. The result is that the correlation peak belonging to the  $90^\circ$  rotation has much more energy and thus amplitude than the  $45^\circ$  correlation peak. A higher correlation amplitude translates into a higher correlation coefficient for the  $90^\circ$  tank rotation than the  $45^\circ$  tank rotation.

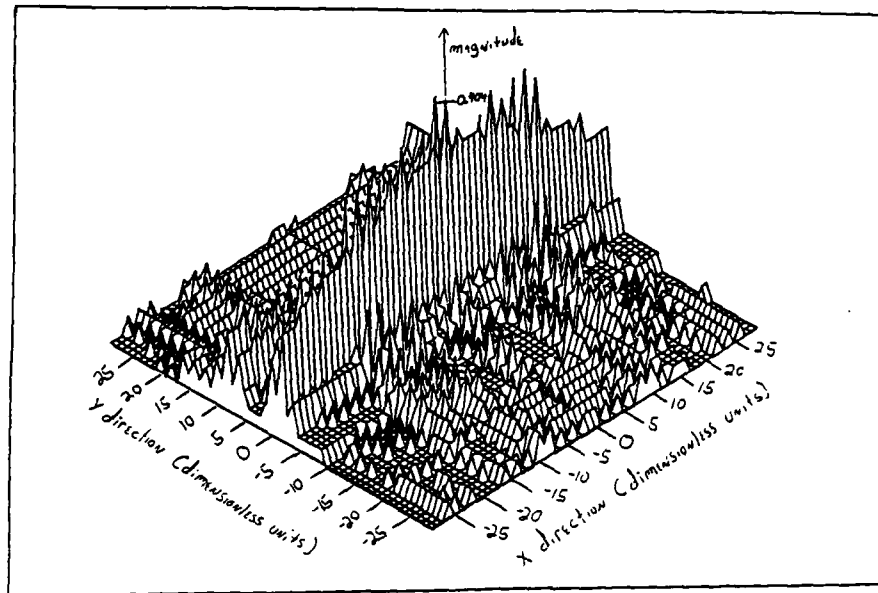


Fig. 36. Correlation of a Rotated (90 Degrees) Model T-72 Tank with a Non-Rotated Model T-72 Tank.

Casasent discovered similar optical results as those of Figure 34, when the input function and a holographic matched filter function were rotated with respect to each other (Casasent and Psaltis, 1976:1796). This problem of rotation is thus not limited to range images but is a problem in all fields of pattern recognition. Rotational variance is a problem that will certainly have to be solved if cross correlation is going to prove to be a viable target recognition technique.

#### Research on Rotation and Scale Invariant Correlations.

Rotation and scale invariant correlations have been the focus of a lot of research in the past several years. This research has been in both the fields of optical and digital correlations and is still being actively studied. One of the ways that researchers have tried to deal with rotation and scale changes is by combining the operations of Fourier and modified Mellin transforms.

#### Fourier-Mellin Correlation.

The Fourier transform is shift invariant, but it is not rotational nor scale invariant. A Mellin transform, on the other hand, is scale invariant but not shift nor rotation invariant. Casasent and Psaltis combined these two transforms, along with a polar transformation and a logarithmic scaling, to produce a correlation that was both rotation and scale invariant (Casasent and Psaltis, 1976). Casasent and Psaltis performed this process optically in their work, but this same process can also be performed digitally (Friday, 1984). A diagram of the correlation process is shown in Figure 37 (Friday, 1985:2). In this process the correlation is performed on the Fourier transform magnitudes of the reference image and the sensed image, not on the images themselves. The reason for using the Fourier transform magnitudes is that the magnitude of the Fourier transform is shift invariant, so that it is always located on the optical axis, when the correlation is optical, and is always located



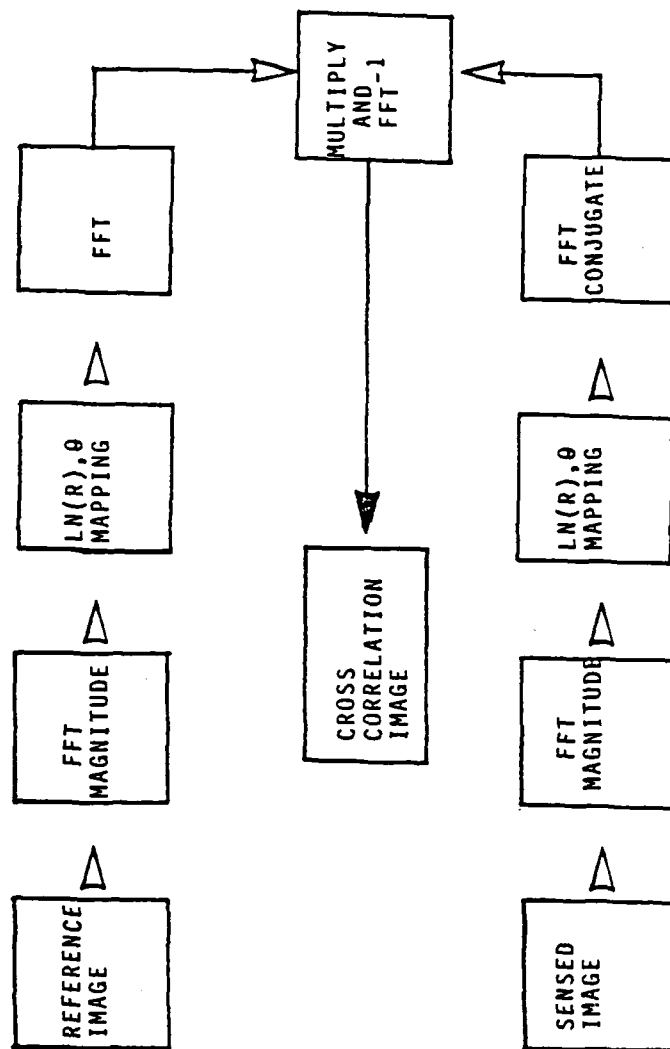


Fig. 37. The Mellin-Fourier Correlation Process

at the center of the output matrix when the correlation is digital.

Casasent and Psaltis found good results when they optically correlated a simple object that was both rotated and scaled, with the same non-rotated and unscaled object (Casasent and Psaltis, 1976). The degree of rotation for the object, a square, was  $45^\circ$  and the scale change was 100%. The magnitude of the correlation peak for the rotated and scaled square was within 8% of the autocorrelation peak for the non-rotated and non-scaled square. This was well within the accuracy of their experiment. By using this procedure, they could also determine the amount of rotation and scale change by the location of the correlation peak. A drawback to using this procedure is that the position of the correlation peak no longer corresponds to the position of the input object. Thus the position of the input object is lost. This is a very important loss if this technique is to be used in an air-to-ground missile.

A recent work into Mellin-Fourier transforms is by E. Friday (Friday, 1984). In this work Friday tried with success to extend the scale invariance of this hybrid transform. He was able to extend the transform's scale invariance so that scale changes ranging from 0.2 to about 1.5 would still have correlation coefficients above 0.85. These correlations were implemented digitally. With his procedure Friday was able to have a rotation difference of  $45^\circ$  and a

scale change of 100% between the input object and the reference object and still obtain a correlation coefficient of 0.89.

The Fourier-Mellin transform method of Casasent and Psaltis would certainly help our problem of multiple target orientations, but the position of the targets would be lost with this method. This might be a loss that one can not afford, for what good is it to recognize a target if one does not know where it is in a range scene? To solve this problem one could first perform the hybrid correlation procedure to detect the target, and then use the ordinary Fourier correlation procedure to locate the target's position. This of course would take more time, which the missile might not have.

#### Circular Harmonic Filters.

Another method of correlation which is rotation invariant is that of correlating with circular harmonic components of objects (Arsenault and others, 1982:266-272). To use this correlation procedure, one must expand the reference object and the input object in a circular harmonic series and then select out a component, e.g. the 7th-order component, from the series to use in the correlation. The problem in selecting the particular component of the series to use, is that the component must be of high enough order to discriminate between the two objects, and still produce

an adequate signal-to-noise ratio (SNR). The usual result is that one must sacrifice SNR for rotation invariance.

Arsenault (Arsenault and others, 1982:266-272) found good experimental results, both digitally and optically, using this circular harmonic correlation method. He found that he could recognize the letter "E" when several rotated versions of it were placed in a field with other similar appearing letters. All of the rotated "E"s were recognized in this experiment and the other letters in the field were rejected as not being "E"s. Thus, this proves that this method of correlation is rotation invariant but still discriminating.

The big advantage that this method has over the Fourier-Mellin method is that the position of the input object is not lost -- the position of the correlation peak is still the position of the input object. The big disadvantage that this method has is the small SNR. This method, though, needs to be further investigated to see if this SNR can be improved or tolerated.

#### Synthetic Discriminant Function.

A correlation procedure that has received much attention in recent years is that of correlating with a synthetic discriminant function (SDF). This SDF serves as the reference function with which one correlates the input function. The SDF allows for object distortion, i.e. rotation and scale change, and will yet discriminate between diffe-

rent objects (Hester and Casasent, 1981:108). There are, though, different SDF's for different purposes: ones for intra-class recognition, i.e. recognition of a single object but which can have multiple orientations and sizes; and ones for intra-class recognition and inter-class discrimination, i.e. an SDF which will perform intra-class recognition for each object used in forming the SDF, but in addition will indicate to which of the objects that the input object corresponds.

The intra-class SDF is formed from a linear combination of single images of an object. The other types of SDF's involve a linear combination of images of different objects. The single images used to form an intra-class SDF are images of different rotated and scaled versions of the input object. The two major factors that have to be determined in forming an intra-class or any other SDF are first which particular images are to be used to form the SDF, and second how the images will be weighted with respect to one another. At first researchers chose these parameters in an "ad hoc" fashion, but recently Casasent has come up with a deterministic procedure to determine these factors (Casasent, 1984: 1620-1627). The procedure is fairly involved and will be left up to the reader to examine. A description and summary of the different SDF's as well as details on their formation is given in an article by Casasent called "Synthetic Discrimi-

minant Functions for Three-Dimensional Object Recognition" (Casasent and others, 1982:136-142).

The results that researchers have obtained with SDF's have been good. Casasent, for example, was able to recognize all of the rotated images, 36, of a ship using only six of the orientations to form his SDF (Casasent and Sharma, 1983:47-55). He had similar success with an intra-class, inter-class SDF (Casasent and Sharma, 1983:47-48). There is one aspect of SDF's on which this researcher could not find too much data. This lack of data has to do with the discrimination ability of SDF's for objects of which the SDF's are not composed. Thus for the case considered in this paper, would an SDF of the model T-72 tank be able to recognize different rotated versions of the model tank, while at the same time discriminate between a tank and a decoy? This needs to be investigated in the near future.

SDF's show promise in solving rotation and scaling problems in object recognition. Using an SDF reference image, a correlation can have not only rotation and scale invariance but can also retain its ability to locate the input object's position. The SDF can also be implemented both optically and digitally.

#### Other Rotation Invariant Techniques for Correlation.

One correlation technique that has been used in the past, achieves rotation and scale invariance by making a

number of sequential correlations with successive reference objects, at different orientations and with different sizes (Fujii and Ohtsuba, 1981:616-620) and (Fujii and others, 1980:1190-1195). This method is very time consuming especially for a missile application. Another correlation technique involves correlating with a multiplexed filter which contains a number of rotated and scaled filters (Leib and others, 1978:2892-2899) and (Mendelsohn and Wohlers, 1980:148-153). This method, though, usually involves a drop in the output SNR, which decreases as some power of the number of individual filters contained on the multiplexed filter (Arsenault and others, 1982:266-272).

This completes the list of the major correlation techniques which are rotation and scale invariant. Considering all of these techniques, the method showing the most promise seems to be the technique involving the SDF. The other methods should not be forgotten as they deserve further investigation.

#### Enhancing Horizontal Edges Only

All of the previous correlations have been with images that were enhanced in both the y and x directions. Since edge enhancing in this manner produced correlations that were very rotationally variant, it was thought edge enhancing in a single direction might produce more rotation invariant correlations. To investigate this possibility, horizontal edge enhancement was performed. To implement this

horizontal edge enhancement, a new version of the image forming computer program was formed which multiplied each frequency component by only its "y" frequency. The frequency components were not weighted by the "x" frequencies. The result of this horizontal edge enhancement is shown in Figure 38 for the non-rotated T-72 tank. Table III contains the correlation coefficients resulting from the correlation of the "horizontally edge enhanced" T-72 tank with other "horizontally edge enhanced" objects.

From the results listed in this table, horizontal edge enhancement does not make a correlation more rotationally invariant, it makes it even less so. Comparing the results of Table III with those listed in Tables I and II, horizontal edge enhancement produces worse results than bidirectional edge enhancement for all of these cases, except for the correlation with the rectangular box. The rectangular box is not as good of a decoy when horizontal edge enhancement is performed, as it is when combined edge enhancement is performed. The lower coefficient for the correlation with the box, though, is not enough to make up for the low coefficients of the other correlations, especially the coefficient for the rotated tank. Therefore it is concluded that for recognizing a T-72 tank, the combined horizontal and vertical edge enhancement is better than just horizontally edge enhancing.



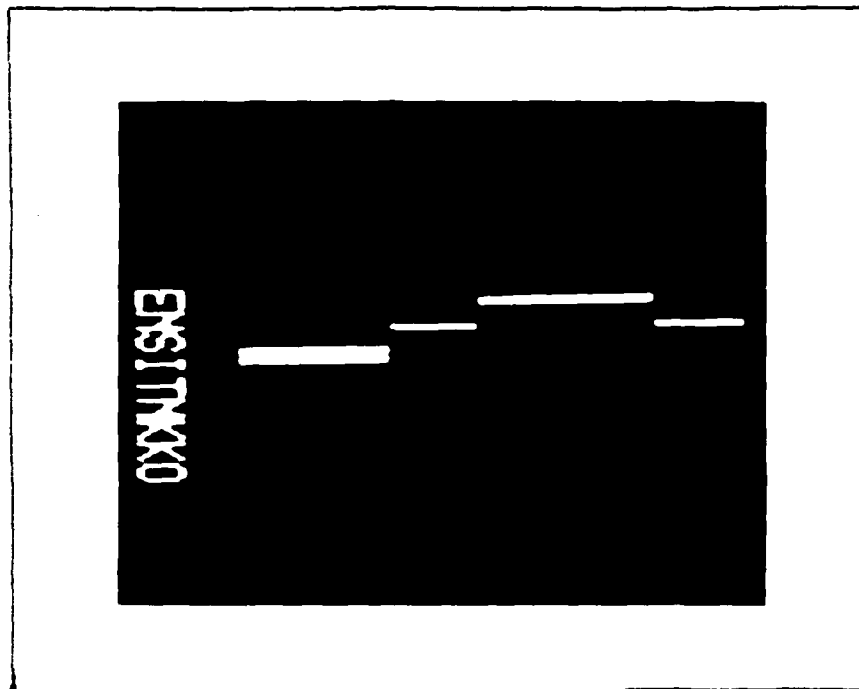


Fig. 38. Horizontally Edge Enhanced Range Image of a Model T-72 Tank.

TABLE III

Correlation Coefficients Resulting from the Correlation of the "Horizontally Edge Enhanced" T-72 Tank with Other "Horizontally Edge Enhanced" Objects

| Objects                          | Correlation Coefficient | Description   |
|----------------------------------|-------------------------|---|
| T-72 Tank Rotated 45°            | 0.056                   | The model T-72 tank was rotated 45°.  |
| Tilted T-72 Tank                 | 0.473                   | The entire tank was tilted 30° from its horizontal position. This tilt was to model a tank sitting on a hill of positive slope. |
| T-72 Tank with Tilted Gun Barrel | 0.346                   | The gun barrel of the tank was tilted 10° upwards from its horizontal position.   |
| Box                              | 0.525                   | The rectangular box had a width of 6.95 m, a depth of 4.75 m, and a height of 2.37 m.   |

Before leaving the subject of horizontal edge enhancement, it would be desirable to see just how the pixel levels belonging to enhanced horizontal edges map to the height of the edges. Figure 39 is a plot of the pixel levels of the enhanced horizontal edges versus their corresponding heights. The pixels used in Figure 39 were taken from the back edges of the tops of horizontally edge enhanced boxes. There were five boxes, all with varying heights, in the range scene that was scanned and edge enhanced. One pixel level was

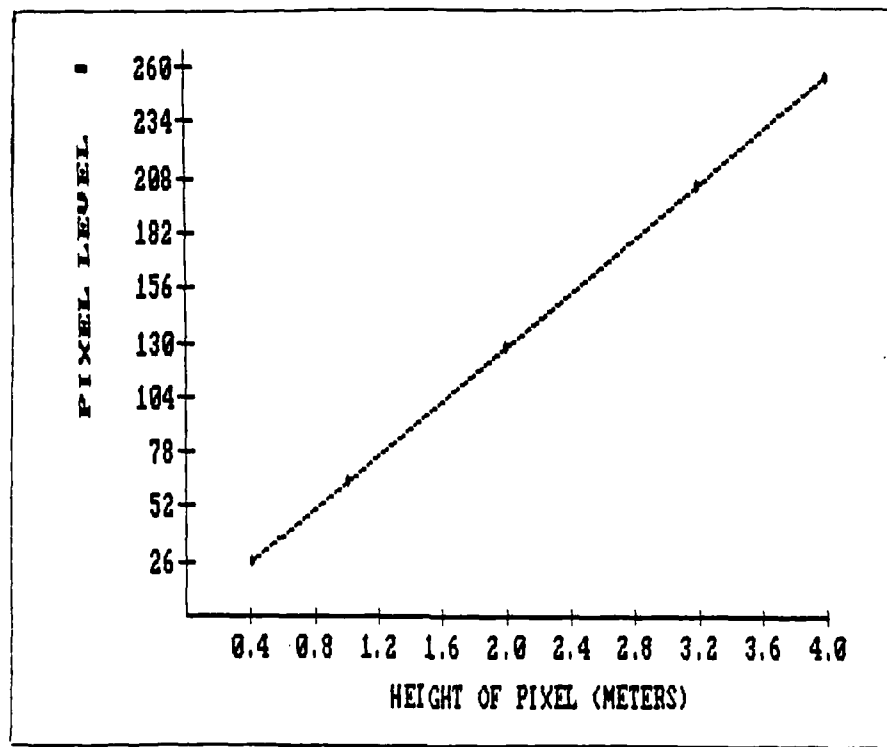


Fig. 39. Pixel Level vs. Height for Horizontally Enhanced Edges.

taken from each box's top back edge. One noticeable result of the horizontal edge enhancement, was that the corners of the boxes were enhanced in the same manner as the edges, not  $\sqrt{2}$  times more than the edges as was the case with the bidirectional edge enhancement.

Examining Figure 39, one can see that the relationship between pixel level and height is again linear. The slope this time though is approximately  $64.2 \text{ m}^{-1}$  whereas for enhancement in two directions it was approximately  $8.33 \text{ m}^{-1}$ .

The difference in the slopes comes from the fact that corners are enhanced much more than edges for bidirectional edge enhancement, whereas for horizontal edge enhancement they are enhanced the same. Thus, for a 4 m high box bidirectionally edge enhanced, the highest pixel level that an edge can have is 148, whereas for horizontal edge enhancement, the highest pixel level that an edge can have is 255. Even though the pixel level mapping is different for the two enhancement methods, both mappings are still linear.

#### Vertical Edge Enhancement

Since horizontal edge enhancement was tried to see if that would improve the correlation's rotational invariance, vertical edge enhancement was also tried. The way that vertical edge enhancement was employed in the range imaging program was that instead of multiplying the frequency components by their "y" frequencies, the frequency components were multiplied by their "x" frequencies. Figure 40 is a vertical edge enhanced image of the non-rotated T-72 tank. Table IV contains the correlation coefficients for the correlation of the same objects listed in Table III, but this time both the objects and the T-72 tank of Figure 40 were vertically edge enhanced.

As one can see by comparing Tables III and IV, for the cases when enhancing only in the horizontal direction improved the correlation results, enhancing in the vertical direction worsened them; and where enhancing only in the

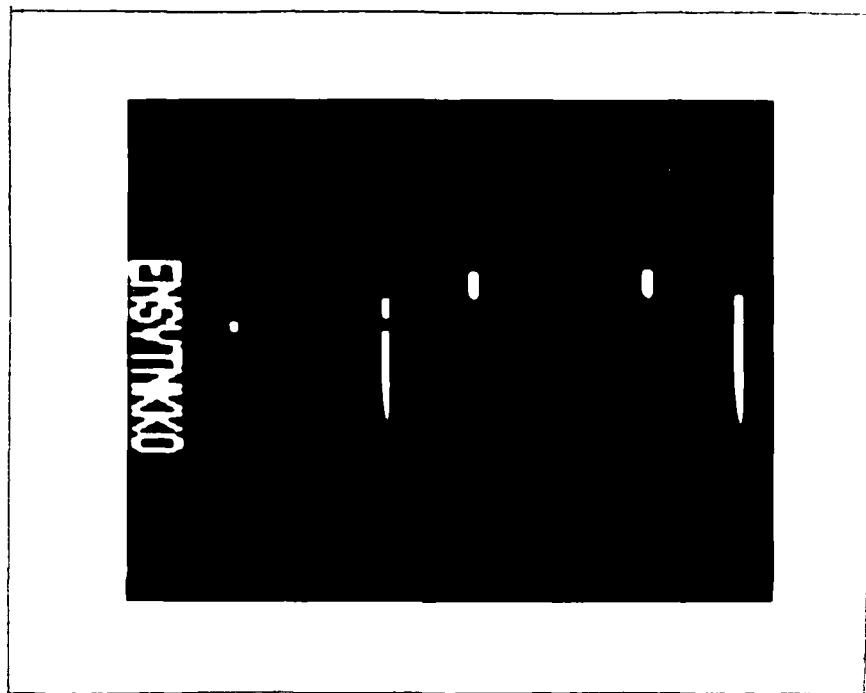


Fig. 40. Vertically Edge Enhanced Range Image of a Model T-72 Tank.

TABLE IV

Correlation Coefficients Resulting from the Correlation of the "Vertically Edge Enhanced" T-72 Tank with Other "Vertically Edge Enhanced" Objects

| Object                           | Correlation Coefficient | Description   |
|----------------------------------|-------------------------|---|
| T-72 Tank Rotated 45°            | 0.161                   | The T-72 tank was rotated by 45°.   |
| Tilted T-72 Tank                 | 0.848                   | The entire tank was tilted 30° upwards from its horizontal position. This tilt was to model a tank sitting on a hill of positive slope. |
| T-72 Tank with Tilted Gun Barrel | 0.623                   | The gun barrel of the tank was tilted 10° upwards from its horizontal position.   |
| Box                              | 0.916                   | The rectangular box had a width of 6.95 m, a depth of 4.75 m, and a height of 37 2.37 m.  |

horizontal direction worsened the correlation results, enhancing in the vertical direction improved them. Though the vertical edge enhancement process improved most of the correlation results, it really hurt the correlation's ability to distinguish the T-72 tank from a rectangular box with the same overall size. This result certainly couldn't be tolerated, for it would push the threshold correlation coefficient all the way up to 0.920. Using this threshold coefficient, any change in the appearance of a T-72 tank would cause the missile not to recognize the tank. Thus overall,

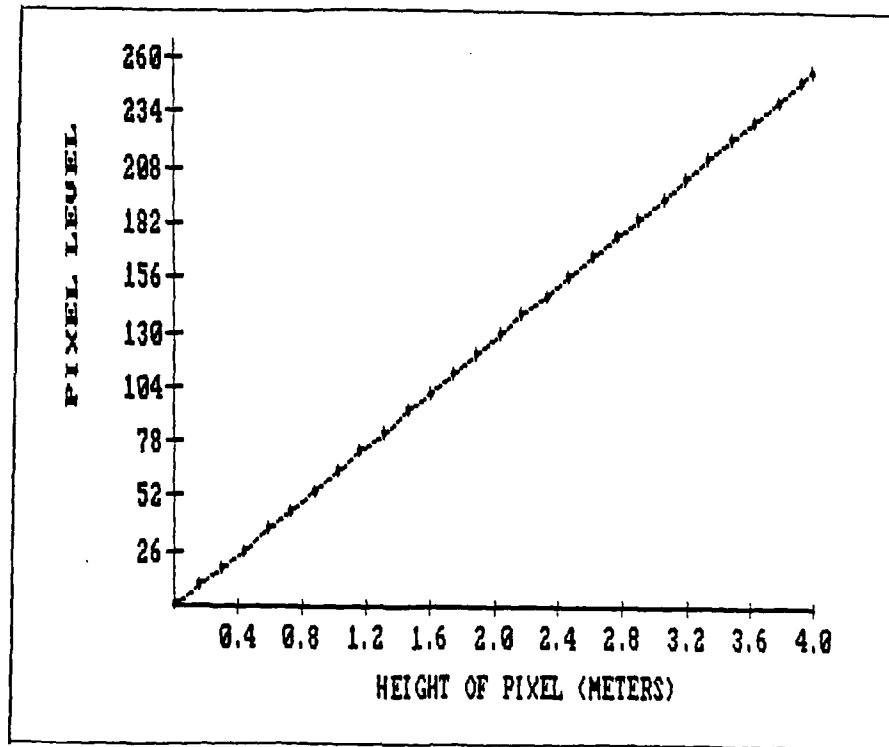


Fig. 41. Pixel Level vs. Height for Vertically Enhanced Edges.

the process using combined horizontal and vertical edge enhancement produces better correlation results than the processes using single direction edge enhancement.

Since the pixel levels of enhanced edges were mapped to their height for the other enhancement methods, this mapping also needs to be examined for the vertical edge enhancement method. Figure 41 is a plot of the pixel level versus height for a vertically enhanced edge of a rectangular box. The box had a height of 4 m and the pixels that are plotted

in Figure 41 belong to the front right hand edge of the box. Examining Figure 41, one can see that the relationship between an edge's pixel level and its corresponding height is again linear. The slope of the line in Figure 41 is approximately  $64.3 \text{ m}^{-1}$ , which is very close to the slope of the graph in Figure 39 for the horizontal edge enhancement method. For vertical edge enhancement, like horizontal enhancement, corners were enhanced in the same manner as the edges.



#### V. Other Factors Affecting the Correlation Coefficients

There are factors beside scene clutter and object rotation, which affect the correlation coefficient of a range scene. Two factors which will be considered in this chapter are the laser's "on target" beam spot size and the pixel dropouts in a range scene. Of the many factors which affect this coefficient, only these two will be considered in this chapter.

##### The Effect of the Laser Beam Spot on Correlation

When the scanning laser's beam divergence is increased, or the scanning occurs farther away from the air-to-ground missile, the laser's spot size on the target is increased. This means that the target is sampled fewer times and as a result one loses some of the target's detail. This would seem to have an effect on the correlation's ability to distinguish potential targets from decoys and ordinary background clutter. Scanning at a larger distance away from the missile though, would give the missile's processor more time to correlate and process the range images. Thus, having the largest possible beam spot on the target while retaining the correlation's "object distinguishing capability" would be very desirable. In this section, it was desired to investigate the effect that an increased beam spot would have on

distinguishing a target from a decoy. The target used, was again the model T-72 tank. Since rectangular boxes don't have a lot of detail, it was decided to use the modified model of the T-72 shown in Figures 6 and 7. This modified model is still crude compared to an actual image of a T-72 tank, but should suffice for the purposes here.

Figure 7 is range image of the model T-72 tank formed with a beam spot diameter, as measured on a vertical surface, of 7.3 cm. Figure 6 is a range image of the model T-72 tank formed with a beam spot diameter of 29.1 cm. As Figure 6 shows, scanning with a beam spot of 29.1 cm distorts the tank's turret as well as the true size of the tank's gun barrel. A beam spot of 7.3 cm on the other hand, retains most of the detail about the tank's turret, as well as maintains the gun barrel's true size. With a larger spot size on a target, one doesn't obtain as much detailed information as with a smaller spot size.

It would seem logical that the less information a laser scanner gathers about targets, the more susceptible it would be to decoys. To check the validity of this hypothesis, the improved model of the T-72 tank was range scanned with different spot diameters, and then correlated with our best decoy, the rectangular box with the overall dimensions of the T-72 tank. For each correlation, the rectangular box was scanned with the same spot diameter as the tank with which it was to be correlated. The result of the correla-

tions is plotted in Figure 42. The laser beam diameter plotted is the diameter that a laser beam would have on a vertical surface of the model tank.

The plot in Figure 42 indicates that the hypothesis was wrong at least for beam diameters between 7 and 60 cm. For beam diameters within this range, the plot shows that as the laser beam diameter increases, the ability of the correlation to distinguish the model tank from the box increases. The most probable explanation of this result, is that increasing the beam diameter results in an enhancing of the basic features of the tank, one being the gun barrel. From Figure 6 and 7 one can see that increasing the laser spot diameter, increases in turn the size of the tank's gun barrel in the range image. Therefore, enlarging this distinguishing feature of the tank, makes it easier for the correlation to discern the tank from a simple decoy.

Increasing the beam diameter is good up to a point, because it helps distinguish the tank's basic geometric features. This is true only up to a point though. As the "on target" beam diameter of the laser is increased, the tank is being sampled less and less times. If the laser beam doesn't sample the tank enough, its range image will become a rectangular blob, and it will correlate very highly with almost anything. There is thus a turning point where increasing the beam diameter doesn't help distinguish an object any more, but instead makes the object less distinc-

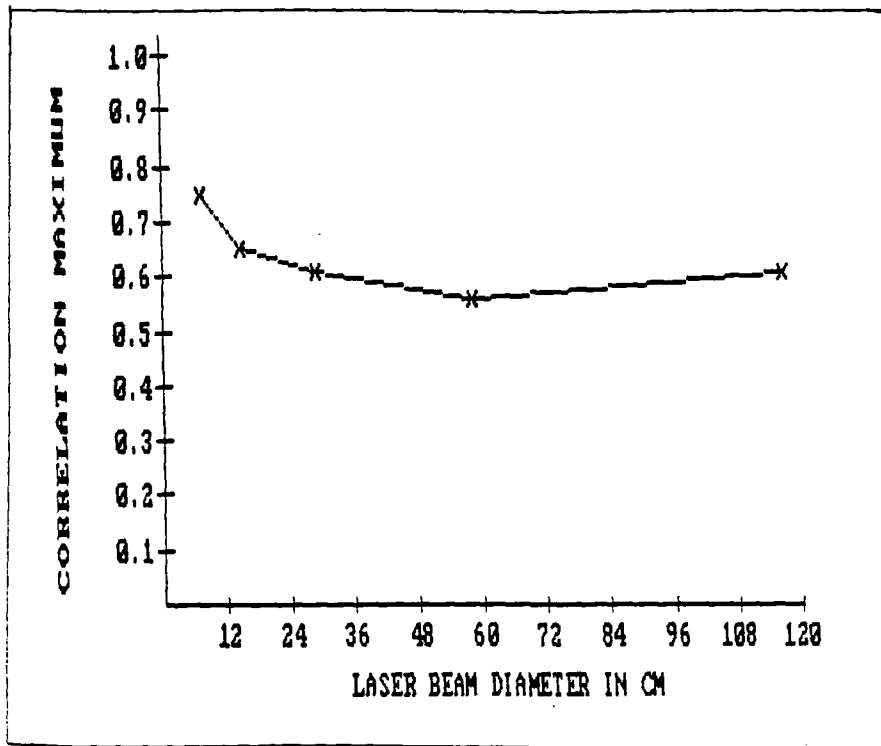


Fig. 42. Correlation Maximum vs. Diameter of the Scanning Laser Beam for a Scanned Tank.

tive. The graph in Figure 42 indicates that the turning point for the T-72 tank occurs when a beam diameter between 60 cm and 120 cm is used. Since a beam diameter of 116.5 cm corresponds to the vertical side of the tank being sampled only 2 times, one can understand why the turning point occurs before this beam diameter is reached. Thus from the graph in Figure 42, the largest "on target" beam diameter that should be used on a T-72 tank is 116.5 cm.

The above result should be used with caution though, for it was derived using a simple model of the T-72 tank and a simple decoy. If the decoys used against a scanning air-to-ground missile become more sophisticated, then a smaller beam spot diameter will have to be used. The value of 116.5 cm should therefore be taken as an upper limit for forming range images.

If the gun barrel of the T-72 tank was not as evident as it is in Figure 7, then the tank would be expected to correlate higher with a rectangular box having its overall dimensions. The laser beam diameter would also be expected to be smaller at the turning point, where the beam stops enhancing the tank's basic geometric features and starts eliminating them. To test this hypothesis, the T-72 tank was rotated  $90^{\circ}$  and range scanned with a number of different beam diameters. Figures 43 and 44 show such rotated T-72 tanks formed with beam diameters of 7.3 cm and 29.1 cm respectively. These rotated tanks were then correlated with correspondingly scanned rectangular boxes having the overall dimensions of the tanks. The result of the correlations is graphed in Figure 45. The graph of Figure 45 shows that without the distinctive feature of the gun barrel so easily seen, the rectangular box becomes a better decoy for the tank. The threshold correlation coefficient of 0.68 now really needs to be increased to 0.81. With this threshold coefficient there is not much room for error in performing

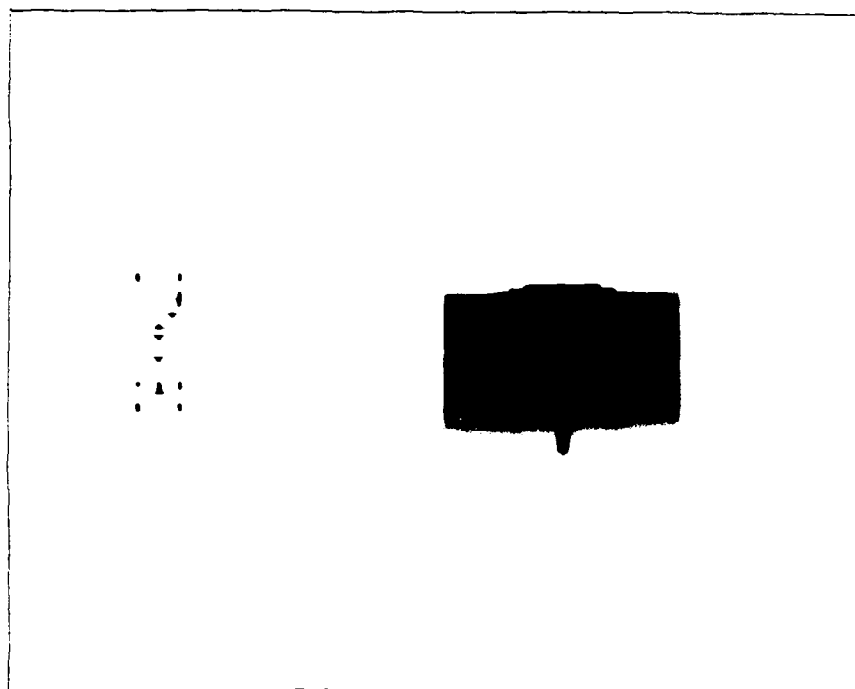


Fig. 43. Range Image of a Model T-72 Tank  
Rotated by 90 Degrees and Formed with a  
Beam Diameter of 7.3 cm.

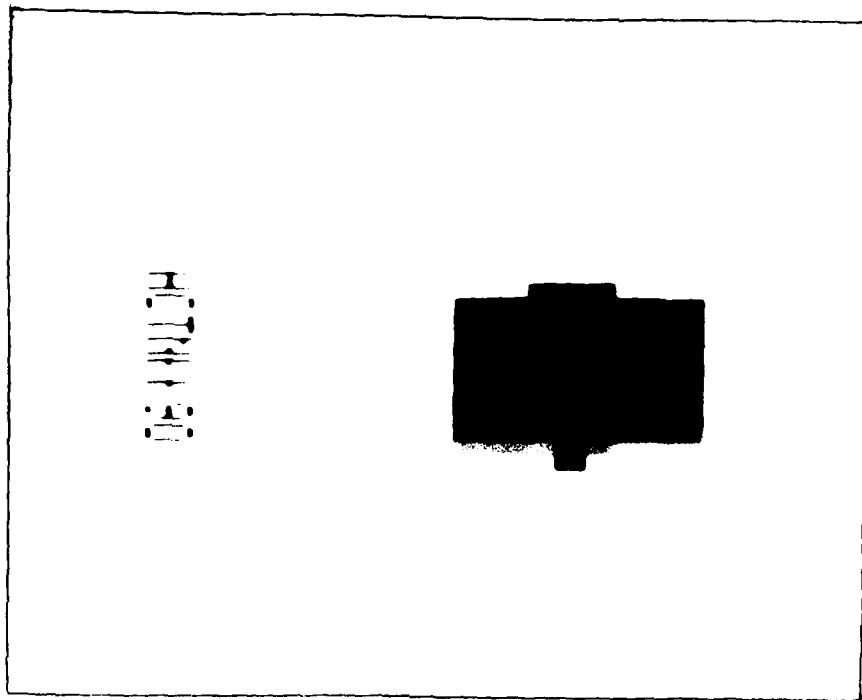


Fig. 44. Range Image of a Model T-72 Tank  
Rotated by 90 Degrees and Formed with a  
Beam Diameter of 29.1 cm.

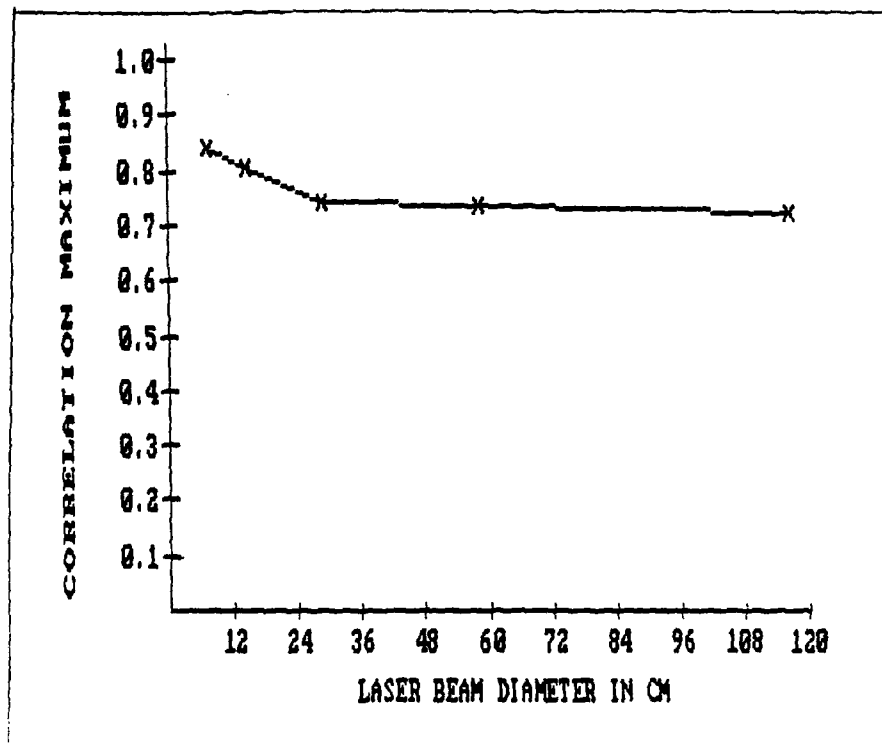


Fig. 45. Correlation Maximum vs. Diameter of the Scanning Laser Beam for a Scanned Tank (Rotated  $90^{\circ}$ ).

the correlation. The graph in Figure 45 also shows that after the laser beam diameter is increased to values larger than 30 cm, the tank's feature are not really being enhanced any more than they were at 30 cm. Thus, the plateau of the turning point was reached with a smaller beam diameter than with the non-rotated tank. This is logical since without the gun barrel, the tank has no real distinctive feature to discern it from a rectangular box. Considering the informa-



tion provided by the graphs in Figures 42 and 45, it should be okay to use beam diameters as large as 116.5 cm with which to scan a tank.

In summary, it appears that if the decoys for the air-to-ground missile are not expected to be too sophisticated, then the laser beam's spot size can be increased on the target. With a larger spot size, the range images will contain less information about potential targets, but can still possibly retain enough detail to distinguish them from simple decoys. The limit on the size of the laser beam is determined by the size of the target and the sophistication of the decoys. Range images of actual targets, though, need to be used to confirm the results obtained here.

#### The Results of Applying the Median Repair Method to Range Images

As was stated in Chapter II., range images are not perfect, since each one will contain dropout pixels. These dropout pixels are due to laser returns with either amplitudes too small to be detected or amplitudes too large to be trusted. The detector is set up so that if either of these two cases occur, then a predetermined range value will be placed in the range matrix for that laser pulse. Figure 46 is a graph that shows the results of what happens to the correlation coefficient, when a degraded range image, i.e. a range image that contains dropouts, is correlated with the same non-degraded reference image. The curve which is drawn

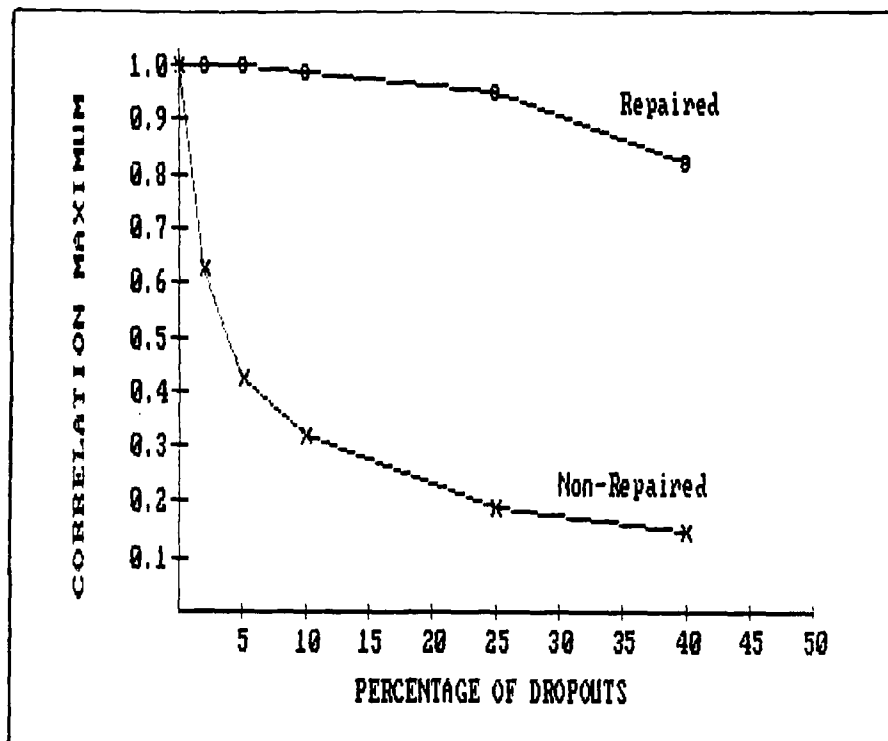


Fig. 46. Correlation Maximum vs. Percentage of Pixel Dropouts (for Both Repaired and Non-Repaired Tanks).

through the x's in Figure 46, is the result of plotting the correlation coefficient for a degraded, non-rotated T-72 tank versus the percentage that the tank in the range image was degraded. The correlation coefficients were the result of correlating the degraded tank with the same non-degraded tank.

As one can see from this graph, the correlation coefficient drops off very quickly when the object is degraded.

Figures 8 and 9 of Chapter II show how the T-72 tank appears when it has been degraded by 10% and 40% respectively. The dropout pixels in these figures have been set to the background range value. Figures 47 and 48 show the edge enhanced versions of Figures 8 and 9 respectively.

From Figures 47 and 48 it is evident why the correlation coefficient drops off so steeply, the dropouts are enhanced tremendously. The enhancement of the dropouts causes much of the energy to go into noise peaks in the correlation. Figure 49 is a graph of the correlation of the 40% degraded tank with the non-degraded tank. The overall correlation form is the same as the autocorrelation of the non-degraded tank, except for the large number of noise peaks. These noise peaks subtract a lot of energy from the autocorrelation peak which results in a low correlation coefficient. Even for only a 2% degradation, the correlation coefficient is below the old threshold of 0.68.

The same graph in Figure 46 though, also reveals the salvation of the median replacement method. The median replacement method was also described in Chapter II. The curve that is drawn through the O's in Figure 46, is the result of plotting correlation coefficients versus percentage of object degradation for the degraded, but then repaired, T-72 tank. The effect of the median replacement method on the correlation coefficient is phenomenal, even for a degradation of 40% the correlation coefficient is

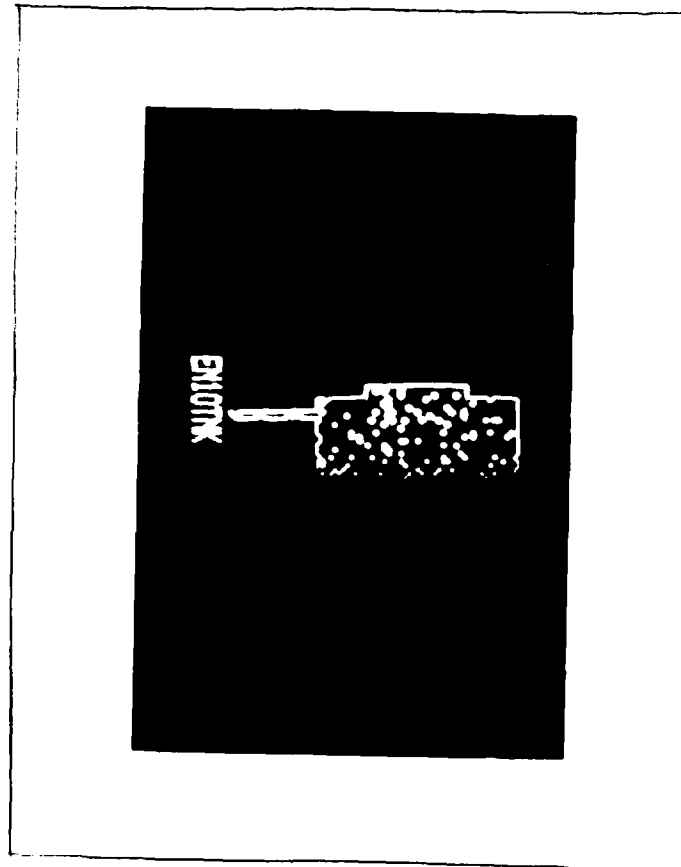


Fig. 47. Enhanced Range Image of the 10% Degraded Model T-72 Tank.

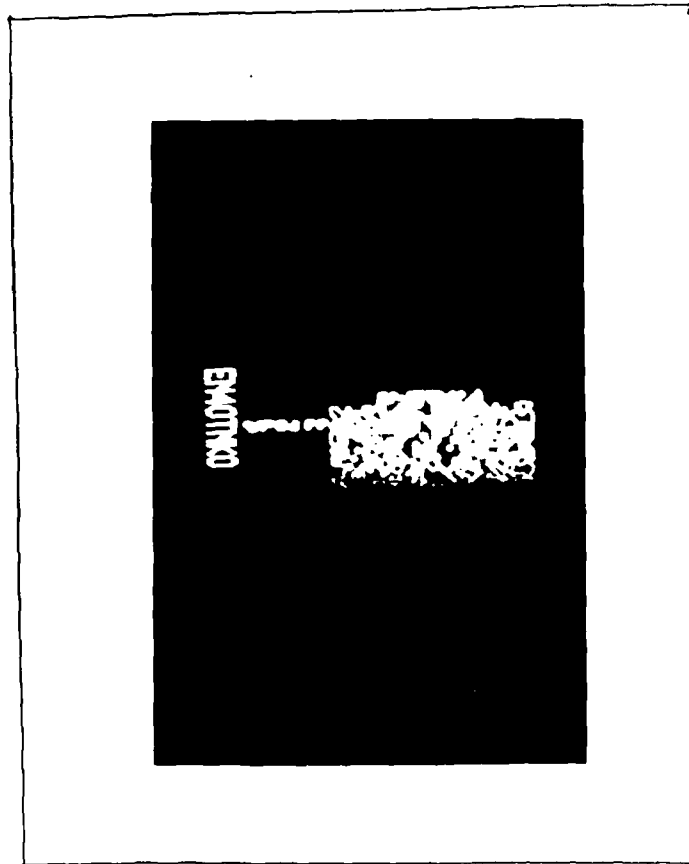


Fig. 48. Enhanced Range Image of a 40% Degraded Model T-72 Tank.

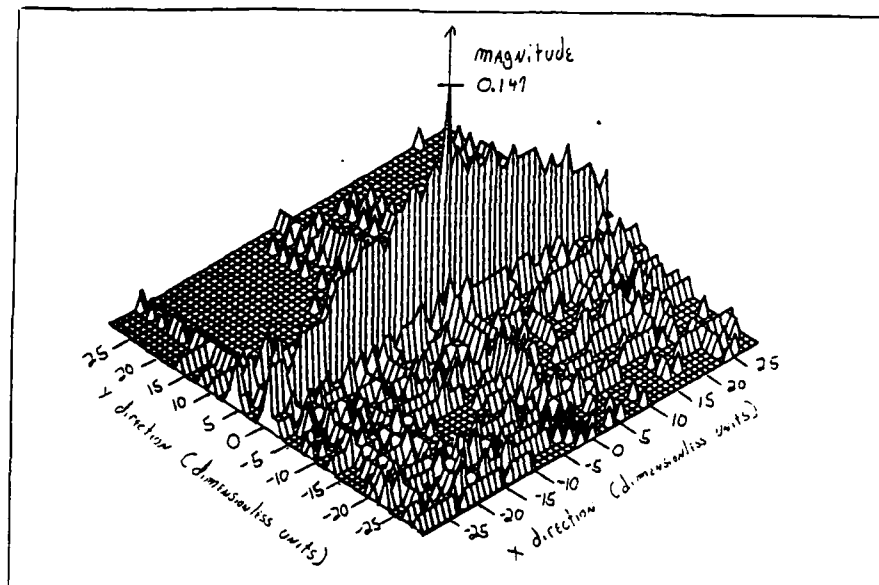


Fig. 49. Correlation of the 40% Degraded Model T-72 Tank With the Non-Degraded Model T-72 Tank.

above 0.8. Figures 10 and 11 of Chapter II. show the repaired results of Figures 8 and 9. From figures 10 and 11, one can see what a good job the replacement method has accomplished in repairing the degraded range images.

The real proof of the effectiveness of the median repair method is given by the correlation magnitude shown in Figure 50. There are no noise spikes anywhere in the correlation, and it will take a very close examination to distinguish this graph from the T-72 tank's non-degraded autocorrelation. With this repair algorithm, dropouts are no longer a problem, even if they comprise 40% of the object's pixels.

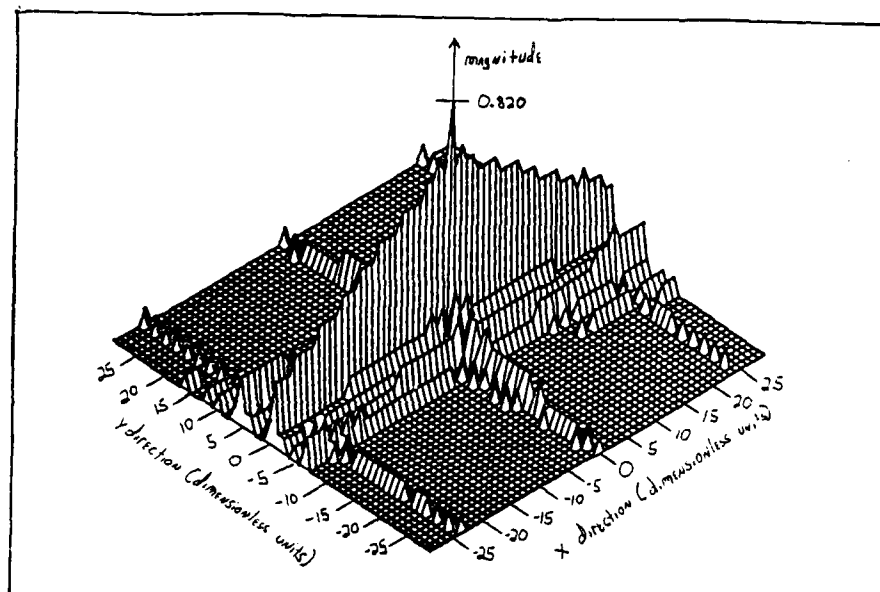


Fig. 50. Correlation of the 40% Degraded (and Then Repaired) Model T-72 Tank with the Non-Degraded T-72 Tank.

## VI. Scanning and Target Recognition for an Actual Air-to-Ground Missile.

In the preceding chapters, range images were formed with a procedure which models the scanning of an air-to-ground missile. The correlation technique of target recognition was also shown to hold a lot of promise for application to an air-to-ground missile. Now, the actual application of these scanning and recognition techniques to an air-to-ground missile needs to be explored. The values for such parameters as beam divergence and pulse rate that will be used throughout this chapter were obtained from the Electro-Optical Terminal Guidance Branch at Eglin AFB FL (Riggins, 1985). These values are only approximate and do not necessarily represent the "state of the art"; they are used only to give some reasonable values with which to work. Currently this branch at Eglin AFB is conducting experiments to test the concept of range imaging.

### The Raster Scanning of the Air-to-Ground Missile

The details of raster scanning were examined in Chapter II; in this section though, such effects on the laser scan as the missile speed and the laser beam spot size will be explored. There are many factors affecting the scan of a laser, but only the major ones will be considered here.



Since the speed of an air-to-ground missile has the biggest effect on the raster scan, it will be considered first.

An air-to-ground missile can travel with a speed anywhere from 200 m/sec to 250 m/sec. With the missile traveling with a speed like this, the scanning of the missile should occur as far ahead of the missile as possible. The further the scan takes place away from the missile, the more time the missile has to form a range scene, determine if a target is contained within the scene, and to send some kind of submunition to the target. If the missile is assumed to be traveling with a speed of 200 m/sec, a scanning distance of 1 km would give the missile 5 sec to perform all of its operations. This is not a lot of time.

The factor limiting the upper bound of the scanning distance is the beam divergence of the scanning laser. The beam divergence should be as small as possible, so that a small laser spot, e.g. less than 1 m, will be formed as far away as possible. Using a pulsed CO<sub>2</sub> laser in its laser scanner, the electro-optical branch at Eglin AFB has obtained a beam diameter of approximately 30 cm on a target 1.2 km away from the scanner. These numbers imply that the beam divergence of the laser that they were using, had a full-angle beam divergence of 0.25 mrad.

This beam diameter, 30 cm, can be used along with the pulse rate, 87 kHz that the branch was using, to compute the minimum possible time that a raster scan would take to

complete. To start off, it will be assumed that a 90 m, i.e. approximately 100 yards, swath will be scanned in front of the missile, and that the scan will take place at 1.2 km in front of the missile. It will also be assumed that the beam spots at 1.2 km will not overlap each other, but will be contiguous. Using these assumptions, one horizontal sweep of the laser over this distance of 90 m will take 300 laser pulses with an elapsed time of 3.44 msec. If it is next assumed that the range scene will be composed of a 300 x 300 matrix, then the whole scan will take 1.03 sec to complete. If the missile is traveling with a speed of 200 m/sec, then during one horizontal sweep of the laser the missile will have traveled 0.69 m, and 207 m for the entire scan. The area of the scan is thus 90 m x 207 m.

The numbers computed above bring out some interesting facts about the raster scan. The first is that the horizontal sweep of the laser does not really correspond to the range scene being sampled in a straight horizontal line. On account of the motion of the missile during the horizontal sweep, the range scene is actually sampled with slanted lines. This would tend to degrade the quality of the range images formed from the scan, but since the slope of the slant would only be 0.008 rad for the parameters considered, it shouldn't affect the range images too much.

Another fact that can be derived from the above paragraph's results is that after subtracting the 1.03 sec used

for scanning, the missile will have 4.97 sec to complete all of its processing and release its submunition. This is not a lot of time to perform all these tasks. The processing time available to the missile can be increased, though, by decreasing the area it has to scan. Thus, if the scanning area shrinks to a 90 m x 90 m area, then the missile would have about 5.56 sec for its processing time.

Of course, if the beam spot at this scanning distance was smaller, then it would take more pulses and therefore more time to complete the horizontal sweep. This longer time translates into a larger distance that the missile travels during the sweep, which in turn causes more distortion in the range image. Consequently, if a more detailed scan is desired (without distortion), then the constant speed of the missile forces the scan to cover less area. There is thus a strong relationship between scan area, beam spot size, pulse rate, and missile speed. When one of these parameters is changed, then the effect on the others must also be considered.

#### Laser Power and Detector Sensitivity

The relationship between the power that the scanning laser sends out and the power that the detector receives, can be derived using optical diagnostics to have the form given by the following equation:

$$\Phi_d = \frac{\rho A_d \Phi_L \cos(\theta)}{\pi R^2} \quad (18)$$

where

$\Phi_L$  = the power produced by the laser

$\Phi_d$  = the power received by the detector

$R$  = the range from the laser to the target

$A_d$  = the receiving area of the dectector

$\theta$  = the incident angle of laser beam as measured from the normal of the target surface

$\rho$  = the diffuse reflectance coefficient of the target surface

In forming equation (18) it has been assumed that the target surface is Lambertian, that the atmospheric absorption is zero for the wavelength of the laser, and that the laser and the detector are coaxial. Equation (18) thus only approximately describes the relationship between the output power of the laser and the power received by the detector. For the purposes of this paper, though, this equation is quite adequate.

If one assumes that laser scanning is taking place 1.2 km away from the missile, that the area of the missile's detector is  $0.25 \text{ cm}^2$ , and that the reflectance coefficient is 1.0, then equation (18) becomes

$$\Phi_d = (5.53 \times 10^{-12}) \Phi_L \cos(\theta) \quad (19)$$

where all of the symbols are defined in the same manner as

for equation (18). The detector size used in obtaining equation (19) was arbitrarily chosen. If the scanning laser produces an average power of 1 W, then the largest power, i.e. normal incidence, that the detector will receive back is  $5.53 \times 10^{-12}$  W. This number doesn't even include atmospheric absorption, nor the fact that the laser beam could be specularly reflected away from the detector. The detector that will be used in the missile will thus have to be very sensitive.

Even if such a detector does exist, one would expect that the blackbody radiation of the earth, whose peak wavelength is about 10  $\mu\text{m}$ , would make it impossible to detect such small returning signals. The electro-optical branch at Eglin is able to accomplish this feat by using a heterodyne method to modulate the output signal and to pull the returning signal out of the blackbody noise. The fact that this branch is forming range images from objects at this distance, 1.2 km, is proof that such a detector exists and that the laser returns can be detected.

If one wants to lessen the demands on the detector, the only way is to either scan closer to the missile or increase the power of the scanning laser. If one scans closer to the missile then, as a result, more of a time demand will be placed on the missile's processor. On the other hand, increasing a laser's power usually means increasing the size of the laser, and the laser that will operate inside an air-

to-ground missile must be very compact. Thus, the demands on the sensitivity of the detector appear as if they are not going to lessen very much.

#### Implementing the Correlation Routine

If one assumes that the range scan takes 0.44 sec, calculated previously, then the missile has about 5.56 sec to perform all the functions involved in detecting and destroying a target. These functions include preprocessing the range image, i.e. edge enhancing and repairing dropouts; correlating the range image with the reference target; using the position of the correlation peak to determine the position of the target; and sending a submunition to the target. These are a lot of tasks for the missile to perform in 5.56 sec.

The first step that the missile must perform after completing the range scan, is to rid the range image of its dropout pixels. The algorithm developed in this research to repair the range images took  $0.108 \pm 0.016$  sec to perform on a VAX-11/785 computer with a VMS version 4.1 operating system. All of the computer work in this research was accomplished on this computer. The time given for repairing the dropouts was actual CPU time, representing an average of measurements taken at different times in the day with different work loads on the computer. The uncertainty in the average is the standard deviation of the mean. The processor in a missile will not have the "computing power" of a

computer of this size, but should still be able to repair the range images within a second. Thus, for the time and the results it produces, the median replacement is well worth implementing.

After repairing the range image, the missile must perform a FFT on it. The FFT used in this research took  $15.56 \pm 0.15$  sec to perform. Again, this value represents the mean of a series of measurements, and the uncertainty represents the standard deviation of the mean. The missile doesn't even have enough time to perform a single FFT, much less performing a correlation and the other tasks necessary in detecting and destroying a target. Though the FFT algorithm used is not the most time efficient algorithm, the fastest FFT algorithm will still probably not give the missile enough time to perform all of its necessary duties. Let's go on though, and see how long the entire target recognition procedure would take, if an air-to-ground missile's processor was a VAX computer.

The next task that the missile must perform is edge enhancing. The edge enhancing algorithm developed in this research took  $2.69 \pm 0.08$  sec to perform, where the time value represents the mean of a series of measurements and the uncertainty is the standard deviation of those measurements. Edge enhancing thus takes a relatively long time to perform on a computer of this size. It has already been

determined previously though, that edge enhancing was necessary for the correlation process to perform properly.

The correlation is carried out by a multiplication in the frequency domain and then an inverse FFT. The combination of performing the multiplication, performing the inverse FFT, and then finding the maximum peak in the correlation took a total of 28.36 +/- 0.23 sec to perform. Adding up all of the previous time measurements, the entire target recognition procedure would take a missile with the "computing power" of a VAX computer 46.72 +/- 0.29 sec to perform. The missile would be long past the target after this amount of time has elapsed. If there is no faster method to perform correlations, some other recognition procedure besides correlation will have to be used to detect targets.

#### Optical Correlation.

Luckily, there is a method of correlation that can be performed in real time -- this method is optical correlation (Goodman, 1968:171-184). There is one problem with optical correlation though; it usually has an entire scene entered at once. With range scanning the image is entered one point at a time. There must be therefore, a combining of digital and optical processing so that the missile can perform all of its tasks in time.

The most logical method of combining the two would be to first have a digital matrix store the range points while



the image is being formed, perform the repair work on the range image digitally, and then perform the rest of the recognition procedure optically. Since the median replacement algorithm took only 0.108 sec to perform, the missile should have at least 4.56 sec to perform the optical correlation and the rest of its duties necessary in destroying a target. The transformation of the digital image into an optical image would be through some kind of spatial light modulator. Optical correlation has been established for a long time, so there shouldn't be any problem in performing a correlation with the reference target and the range image. Before this correlation is performed, edge enhancing has to be performed.

Edge enhancing can be performed at the same time as the correlation is performed. The way that one would accomplish this feat, would be to place a filter in the Fourier transform plane of the transforming lens. Immediately behind the filter would be the edge enhanced target image. The filter would be opaque in the center to block the dc component of the range image, and would become less opaque the farther one moves radially outward from the center. Thus, since the highest spatial frequencies are the farthest from the optical axis, these would pass through the filter the least attenuated. Other than using the enhancement filter, the correlation could be performed in exactly the same manner as Goodman (Goodman, 1968:166-176) has outlined. To detect the

magnitude and position of the correlation peak one could place some kind of array detector in the correlation plane of the correlator.

Though the optical correlation does not have to be performed with the procedure described, the procedure does show that it is theoretically possible to combine digital and optical operations in detecting targets from a range scene. Whether even this hybrid method is fast enough to allow the missile to detect, locate, and destroy a target has yet to be determined. It does, though, give the correlation technique some hope of being applied in air-to-ground missiles. If it turns out that this method is fast enough for use in missiles, then the technical problems of actually implementing the method on an air-to-ground missile would have to then be addressed. The technical problems would include such things as building the correlation apparatus small enough to fit inside an air-to-ground missile, yet rugged enough to withstand the vibrations of the missile.

## VII. Conclusion and Recommendations

### Conclusion

A computer program was developed in this research to form range images in a manner which models the laser scanning of an air-to-ground missile. This computer program was then used to form range images of a simple model of a Russian T-72 tank. These range images were then subsequently used to investigate a correlation technique of target recognition. In this investigation, it was shown that edge enhancing the range images was vital in distinguishing objects from one another.

It was soon discovered in this search that it was practically impossible to establish a threshold correlation coefficient for recognition, which would handle scene clutter and target rotation and at the same time be able to distinguish the model tank from a simple decoy. Methods of solving the problems of scene clutter and target rotation were then concisely summarized and referenced. Different types of edge enhancement were also tried in hopes of mitigating the effect of target rotation on the correlation coefficient. It was concluded though, that bidirectional edge enhancement was the best overall technique.

One surprising result of this study had to do with the "on target" beam diameter of the image forming laser beam. It was found that for a certain range of diameters, increasing the beam diameter impinging on a model tank would in turn, increase the correlation's ability to distinguish the tank from a simple decoy. Thus, it might not be so good to form a very detailed scan of a range scene.

One of the major successes of this study was in showing how quickly and easily the pixel dropouts in range images could be repaired. These pixel dropouts were found to have a very detrimental effect on the correlation coefficients of range images, but which could be corrected by using a technique called the "median replacement method". With this technique, a correlation coefficient of degraded range image could be raised from a value of 0.147 to a value of 0.820, a significant increase.

To close out this study, the actual implementation of the correlation technique of target recognition was explored. It was determined that using a strickly digital means to process the range images and to perform correlations would be far too slow to be useful in an air-to-ground missile. As a result, a combination of digital and optical operations would have to be combined to perform the operations of processing and correlations.

### Recommendations

The first step in continuing this research would be to create a more sophisticated model of a tank. This tank could then be used to establish a more accurate "threshold correlation coefficient", and also to see how well a more sophisticated tank model correlates with simple decoys. It would also be very desirable to use an actual range image of a tank to test whether a simple decoy would fool the correlation technique, or whether it would take a more sophisticated decoy to fool it. Both the simple and sophisticated decoys could be formed with this computer program.

The method of Mills' multiple pass correlations (Mills, 1984) should also be implemented into the correlation algorithm, if one intends to extend this research. With this implementation, the correlation should be less susceptible to the problems of scene clutter, i.e. multiple objects in a range scene. Once this algorithm has been incorporated into the correlation procedure, then experiments should be run on a computer to see how close objects have to be to the target, before this new algorithm ceases to be of use.

Another extension of this research, would be to form a SDF from computer range images of the T-72 tank, and then test it for rotation invariance. This SDF should also be tested against decoys to see if it is still discriminating. Thus, the SDF should be formed so that there is a balance

between possessing rotation invariance and possessing object discrimination. The SDF could also be built and tested for scale invariance.

Another possible extension of this research, would be to have the Electro-Optical Terminal Guidance Branch of Eglin AFB form a series of range images of actual tanks, all with differing spot sizes. These images would then need to be correlated with computer-generated images of decoys, formed with spot sizes corresponding to the tank images. This would further test the hypothesis made in this paper that for a certain range of spot sizes, the larger the "on target" spot size, the easier it is for the correlation to discriminate a tank from a simple decoy. Both sophisticated decoys and non-sophisticated decoys should be used in this test, as well as range images with the tank's barrel clearly evident and not so evident.

### Bibliography

- Arsenault, H. H. and others. "Rotation Invariant Pattern Recognition," SPIE, 359: 266-272 (1982).
- Bjorklund, C. M. and R. S. Loe. "Target Identification Using Three-Dimensional Features," SPIE, 367: (1982).
- Brigham, E. Oran. The Fast Fourier Transform. Englewood Cliffs: Prentice Hall, Inc., 1974.
- Butler, Steve. "Three Dimensional Pattern Recognition." Unpublished report. Electro-Optical Terminal Guidance Branch, Eglin AFB FL, 1985.
- Casasent, David. "Unified Synthetic Discriminant Function Computational Formulation," Applied Optics, 23: (May 1984).
- Casasent, David and Demetri Psaltis. "Position, Rotation, and Scale Invariant Optical Correlation," Applied Optics, 15: 1795-1799 (July 1976).
- Casasent, David and Vinod Sharma. "Shift-Invariant and Distortion-Invariant Object Recognition," Proceedings of the Society of Photo-Opt. Instrum. Eng., 360: 47-55 (August 1982).
- Casasent, David and others. "Synthetic Discriminant Functions for Three-Dimensional Object Recognition," SPIE, 360: 136-142 (1982).
- Cooley, James W. and John W. Tukey. "An Algorithm for the Machine Calculation of Complex Fourier Series," Mathematics of Computations, 19: 297-301 (April 1965).
- Duda, Richard O. "Use of Range and Reflectance Data to Find Planar Surface Regions," IEEE Transactions on Pattern Recognition and Machine Intelligence, PAMI-1: 259-271 (July 1979).
- Foss, Christopher F. Jane's Armour and Artillery 1983-1984 (Fifth Edition). New York: Janes Publication Inc., 1984.
- Friday, Edward C. Mellin-Fourier Correlation: Final Report, June 1982-January 1984. Electro-Optical Terminal Guidance Branch, Eglin AFB FL, August 1985.

- Fujii, H. and Y. Ohtsuba. "Rotational Filtering for Randomly Oriented Pattern Recognition," Optics Communication, 36: 255-257 (1981).
- Fujii, H. and others. "Rotational Matched Spatial Filter for Biological Pattern Recognition," Applied Optics, 19: 1190-1195 (June 1980).
- Gaskill, Jack D. Linear Systems, Fourier Transforms, and Optics. New York: John Wiley and Sons, 1978.
- Goodman, Joseph W. Introduction to Fourier Optics. New York: McGraw-Hill Book Company, 1968.
- Hester, Charles F. and David Casasent. "Multivariant Technique for Multiclass Recognition," Applied Optics, 19: 1758-1761 (June 1980).
- Jarvis, R. A. "A Laser Time-of-Flight Range Scanner for Robotic Vision," IEEE Transactions on Pattern Analysis and Machine Intelligence, PAMI-5: 505-511 (September 1983).
- Leib, Kenneth G. and others. "Aerial Reconnaissance Film Screening Using Optical Matched-Filter Image-Correlator Technology," Applied Optics, 17: 2892-2899 (September 1978).
- Mendelsohn, J. and M. R. Wohlers. "Digital Methods in the Design of Optical Matched Filters for Target Recognition," SPIE, 128: 148-153 (1980).
- Mills, Richard L. Scene Analysis Using Recursive Frequency Domain Correlation with Energy Normalization. MS thesis, School of Engineering, Air Force Institute of Technology (AU). Wright Patterson AFB OH, December 1984.
- Nitzan, David and others. "The Measurement and Use of Registered Reflectance and Range Data in Scene Analysis," Proceedings of the IEEE, 65: 206-219 (February 1977).
- Popplestone R. J. and others. "Forming Models of Plane-and-Cylinder Faceted Bodies from Light Stripes," Proceedings of the Fourth International Joint Conference on Artificial Intelligence: 664-668 (September 1975).
- Protter, Murray H. and Charles B. Morrey, Jr. Analytic Geometry (Second Edition). Reading: Addison-Wesley Publication Company, 1975.



Riggins, Capt Jim. Personal Correspondence. Electro-Optical Terminal Guidance Branch, Eglin AFB FL, June 1985.

Rocker F. and A. Kiessling. "Methods for analyzing Three Dimensional Scenes," Proceedings of the Fourth International Joint Conference on Artificial Intelligence: 669-673 (September 1975).

Shirai, Y. "A Step Towards Context-Sensitive Recognition of Irregular Objects," Computer Graphics and Image Processing, 2: 298-307 (December 1973).

Shirai, Y. and M. Suwa. "Recognition of Polyhedrons with a Range Finder," Proceedings of the Second International Joint Conference on Artificial Intelligence: 80-87 (September 1971).

#### VITA

Jeffrey W. Grantham was born June 9, 1962 in Perry, Florida. He graduated from Taylor County High School in 1980. He then attended Florida State University on a 4-year ROTC scholarship. He graduated in 1984 with highest honors receiving the degree of Bachelor of Science with a major in Physics and a minor in Applied Mathematics. At that time he was commissioned in the United States Air Force through the ROTC program.

After graduation, his first active duty assignment was to the Air Force Institute of Technology in May 1984.

Permanent address: 614 W. Julia Dr.  
Perry, Fl. 32347

Unclassified

SECURITY CLASSIFICATION OF THIS PAGE

## REPORT DOCUMENTATION PAGE

|   |       |  |  |
|---|-------|--|--|
| 1a. REPORT SECURITY CLASSIFICATION<br>Unclassified  |       | 1b. RESTRICTIVE MARKINGS   |  |
| 2a. SECURITY CLASSIFICATION AUTHORITY   |       | 3. DISTRIBUTION/AVAILABILITY OF REPORT<br>Approved for public release;<br>distribution unlimited |  |
| 2b. DECLASSIFICATION/DOWNGRADING SCHEDULE   |       | 5. MONITORING ORGANIZATION REPORT NUMBER(S)  |  |
| 4. PERFORMING ORGANIZATION REPORT NUMBER(S)<br>AFIT/ENP/85D-4   |       | 7a. NAME OF MONITORING ORGANIZATION  |  |
| 6a. NAME OF PERFORMING ORGANIZATION<br>Department of Engineering<br>Eglin AFB, OH 45433   |       | 6b. OFFICE SYMBOL<br>(If applicable)<br>AFIT/ENP   |  |
| 8a. NAME OF FUNDING/SPONSORING ORGANIZATION<br>Air Force Armament Test Lab  |       | 8b. OFFICE SYMBOL<br>(If applicable)<br>AFATL/DLMI   |  |
| 8c. ADDRESS (City, State and ZIP Code)<br>Eglin AFB FL 32542-5000   |       | 9. PROCUREMENT INSTRUMENT IDENTIFICATION NUMBER  |  |
| 11. TITLE (Include Security Classification)<br>See Box 19   |       | 10. SOURCE OF FUNDING NOS.   |  |
| 12. PERSONAL AUTHOR(S)<br>Grantham, Jeffrey W., 2nd Lt, USAF  |       | PROGRAM ELEMENT NO.  |  |
| 13a. TYPE OF REPORT<br>MS Thesis  |       | PROJECT NO.  |  |
| 13b. TIME COVERED<br>FROM _____ TO _____  |       | TASK NO.   |  |
| 14. DATE OF REPORT (Yr., Mo., Day)<br>1985 December   |       | WORK UNIT NO.  |  |
| 15. PAGE COUNT<br>151   |       | 16. SUPPLEMENTARY NOTATION   |  |
| 17. COSATI CODES  |       | 18. SUBJECT TERMS (Continue on reverse if necessary and identify by block number)                |  |
| FIELD   | GROUP | SUB. GR.   |  |
| 20  | 06    | Cross Correlation, Optical Images, Optical Radar, Range Imaging                                  |  |
| 19. ABSTRACT (Continue on reverse if necessary and identify by block number)  |       |  |  |
| Title: OBJECT RECOGNITION USING RANGE IMAGES  |       |  |  |
| Thesis Chairman: John J. Wharton Jr., Major, USAF<br>Deputy Head and Assistant Professor<br>Department of Engineering Physics   |       |  |  |
| <div style="text-align: right;"> <p>Approved for Public Release DATE 12/1/85 BY 13548</p> <p>LENN E. WOLAVICH</p> <p>Dean for Research and Professional Development</p> <p>Air Force Institute of Technology (AFIT)</p> <p>Wright-Patterson AFB OH 45433</p> </div> |       |  |  |
| 20. DISTRIBUTION/AVAILABILITY OF ABSTRACT<br>UNCLASSIFIED/UNLIMITED <input checked="" type="checkbox"/> SAME AS RPT. <input type="checkbox"/> DTIC USERS <input type="checkbox"/>   |       | 21. ABSTRACT SECURITY CLASSIFICATION<br>Unclassified   |  |
| 22a. NAME OF RESPONSIBLE INDIVIDUAL<br>John J. Wharton Jr., Maj, USAF   |       | 22b. TELEPHONE NUMBER<br>(Include Area Code)<br>513-255-4498                                     |  |
|   |       | 22c. OFFICE SYMBOL<br>AFIT/ENP   |  |

DD FORM 1473, 83 APR

EDITION OF 1 JAN 73 IS OBSOLETE.

Unclassified  
SECURITY CLASSIFICATION OF THIS PAGE

Unclassified

SECURITY CLASSIFICATION OF THIS PAGE

This study involved forming synthetic range images and investigating correlation as a target recognition technique. The synthetic range images were formed with a computer program, which models the laser scanning of an air-to-ground missile. With this range imaging program, a model of a Russian T-72 tank was formed, which was subsequently used in investigating image correlation.

In the investigation into image correlation, the effects of background clutter and target rotation on a range image's correlation coefficient were examined, as well as possible methods of correcting for these effects. Other factors affecting the correlation coefficient that were considered were pixel dropouts and the beam spot size of the laser. Pixel dropouts were shown to be detrimental to a range image's correlation coefficient, but could be corrected by using a "median replacement" technique. Also shown was that for a certain range of "on target" beam diameters, as the diameter of the scanning laser beam increased, so did the correlation's discerning ability. The last part of this study revealed that actually implementing range imaging and correlation into an air-to-ground missile was possible, but would require both digital and optical operations.

Unclassified

SECURITY CLASSIFICATION OF THIS PAGE

END

DATE  
FILMED

6-86

DTIC